ENHANCEMENT OF AROMATIC HYDROCARBON PRODUCTION AND SUPPRESSION OF COKE FORMATION IN CATALYTIC PYROLYSIS OF BIOMASS

POUYA SIROUS REZAEI

THESIS SUBMITTED IN FULFILLMENT OF THE REQUIREMENTS FOR THE DEGREE OF DOCTOR OF PHILOSOPHY

FACULTY OF ENGINEERING
UNIVERSITY OF MALAYA
KUALA LUMPUR

2016

UNIVERSITI MALAYA

ORIGINAL LITERARY WORK DECLARATION

Name of Candidate: Pouya Sirous Rezaei **(I.C/Passport No:**

Registration/Matric No: KHA110092

Name of Degree: DOCTOR OF PHILOSOPHY

Title of Project Paper/Research Report/Dissertation/Thesis ("this Work"):

ENHANCEMENT OF AROMATIC HYDROCARBON PRODUCTION AND SUPPRESSION OF COKE FORMATION IN CATALYTIC PYROLYSIS OF BIOMASS

Field of Study: Reaction Engineering

I do solemnly and sincerely declare that:

(1) I am the sole author/writer of this Work;
(2) This Work is original;
(3) Any use of any work in which copyright exists was done by way of fair dealing and for permitted purposes and any excerpt or extract from, or reference to or reproduction of any copyright work has been disclosed expressly and sufficiently and the title of the Work and its authorship have been acknowledged in this Work;
(4) I do not have any actual knowledge nor ought I reasonably to know that the making of this work constitutes an infringement of any copyright work;
(5) I hereby assign all and every rights in the copyright to this Work to the University of Malaya ("UM"), who henceforth shall be owner of the copyright in this Work and that any reproduction or use in any form or by any means whatsoever is prohibited without the written consent of UM having been first had and obtained;
(6) I am fully aware that if in the course of making this Work I have infringed any copyright whether intentionally or otherwise, I may be subject to legal action or any other action as may be determined by UM.

Candidate's Signature **Date: 4 April 2016**

Subscribed and solemnly declared before,

Witness's Signature **Date: 4 April 2016**

Name: Hoda Shafaghat
Designation: Department of Chemical Engineering,
Faculty of Engineering, University of Malaya

ABSTRACT

The concern for depletion of fossil fuels and their growing environmental threats necessitates to develop efficient techniques for utilization of lignocellulosic biomass as an alternative fuel source which is renewable and environmentally safe. Pyrolysis is an economically feasible process for large-scale exploitation of biomass. However, bio-oil which is the liquid product of biomass pyrolysis has high oxygen content, and needs to be deoxygenated to hydrocarbons in order to be used as fuel additive. Catalytic pyrolysis using zeolites as catalyst is considered as an efficient technology since it includes both steps of pyrolysis and catalytic upgrading in one unit. Among the three major lignocellulosic components (cellulose, hemicellulose and lignin), lignin is the most difficult fraction of biomass to be deoxygenated. In catalytic conversion of methanol co-fed with *m*-cresol or phenol as lignin model compounds over HBeta catalyst in a fixed-bed reactor, it was revealed that co-feeding phenol or *m*-cresol with methanol causes significant deactivation of HBeta and remarkable reduction in aromatic hydrocarbons yield due to strong adsorption of phenolics on zeolite acid sites. Hence, pure zeolites are not appropriate catalysts for upgrading of the lignocellulosic biomass with high content of lignin. In this research, bifunctional Fe/HBeta catalyst showed to be efficient for production of aromatic hydrocarbons in catalytic pyrolysis of palm kernel shell waste with high lignin content of about 50 wt%. Lignin derived phenolics were deoxygenated through hydrogenolysis reaction promoted by Fe active sites. The adsorption of phenol on zeolite was shown to be highly affected by reaction temperature and catalyst properties such as pore size, crystallite size and strength distribution of zeolite acid sites. One main challenge in atmospheric upgrading of biomass derived feedstocks over zeolites is high formation and deposition of coke which results in rapid catalyst deactivation. Meanwhile, coke formation is a competing reaction with production of valuable compounds like aromatic hydrocarbons. Coke is one major undesired product of this process which its

high yield is due to low hydrogen to carbon effective ratio of biomass and in turn low hydrogen content in hydrocarbon pool inside catalyst. In this study, catalytic pyrolysis of cellulose as biomass model compound was conducted using HZSM-5 (Si/Al: 30), HY (Si/Al: 30) and physically mixed catalysts of HZSM-5 (Si/Al: 30) and dealuminated HY (Si/Al: 327) in order to investigate the dependency of formation of both types of thermal and catalytic coke on zeolite characteristics. Coke formation over physically mixed catalysts of HZSM-5 and dealuminated HY was remarkably lower than that over HZSM-5 and HY. The aromatic hydrocarbons yield was also considerably enhanced over the physically mixed catalysts compared to HZSM-5 and HY. It was shown that there is a significant interaction between zeolite pore structure and density of acid sites which could be taken into account for designing more efficient catalysts to achieve lower coke formation and higher production of desired products. The catalysts used in this study were characterized by XRF, XRD, N_2 adsorption, NH_3-TPD, H_2-TPR, FTIR and TGA, and liquid products were analyzed by GC/MS.

ABSTRAK

Kebimbangan untuk pengurangan bahan api fosil dan ancaman alam sekitar yang sedang membesar memerlukan untuk membangunkan teknik-teknik berkesan untuk penggunaan biomas lignoselulosa sebagai sumber bahan api alternatif yang boleh diperbaharui dan mesra alam. Pirolisis adalah satu proses yang dilaksanakan dari segi ekonomi untuk eksploitasi besar-besaran biomas. Walau bagaimanapun, bio-oil yang merupakan produk cecair pirolisis biomas mempunyai kandungan oksigen yang tinggi, dan perlu terdeoksigen kepada hidrokarbon untuk digunakan sebagai bahan tambahan bahan api. Pirolisis pemangkin menggunakan zeolite sebagai pemangkin dianggap sebagai teknologi yang cekap kerana ia merangkumi kedua-dua langkah pirolisis dan menaik taraf pemangkin dalam satu unit. Antara ketiga-tiga komponen lignoselulosa utama (selulosa, hemiselulosa dan lignin), lignin adalah pecahan yang paling sukar biomas sebagai terdeoksigen. Dalam penukaran pemangkin metanol bersama makan dengan *m*-cresol atau fenol sebagai sebatian model lignin lebih HBeta pemangkin dalam reaktor tetap tidur, ia telah mendedahkan bahawa bersama makan fenol atau *m*-cresol dengan metanol menyebabkan penyahaktifan besar HBeta dan pengurangan yang luar biasa dalam hidrokarbon aromatik hasil kerana penyerapan yang kuat fenolik pada tapak asid zeolite. Oleh itu, zeolite tulen tidak pemangkin sesuai untuk menaik taraf biomas lignoselulosa yang tinggi kandungan lignin. Dalam kajian ini, bifunctional Fe/HBeta pemangkin menunjukkan untuk menjadi tinggi untuk pengeluaran hidrokarbon aromatik dalam pirolisis pemangkin sisa shell isirong sawit dengan kandungan lignin tinggi kira-kira 50% berat. Lignin fenolik yang diperolehi adalah terdeoksigen melalui tindak balas hydrogenolysis digalakkan oleh Fe tapak aktif. Penjerapan fenol pada zeolite telah ditunjukkan untuk menjadi sangat dipengaruhi oleh tindak balas suhu dan pemangkin sifat seperti saiz liang, saiz crystallite dan pengedaran kekuatan tapak asid zeolite. Salah satu cabaran utama dalam menaik taraf atmosfera biomas yang dihasilkan bahan suapan

lebih zeolite adalah pembentukan yang tinggi dan pemendapan coke yang menyebabkan pemangkin penyahaktifan pesat. Sementara itu, pembentukan coke adalah reaksi bersaing dengan pengeluaran sebatian berharga seperti hidrokarbon aromatik. Coke adalah salah satu produk utama yang tidak diingini daripada proses ini yang hasil yang tinggi adalah disebabkan oleh hidrogen yang rendah nisbah karbon berkesan biomas dan seterusnya kandungan hidrogen yang rendah dalam kolam hidrokarbon dalam pemangkin. Dalam kajian ini, pirolisis pemangkin selulosa sebagai sebatian model biomas dijalankan dengan menggunakan HZSM-5 (Si/Al: 30), HY (Si/Al: 30) dan pemangkin campuran secara fizikal daripada HZSM-5 (Si/Al: 30) dan dealuminated HY (Si/Al: 327) untuk menyiasat pergantungan pembentukan kedua-dua jenis coke haba dan pemangkin kepada ciri-ciri zeolite. Pembentukan coke lebih pemangkin campuran secara fizikal daripada HZSM-5 dan dealuminated HY adalah amat rendah berbanding lebih HZSM-5 dan HY. Hasil hidrokarbon aromatik juga jauh dipertingkatkan ke atas pemangkin campuran secara fizikal berbanding HZSM-5 dan HY. Ia telah menunjukkan bahawa terdapat interaksi yang signifikan antara struktur liang zeolite dan ketumpatan tapak asid yang boleh diambil kira untuk mereka bentuk pemangkin yang lebih cekap untuk mencapai pembentukan coke lebih rendah dan peningkatan pengeluaran produk yang dikehendaki. Pemangkin yang digunakan dalam kajian ini telah disifatkan oleh XRF, XRD, penjerapan N_2, NH_3-TPD, H_2-TPR, FTIR dan TGA, dan produk cecair dianalisis dengan GC/MS.

To my beloved parents for their constant support and encouragement

To my beloved wife, Hoda, for her unconditional love, continuous encouragement and devotion

ACKNOWLEDGEMENTS

I express my deep sense of gratitude to my advisor, Prof. Dr. Wan Mohd Ashri Wan Daud. His inspiring guidance and constant encouragement always helped me to shape my research towards something more meaningful. This thesis could not have been accomplished without his insight, patience and support.

I am thankful to my colleague, Masoud Asadieraghi, for all his help and encouragement during this research work. My special thanks goes to my colleague, friend and wife, Hoda Shafaghat, who has always been a source of encouragement and support for me, and provided me with her help and suggestions in every step of my education.

I am greatly appreciative of my family, my parents and sisters, for their love and support.

TABLE OF CONTENTS

LIST OF FIGURES

LIST OF SCHEMES

LIST OF TABLES

LIST OF SYMBOLS AND ABBREVIATIONS

BET	Brunauer, Emmett and Teller
BJH	Barrett-Joyner-Halenda
β	Line broadening full width at half maximum after subtracting the instrumental line broadening (in radians)
C	Carbon
C_{C1}	Thermal coke
C_{C2}	Catalytic coke
C_{CT}	Total coke
D	Crystallite size
DTG	Differential thermogravimetry
FCC	Fluid catalytic cracking
f_{C1}	Fraction of thermal coke
FTIR	Fourier transform infrared spectroscopy
GC	Gas chromatograph
H	Hydrogen
H/C_{eff}	Hydrogen to carbon effective ratio
HDO	Hydrodeoxygenation
LPG	Liquefied petroleum gas
MS	Mass spectrometer
N	Nitrogen
NIST	National Institute of Standards and Technology
O	Oxygen
PAH	Polycyclic aromatic hydrocarbon
P_c	Critical pressure

PKS	Palm kernel shell
S	Sulfur
T	Temperature
T_c	Critical temperature
TCD	Thermal conductivity detector
TCE	Thermo-catalytic effect
TE	Thermal effect
TGA	Thermogravimetric analysis
TPD	Temperature-programmed desorption
TPR	Temperature-programmed reduction
VGO	Vacuum gas oil
WHSV	Weight hourly space velocity
XRD	X-ray diffraction
XRF	X-ray flouresence
σ	Kinetic diameter
θ	Bragg angle
λ	X-ray wavelength

CHAPTER 1: INTRODUCTION

1.1 General

Current utilization rate of fossil fuels is much higher than their natural regeneration rate leading to the shortage of fossil fuels. Considering the depletion of fossil fuel reserves as well as the increasing environmental threats like global warming and air pollution caused by large-scale consumption of fossil fuels, there is a growing demand for renewable, sustainable and environmentally friendly fuels (Fogassy et al., 2010; Hew, Tamidi, Yusup, Lee, & Ahmad, 2010; Kwon, Mayfield, Marolla, Nichols, & Mashburn, 2011; Perego & Bosetti, 2011; Serrano-Ruiz & Dumesic, 2011). Lignocellulosic biomass seems to be a highly potential renewable source of energy. Fuels obtained from biomass are considered carbon dioxide neutral since CO_2 produced from biofuel combustion has been previously absorbed from atmosphere through photosynthesis process of plants (Zhang, Chang, Wang, & Xu, 2006).

The processes for conversion of biomass into biofuels are generally divided into two broad categories: biological (fermentation and anaerobic digestion) and thermochemical (combustion, gasification, hydrothermal liquefaction and pyrolysis) processes (Iliopoulou et al., 2007; Toor, Rosendahl, & Rudolf, 2011). Fast pyrolysis is one of the most promising thermochemical conversion techniques for large-scale exploitation of biomass material and production of liquid fuel (Zhang, Brown, Hu, & Brown, 2013). Pyrolysis is the thermal decomposition process in which organic compounds are degraded in an oxygen-free environment. The products of pyrolysis are a liquid fraction called bio-oil (about 75 wt% based on biomass) as well as solid residue containing carbon deposits and non-condensable gases (de Miguel Mercader et al., 2010). Pyrolysis-derived bio-oil is considered a potential liquid fuel due to its remarkable advantages like slight content of

sulfur and nitrogen, renewability and availability of large amounts of biomass and CO_2 neutrality (Wang, Yang, Luo, Hu, & Liu, 2011).

However, composition of pyrolysis-derived bio-oils is different from that of petroleum and contains high content of oxygen and water (Graça, Ribeiro, Cerqueira, Lam, & de Almeida, 2009; Samolada, Papafotica, & Vasalos, 2000). Bio-oil has low heating value compared to conventional fossil oil, poor thermal and chemical stabilities and high viscosity. It is also corrosive and immiscible with conventional fossil fuels. The corrosiveness is due to high amounts of organic acids which cause a pH value of 2-3 (Peralta, Sooknoi, Danuthai, & Resasco, 2009; Song, Zhong, & Dai, 2010; Thegarid et al., 2014; Wang, Chang, & Fan, 2010; Williams & Nugranad, 2000; Yu et al., 2011; Zhang, Xiao, Huang, & Xiao, 2009). There are typically more than 400 different organic compounds (such as ketones, aldehydes, alcohols, esters, ethers, sugars, carboxylic acids, phenols and furans) in bio-oil which are derived from depolymerization of the three major lignocellulosic components: cellulose, hemicellulose and lignin. Table 1.1 shows a summary of the main components present in the bio-oil derived from pyrolysis of pine sawdust. This multicomponent composition containing unsaturated compounds causes low stability under storage conditions (Fisk et al., 2009; Graça, Comparot, et al., 2009; Graça et al., 2010; Li et al., 2011). Due to these drawbacks of bio-oil, it needs to be upgraded.

Table 1.1: Chemical composition of bio-oil derived from pyrolysis of pine sawdust (Gayubo, Valle, Aguayo, Olazar, & Bilbao, 2010).

Component or group	**wt%**
Acids and esters	26.17
Acetic acid	15.33
Formic acid	1.77
2(5H)-furanone	1.12
Diethoxymethylacetate	0.98
Methyl acetate	0.78
Propanoic acid	0.55
4-Oxopentanoic acid	0.55
Hexyl 2-methylpropanoate	0.45
Other acids and esters	4.64

'Table 1.1, continued'

Component or group	wt%
Ketones	27.03
1-Hydroxy-2-propanone	14.97
Acetone	5.29
2-Hydroxy-2-cyclopenten-1-one	1.89
3-Methyl-1,2-cyclopentenodione	1.06
1-Acetyloxy-2-propanone	0.52
Other ketones	3.3
Aldehydes	19.33
Hydroxyacetaldehyde	10.58
Butanedial	2.15
Formaldehyde	2.03
Heptanal	1.26
Pentanal	1.14
Furfural	0.95
Other aldehydes	1.22
Phenols	8.20
2-Methoxyphenol	1.18
1,2-Benzenediol	1.11
2-Methoxy-4-methylphenol	1.07
3-Methylphenol	1.00
2-Methylphenol	0.73
Other phenols	3.11
Ethers	0.94
Tetrahydrofuran	0.30
2-Butyl-3-methyl-oxirane	0.16
3-Methyl-3-(1-ethoxyethoxy)-1-buten	0.16
Other ethers	0.32
Alcohols	11.45
Methanol	4.59
Ethylenglycol	1.76
Glycidol	0.78
Cyclopropyl carbinol	0.73
Other alcohols	3.59
Levoglucosan	3.94

In the previous years, catalytic treatment has been the focus of many researchers to produce a liquid fuel similar to refined petroleum fuel. Currently, there are two main methods studied for upgrading of biomass pyrolysis liquids. One technique called hydrodeoxygenation (HDO) is a catalytic hydrotreating with hydrogen under high pressure (mostly in the pressure range of 30-140 bar) or in the presence of hydrogen donor solvents (Furimsky, 2000). Alternatively, upgrading of biomass pyrolysis vapors/bio-oil can be performed through catalytic cracking using solid acid catalysts under atmospheric pressure without hydrogen consumption (Putun, Uzun, & Putun, 2006; Williams & Horne, 1995a). Multicomponent composition of bio-oil has attracted several researchers to study the transformation of different bio-oil model compounds such as aldehydes,

ketones, acids, alcohols, phenols and their mixtures in order to find out the reaction pathway for their conversion and to determine an overall reaction pathway for conversion of biomass pyrolysis vapors/bio-oil. Several catalyst properties like particle size, pore size, acidity and mesoporosity as well as operational parameters such as temperature, gas residence time and ratio of catalyst to reactants have been reported in literature as the factors which significantly affect reaction pathway and products yields and selectivities. Therefore, it is necessary to design selective catalysts and optimize upgrading process in order to maximize the yield of value-added chemicals and minimize the formation of undesired compounds.

Aromatic hydrocarbons are among the main products obtained by catalytic cracking of biomass pyrolysis vapors/bio-oil, and are the building blocks of petrochemical industry. Considering the wide range of applications of aromatic hydrocarbons, it seems worthwhile to determine the factors which influence their production in catalytic cracking of biomass pyrolysis vapors/bio-oil. Selectively production of high yields of green aromatic hydrocarbons through catalytic conversion of biomass derived feedstocks can be a viable alternative for production of these compounds from fossil fuel.

1.2 Conversion of lignin-derived phenolics into aromatic hydrocarbons

It is well described in literature that among the three lignocellulosic components (cellulose, hemicellulose and lignin), lignin is the most difficult fraction to be converted to hydrocarbons (Ben & Ragauskas, 2011; Huang et al., 2012; Li et al., 2012). So far, catalytic pyrolysis processes for conversion of lignin into aromatic hydrocarbons have been conducted at high temperatures above 600 °C, high ratios of zeolite to lignin and fast heating rates (Jackson, Compton, & Boateng, 2009; Kim et al., 2015; Ma, Troussard, & van Bokhoven, 2012; Y. Yu et al., 2012; Zhang, Resende, & Moutsoglou, 2014). In catalytic pyrolysis of lignin over HZSM-5 using a pyroprobe pyrolyzer, it was observed

that aromatic hydrocarbon yield was significantly enhanced by increase of reaction temperature from 550 to 650 °C (Shen, Zhao, Xiao, & Gu, 2015; Zhang & Moutsoglou, 2014). Li et al. (2012) showed that aromatic hydrocarbon yield was a strong function of catalyst to lignin ratio; the aromatic hydrocarbon production was maximized at high HZSM-5 to lignin ratio of 15. However, cellulose could be remarkably converted into aromatic hydrocarbons by catalytic pyrolysis at lower temperatures (below 600 °C) and catalyst to feed ratios (Karanjkar et al., 2014; Srinivasan, Adhikari, Chattanathan, Tu, & Park, 2014). The reasons for difficulty of lignin deoxygenation are low reactivity of lignin-derived phenolics over zeolite acid sites and rapid deactivation of zeolites exposed to phenolic compounds. In a study held by Mullen and Boateng (2010), it was revealed that lignin-derived phenolics especially those simple phenolics obtained from pyrolysis of *p*-hydroxyphenyl unit of lignin have high potential to form tight bond with HZSM-5 acid sites, and cause zeolite deactivation. Catalyst deactivation caused by strong adsorption of phenols on zeolite was also observed by addition of phenol to methylcyclohexane and n-heptane in transformation of these compounds over HZSM-5 and HY zeolites (Graça, Comparot, et al., 2009; Graça et al., 2010; Graça et al., 2009). It could be inferred that pure zeolites are not suitable catalysts for deoxygenation of lignin or feedstocks derived from biomass with high lignin content. Zeolite modification could be implemented in order to design novel catalysts with enhanced catalytic performance for conversion of lignin-derived phenolics into aromatic hydrocarbons.

1.3 Catalyst deactivation by coke formation

One major challenge in catalytic conversion of biomass materials into value-added chemicals and fuels is high formation and deposition of coke which causes high deactivation of catalyst (Rezaei, Shafaghat, & Daud, 2014). The reason for high yield of coke is low hydrogen to carbon effective ratio of biomass which leads to low hydrogen

content in hydrocarbon pool inside catalyst. Coke deposited on catalyst is divided into two types of thermal and catalytic origin (Gayubo et al., 2010). Thermal coke is produced by homogeneous thermal polymerization of compounds in gas phase, and is mainly deposited on outer surface of catalyst (Carlson, Vispute, & Huber, 2008). Catalytic coke is formed in the internal channels of catalyst as a result of heterogeneous transformation of oxygenate compounds over zeolite acid sites through reactions of oligomerization, cyclization, aromatization and condensation (Gayubo, Aguayo, Atutxa, Prieto, & Bilbao, 2004; Gayubo, Valle, Aguayo, Olazar, & Bilbao, 2009; Gayubo, Valle, Aguayo, Olazar, & Bilbao, 2010). Coke deposition results in catalyst deactivation through poisoning zeolite acid sites and pore blockage. In addition to catalyst deactivation, coke formation is a competing reaction with production of desired products. The Characteristics of pore structure of zeolites such as total porosity, pore size and shape, the amount of intercrystalline pores and connectivity of zeolite channels have significant impact on the amount of coke formation. Catalyst pore size influences the yield of both thermal and catalytic coke by affecting the diffusivity of reactants and products into and out of catalyst; smaller pore size restricts the diffusion of large molecules into catalyst which could result in homogeneous thermal polymerization of these molecules in gas phase (Aho et al., 2010; Williams & Horne, 1995b). Pore shape could cause steric constraints for formation of the transition states which are involved in production of coke precursors (Zhang, Cheng, Vispute, Xiao, & Huber, 2011). Meso- and macropores between zeolite crystals allow high degree of polymerization resulting in the growth of coke (Mortensen, Grunwaldt, Jensen, Knudsen, & Jensen, 2011; Valle, Castaño, Olazar, Bilbao, & Gayubo, 2012). Three-dimensional porous structure could reduce coke formation due to high connectivity of channels which results in enhanced movement of coke precursor intermediates to the outside of zeolite crystals (Ibáñez, Valle, Bilbao, Gayubo, & Castaño, 2012). Apart from pore structure, zeolite acidity is also influential on the amount of coke

formation. Since catalytic coke is formed over zeolite acid sites, its yield is dependent on strength distribution and density of acid sites. Catalytic coke content of zeolite is expected to be increased by increase in strength and number of acid sites. Therefore, it is essential to optimize zeolite properties such as pore structure and acidity in order to lower coke formation.

1.4 Thesis objectives

The main target of this thesis is to investigate the improvement of the process of catalytic pyrolysis of biomass in terms of suppression of coke formation and enhanced production of aromatic hydrocarbons. More precisely, the objectives of this study are as follows:

- To study the origin of zeolite deactivation in catalytic conversion of lignin-derived phenolic compounds.
- To design an efficient catalyst for enhanced conversion of lignin-derived phenolics into aromatic hydrocarbons.
- To study and optimize the interactive effects of zeolite characteristics such as pore structure and acidity in order to suppress the formation of both types of thermal and catalytic coke in catalytic pyrolysis of biomass.

1.5 Thesis organization

The present thesis includes five chapters as follows:

- CHAPTER 1: This chapter briefly introduces the pyrolysis of biomass and the various methods for catalytic upgrading of biomass pyrolysis vapors/bio-oil. The two challenging issues in catalytic conversion of biomass derived feedstocks into aromatic hydrocarbons are discussed. Since aromatic hydrocarbons have wide range of applications and are the building blocks for petrochemical industry, these

highly desirable compounds are considered as target products of catalytic reactions in this work. The main objectives of the study are also explained.

- CHAPTER 2: This chapter presents a review on the recent researches in catalytic conversion of biomass pyrolysis vapors/bio-oil and bio-oil model compounds focusing on the effects of catalyst properties and reaction conditions on reaction selectivity toward aromatic hydrocarbons. The dependency of coke formation on catalyst properties and reaction conditions is also reviewed in this chapter.
- CHAPTER 3: This chapter describes all the experimental procedures employed in this work for catalytic activity measurements, catalyst preparation and modification as well as characterization of biomass, bio-oil and catalysts. Details on the raw material, equipment and other related procedures are explained as well.
- CHAPTER 4: This chapter presents the experimental data and results. In this chapter, the results are discussed in three parts. Part 1 investigates the effects of lignin-derived phenolic compounds on zeolite deactivation. Phenol and *m*-cresol as model compounds of lignin were co-fed with methanol in order to show how catalytic performance of HBeta zeolite could be affected by simple phenols derived from *p*-hydroxyphenyl units of lignin. Furthermore, the possibility of atmospheric conversion of phenolic compounds into aromatic hydrocarbons is studied over a bifunctional iron impregnated HBeta catalyst as a modified zeolite. Part 2 studies the conversion of palm kernel shell waste with high lignin content (about 50 wt%) into aromatic hydrocarbons by catalytic pyrolysis using bifunctional Fe/HBeta catalyst. Meanwhile, the effects of cellulose and lignin on zeolite deactivation and the reactivities of the oxygenate compounds derived from these two lignocellulosic components over zeolite acid sites are discussed. Furthermore, the dependency of zeolite deactivation on catalyst pore size and strength of zeolite acid sites is investigated in catalytic pyrolysis of palm kernel

shell using HBeta and HZSM-5 zeolites. In part 3, the interactive effects of zeolite pore structure and density of acid sites on coke formation is studied. Cellulose which is the most abundant organic polymer in nature is used as feedstock in this part. Considering the interaction between zeolite pore structure and density of acid sites, a physically mixed catalyst system including HZSM-5 and dealuminated HY was used in order to supress coke formation and to enhance the yield of aromatic hydrocarbons.

- CHAPTER 5: The conclusions based on the results and discussion chapter are presented part by part. In addition, the recommendations and suggestions for future works are explained.

CHAPTER 2: LITERATURE REVIEW

2.1 Catalytic cracking of biomass pyrolysis-derived feedstocks

Biomass pyrolysis-derived feedstocks can be upgraded using cracking catalysts (zeolites, silica-alumina and molecular sieves) at atmospheric pressure and temperature range of 350-650 °C. Upgrading process can also be integrated with biomass pyrolysis using in situ upgrading technique. In this method which is called catalytic pyrolysis, vapors derived from biomass pyrolysis are directly deoxygenated by passing through a catalyst bed. However, it should be noticed that composition of bio-oil is different from that of biomass pyrolysis vapors due to oligomerization reactions which occur through condensation of pyrolysis vapors to bio-oil. This change in composition might cause a difference in product yields obtained from bio-oil upgrading and in situ upgrading of biomass pyrolysis vapors. Being operated at atmospheric pressure without hydrogen consumption, catalytic cracking seems to be economical method compared to HDO (Zhang, Luo, Dang, Wang, & Chen, 2012). However, some challenges like rapid catalyst deactivation caused by coke deposition, low yields of organic liquids and formation of polycyclic aromatic hydrocarbons (PAHs) have been encountered in this method (Horne & Williams, 1996). So far, several types of zeolite catalysts and mesoporous materials have been investigated to attenuate these problems. It was generally shown that a large variety of oxygenate compounds derived from biomass can be converted into hydrocarbons, CO, CO_2 and H_2O over acidic zeolite catalysts through reactions of decarbonylation, decarboxylation, dehydration, oligomerization, isomerization and dehydrogenation. An overall reaction pathway for conversion of bio-oil over zeolite catalysts is proposed in Scheme 2.1 (Adjaye & Bakhshi, 1995b).

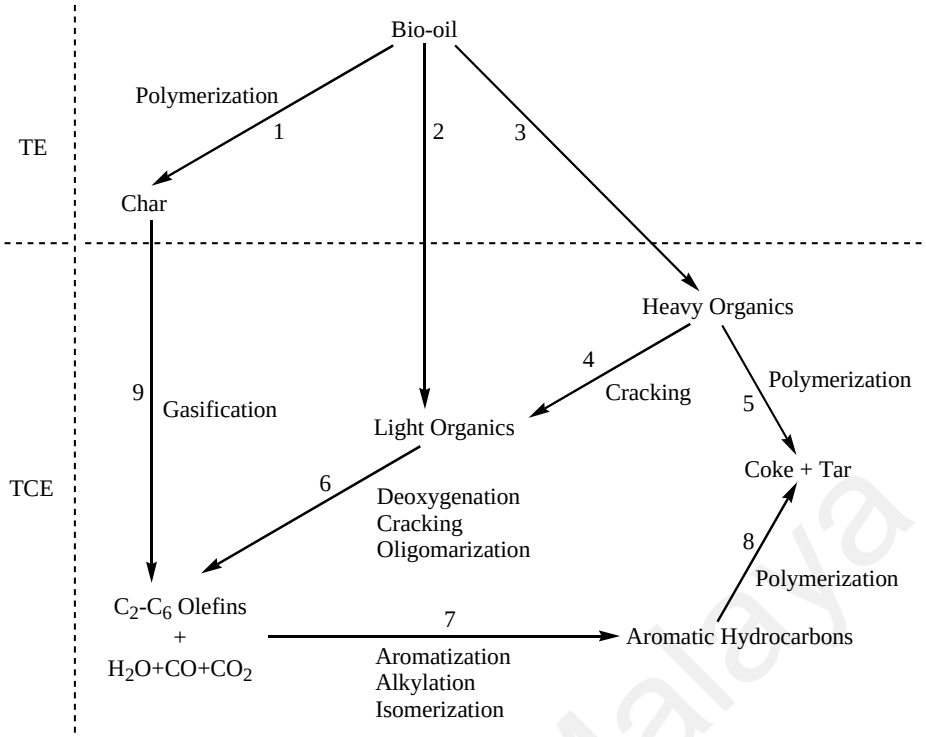

Scheme 2.1: Overall reaction pathway proposed for conversion of bio-oil over zeolite catalysts (TE: thermal effect; TCE: thermo-catalytic effect) (Adjaye & Bakhshi, 1995b).

Catalytic cracking of biomass pyrolysis-derived feedstocks is principally similar to the catalytic cracking technology which is used in oil refineries for conversion of high molecular weight hydrocarbons derived from crude oil into valuable products. The ability to utilize existing petroleum-refining infrastructure for biorefinery purposes makes bio-oil upgrading a feasible technology through significant reduction in capital investments (Huber & Corma, 2007). Co-processing of biomass derived oil with conventional crude oil fractions could also be an economical technique for bio-oil upgrading in standard refineries (Fogassy et al., 2010; Graça, Ribeiro, et al., 2009; Lappas, Bezergianni, & Vasalos, 2009). Fluid catalytic cracking (FCC) as the heart of a modern refinery has high flexibility to changing feedstock and product demands, and could be implemented for upgrading of biomass derived feedstocks. The main aim of this process is to convert the low value heavy fraction of crude oil into lighter and more valuable products such as liquefied petroleum gases (LPGs) and gasoline (Chen, 2006; Vieira, Pinto, Biscaia, Baptista, & Cerqueira, 2004). Table 2.1 illustrates the yields obtained from FCC pilot-

plant fed by vacuum gas oil (VGO), pyrolysis oil lignin fraction and mixtures of VGO and either pyrolysis oil or pyrolysis oil lignin fraction. The yields of produced gasoline and other hydrocarbons shown in this Table demonstrates the feasibility of FCC process for upgrading of pyrolysis oil. However, catalytic cracking of biomass pyrolysis-derived feedstock leads to high yield of coke formation. This problem is mainly due to low hydrogen to carbon effective ratio (H/C_{eff}) ratio of biomass derived feedstock which is the result of high oxygen content. The difference between properties of bio-oil and crude oil depicted in Table 2.2 illustrates that new catalysts and process conditions should be designed in order for commercialization of catalytic cracking of biomass pyrolysis-derived feedstocks.

Table 2.1: Yields (wt%) obtained from fluid catalytic cracking of VGO, pyrolysis oil lignin fraction and mixtures of VGO and either pyrolysis oil or pyrolysis oil lignin fraction (Marinangeli et al., 2006).

Product	**VGO**	**VGO + 20 wt% pyrolysis oil**	**VGO + 20 wt% lignin fraction**	**Lignin fraction**
Ethylene	2.0	3.3	3.6	3.8
Propane	1.2	2.1	2.4	0.7
Propylene	5.9	6.1	6.3	2.6
Butanes	11.1	13.5	14.3	2.7
Gasoline	42.7	40.6	41.3	28.8
LCO[a]	14.8	9.1	9.7	15.6
CSO[b]	18.5	4.8	4.7	6.2
Coke	3.8	7.1	9.2	16.1
Water + CO_2	0.0	13.5	8.5	23.5

[a] Light cycle oil
[b] Clarified slurry oil

Table 2.2: Comparison between bio-oil and crude oil (Mortensen et al., 2011).

Physical property	**Bio-oil**	**Crude oil**
Water (wt%)	15-30	0.1
pH	2.8-3.8	-
density (kg/l)	1.05-1.25	0.86
Viscosity, at 50 °C (cP)	40-100	180
HHV (MJ/kg)	16-19	44
Elemental composition (wt%)		
C	55-65	83-86
O	28-40	<1
H	5-7	11-14
S	<0.05	<4
N	<0.4	<1
Ash	<0.2	0.1

2.2 Aromatics selectivity

Aromatic hydrocarbons are highly desirable products since they have high octane numbers and can be used in gasoline as octane enhancers. Also, aromatics can be used for production of several value-added chemicals and polymers (Thring, Katikaneni, & Bakhshi, 2000). So far, several attempts have been done in order to increase the aromatics yield of bio-oil upgrading process. A variety of microporous zeolites and mesoporous materials have been studied for catalytic cracking of biomass pyrolysis vapors/bio-oil. Acidity caused by Brønsted and Lewis acid sites as well as shape selectivity are the two main properties of solid acid catalysts which need to be optimized in order to achieve maximum aromatics selectivity and minimum coke formation. Table 2.3 presents some previously reported yields of aromatics produced by catalytic cracking of biomass pyrolysis vapors/bio-oil over HZSM-5. Considering the vast variety of compounds present in bio-oil, it is essential to conduct catalytic cracking of different biomass derived oxygenates in order to achieve a better understanding of the reactions which are taken place in catalytic cracking of biomass pyrolysis vapors/bio-oil. The use of model compounds helps to predict the effect of each compound on final product yields and facilitates the proposition of an overall reaction pathway for conversion of biomass pyrolysis vapors/bio-oil. Yields of aromatics produced by catalytic cracking of some bio-oil model compounds are depicted in Table 2.4. This section is a review on how aromatics selectivity is influenced by catalyst properties and operating conditions in catalytic cracking of biomass pyrolysis vapors/bio-oil and bio-oil model compounds.

Table 2.3: Aromatic selectivity obtained by catalytic cracking of biomass pyrolysis vapors/bio-oil over zeolite.

entry	Catalyst (Si/Al ratio)	Feed	Reactor	T (°C)	feed/cat ratio	Aromatic yield	Aromatic distribution			Ref
							Benzene	Toluene	Xylene	
1	HZSM-5 (30)	Pine wood sawdust	Fluidized-bed	600	0.2 g feed/ g cat.h	11 C% of feed	23.1 C% of aromatics	30 C% of aromatics	13.9 C% of aromatics	(Carlson, Cheng, Jae, & Huber, 2011)
2	ZSM-5	Pine wood	Fluidized-bed	600	0.35	13.9	20.8	37.1	19.8	(Huiyan Zhang, Carlson, Xiao, & Huber, 2012)
3	ZSM-5	Pine wood	Fluidized-bed	450	0.35	5.9	10.8	32.2	38	
4	ZSM-5	Pine wood (36 wt%) + Methanol (64 wt%)	Fluidized-bed	450	0.56	21.1	5.8	16.9	62.9	
5	ZSM-5	Pine wood (41 wt%) + 1-Propanol (59 wt%)	Fluidized-bed	450	0.58	16.3	11.0	39.3	39.2	
6	ZSM-5	Pine wood (47 wt%) + 1-Butanol (53 wt%)	Fluidized-bed	450	0.64	17.2	10.6	38.7	40.2	
7	ZSM-5	Pine wood (45 wt%) + 2-Butanol (55 wt%)	Fluidized-bed	450	0.64	15.6	10.4	38.6	40.2	
8	HZSM-5 (30)	White oak bio-oil	-	600	11.7	9.8	17.3	40.8	23.5	(Vispute, Zhang, Sanna, Xiao, & Huber, 2010)
9	HZSM-5 (30)	White oak bio-oil hydrogenated over Ru/C	-	600	11.7	14.4	16.9	37.2	38.5	
10	HZSM-5 (30)	WSBO[a]	-	600	11.7	8.2	26.8	46.3	20.7	
11	HZSM-5 (30)	WSBO hydrogenated over Ru/C	-	600	11.7	21.6	17.6	45.5	31.3	
12	HZSM-5 (30)	WSBO hydrogenated over Ru/C and Pt/C	-	600	11.7	18.3	27.0	49.3	19.1	

'Table 2.3, continued'

entry	Catalyst (Si/Al ratio)	Feed	Reactor	T (°C)	feed/cat ratio	Aromatic yield	Aromatic distribution			Ref
							Benzene	Toluene	Xylene	
13	HZSM-5	Maple wood bio-oil	Packed-bed	330	1.8	45.9 wt% of OLP[b]	1.5 wt% of OLP	6.4 wt% of OLP	10.1 wt% of OLP	(Adjaye, Katikaneni, & Bakhshi, 1996)
14	HZSM-5	Maple wood bio-oil	Packed-bed	330	3.6	30.7	2.3	6.0	8.1	
15	HZSM-5	Maple wood bio-oil	Packed-bed	330	7.2	28.2	3.5	3.8	4.2	
16	HZSM-5	Maple wood bio-oil	Packed-bed	370	1.8	75.1	4.4	16.7	23.2	
17	HZSM-5	Maple wood bio-oil	Packed-bed	370	3.6	79.5	3.5	16.9	22.1	
18	HZSM-5	Maple wood bio-oil	Packed-bed	370	7.2	68.4	6.4	14.1	20.3	
19	HZSM-5	Maple wood bio-oil	Packed-bed	410	1.8	88.8	5.5	31.8	33.1	
20	HZSM-5	Maple wood bio-oil	Packed-bed	410	3.6	85.9	3.8	30.1	24.3	
21	HZSM-5	Maple wood bio-oil	Packed-bed	410	7.2	76.9	4.9	26.1	23.0	
22	HZSM-5 (59)	Maple wood bio-oil	Packed-bed	390	2.3	83.4	-	-	-	(Sharma & Bakhshi, 1993)
23	HZSM-5	Aspen poplar wood bio-oil	Packed-bed	390	3.6	38.3 wt% of feed	-	-	-	(Adjaye & Bakhshi, 1995a)
24	HZSM-5 (30)	40 wt% pine sawdust bio-oil + 60 wt% methanol	Fluidized-bed[c]	500	2.7	35	-	-	-	(Valle, Gayubo, Alonso, Aguayo, & Bilbao, 2010)

[a] WSBO: water-soluble fraction of pine wood bio-oil
[b] OLP: organic liquid product
[c] Catalytic upgrading was performed after thermal treatment

Table 2.4: Aromatic selectivity obtained by catalytic cracking of bio-oil model compounds over zeolite.

entry	Catalyst (Si/Al ratio)	Feed	Conv. (%)	Reactor	T (°C)	feed/cat ratio	Aromatic yield	Aromatic distribution			Ref
								Benzene	Toluene	Xylene	
1	HZSM-5 (56)	Lignin-acetone (1:2 wt ratio)	-	Packed-bed	500	5 g feed/g cat.h	89.4 wt% of liquid product	8.6 wt% of liquid product	33.1 wt% of liquid product	31.5 wt% of liquid product	(Thring et al., 2000)
2	HZSM-5 (56)	Lignin-acetone (1:2 wt ratio)	-	Packed-bed	600	5	87.9	13.6	42.4	22.7	
3	HZSM-5 (56)	Lignin-acetone (1:2 wt ratio)	-	Packed-bed	600	2.5	74.6	9.3	31.0	25.0	
4	HZSM-5 (30) V_{meso}:0.054 cm^3/g	Furan	35.9	Packed-bed	600	10.4	44.7 C% of products	21.0 C% of products	18.6 C% of products	8.8[a] C% of products	(Foster, Jae, Cheng, Huber, & Lobo, 2012)
5	HZSM-5 (30) V_{meso}:0.550 cm^3/g	Furan	36.3	Packed-bed	600	10.4	35.8	18.3	17.7	8.7[a]	
6	L-tartaric acid treated HZSM-5 (30) V_{meso}:0.062 cm^3/g	Furan	40.3	Packed-bed	600	10.4	40.5	20.7	18.1	8.1[a]	
7	L-tartaric acid treated HZSM-5 (30) V_{meso}:0.709 cm^3/g	Furan	29.5	Packed-bed	600	10.4	37.0	17.8	18.2	8.7[a]	
8	HZSM-5 (30)	Furan	22	Packed-bed	450	10.4	37.7	3.6	4.2	1.5	(Cheng & Huber, 2011)
9	ZSM-5	Lignin derived from rice husk bio-oil		Packed-bed	600	20	-	9.20	31.57	-	(Yan Zhao, Deng, Liao, Fu, & Guo, 2010)

'Table 2.4, continued'

entry	Catalyst (Si/Al ratio)	Feed	Conv. (%)	Reactor	T (°C)	feed/cat ratio	Aromatic yield	Aromatic distribution			Ref
								Benzene	Toluene	Xylene	
10	Ferrierite (20)	Glucose	-	Pyroprobe	600	0.05 g feed/g cat	2.5	3.1	18.4	8. 2[b]	(Jae et al., 2011)
11	ZSM-23 (160)	Glucose	-	Pyroprobe	600	0.05	12.0	10.6	25.8	19.3[b]	
12	MCM-22 (30)	Glucose	-	Pyroprobe	600	0.05	3.6	29.4	25.2	10.2[b]	
13	SSZ-20 (90)	Glucose	-	Pyroprobe	600	0.05	10.3	7.3	23.1	16.8[b]	
14	ZSM-11 (30)	Glucose	-	Pyroprobe	600	0.05	25.3	14.2	27.1	17.3[b]	
15	HZSM-5 (30)	Glucose	-	Pyroprobe	600	0.05	35.5	12.8	18.5	12.9[b]	
16	IM-5 (40)	Glucose	-	Pyroprobe	600	0.05	17.3	17.4	25.4	11.4[b]	
17	TNU-9 (40)	Glucose	-	Pyroprobe	600	0.05	2.3	31.9	40.0	11.1[b]	
18	Beta zeolite (38)	Glucose	-	Pyroprobe	600	0.05	4.3	30.9	34.7	13.4[b]	
19	SSZ-55 (54)	Glucose	-	Pyroprobe	600	0.05	2.7	13.3	27.9	9.1[b]	
20	Y zeolite (5.2)	Glucose	-	Pyroprobe	600	0.05	1.6	20.6	31.0	12.5[b]	
21	HZSM-5 (30)	Furan	-	Packed-bed	600	10.4 g feed/g cat.h	24.3 C% of feed	33.5 C% of aromatics	30.0 C% of aromatics	5.4 C% of aromatics	(Carlson et al., 2011)
22	HZSM-5 (30)	Furan	64	Packed-bed	600	5.9	42.6 C% of products	24.3	21.8	3.9	(Cheng & Huber, 2012)
23	HZSM-5 (30)	2-Methylfuran	98	Packed-bed	600	5.7	47.3	23.8	24.5	9.2	
24	HZSM-5 (30)	Furfural	100	Packed-bed	600	9.0	16.7	35.5	28.6	6.9	
25	HZSM-5 (30)	Furfuryl alcohol	100	Packed-bed	600	3.3	42.4	9.1	13.1	13.3	
26	HZSM-5 (30)	Furan	48	Packed-bed	600	10.4	31.0 wt% of feed	25.9 wt% of aromatics	23.6 wt% of aromatics	4.3 wt% of aromatics	(Cheng, Jae, Shi, Fan, & Huber, 2012)
27	HZSM-5 (25)	Kraft lignin (Sulfur content: 4.10 %)	-	Curie-point pyrolyzer	650	0.05 g feed/g cat	2	15.0	23.9	24.5	(Li et al., 2012)

‘Table 2.4, continued’

entry	Catalyst (Si/Al ratio)	Feed	Conv. (%)	Reactor	T (°C)	feed/cat ratio	Aromatic yield	Aromatic distribution			Ref
								Benzene	Toluene	Xylene	
28	HZSM-5 (25)	Kraft lignin (Sulfur content: 1.49 %)	-	Curie-point pyrolyzer	650	0.05	5.2	18.4	25.5	14.4	
29	HZSM-5	Propanoic acid	99.9	Packed-bed	410	3.6 g feed/g cat.h	8	-	-	-	(Adjaye & Bakhshi, 1995a)
30	HZSM-5	4-Methylcyclohexanol	98.2	Packed-bed	410	3.6	39.9	-	-	-	
31	HZSM-5	2-Methylcyclopentanone	94.8	Packed-bed	410	3.6	48.5	-	-	-	
32	HZSM-5	Ethoxybenzene	49.9	Packed-bed	410	3.6	3.1	-	-	-	
33	HZSM-5	Eugenol	60	Packed-bed	410	3.6	1.1	-	-	-	
34	ZSM-5 (60)	Cellulose	-	Pyroprobe	600	9.9	13.5	-	-	-	(Carlson, Tompsett, Conner, & Huber, 2009)
35	ZSM-5 (60)	Glucose	-	Pyroprobe	600	9.9	13.6	-	-	-	

[a] Including ethylbenzene and styrene in addition to xylene
[b] Including ethylbenzene in addition to xylene

2.2.1 Overview of solid acid catalysts for aromatics production

So far, several micro- and mesoporous solid acid catalysts have been examined for catalytic cracking of biomass derived feedstocks. Zeolites as the most widely used solid acids are aluminosilicate materials with three dimensional crystalline structure. The primary building units of zeolites are SiO_4 and AlO_4 tetrahedra which are linked together via a common oxygen atom forming a network of interconnected cavities and channels of molecular dimensions. The molecular size dimensions of pores and channels of zeolites make them suitable for shape selective catalysis in which the reaction selectivity depends on the size and architecture of the pores (Weitkamp, 2000). Containing both Brønsted and Lewis acid sites, zeolites are appropriate for cracking reactions. The density and strength distribution of acid sites could be controlled in order to achieve the desired reaction selectivity. Among the zeolites used for catalytic cracking of biomass pyrolysis vapors/bio-oil, HZSM-5 zeolite has been shown to be an effective catalyst for conversion of biomass derived oxygenates to aromatics. High yields of benzene, toluene and alkylated benzenes as well as naphthalenes and alkylated naphthalenes are obtained by upgrading of bio-oil over HZSM-5 (Robert & Milne, 1988; Mathews, Tepylo, Eager, & Pepper, 1985; Sharma & Bakhshi, 1991). Use of catalysts such as HZSM-5, Y zeolite and activated alumina in pyrolysis of wood biomass was shown to significantly increase aromatics production compared to non-catalytic pyrolysis (Williams & Horne, 1995b). The single ring aromatics yield decreased in the order HZSM-5 > Y zeolite > activated alumina. Also, the yield of naphthalene and alkylated homologues decreased in the order Y zeolite > HZSM-5 > activated alumina. Mihalcik et al. (2011) used five zeolites (HZSM-5, H-Y, H-Beta, H-Mordenite and H-Ferrierite) for catalytic fast pyrolysis of different biomass feedstocks. They found that the activity of zeolites on basis of aromatics production was as the following order: HZSM-5 > H-Beta > H-Mordenite > H-Ferrierite ~ H-Y. It was shown that by decrease of Si/Al ratio (increase of acidity), HZSM-5 and

H-Beta produced more aromatics. HZSM-5 is also potential for production of high yields of aromatic hydrocarbons from other waste materials such as plastic derived oil and vegetable oils (Hilten, Speir, Kastner, & Das, 2011; Katikaneni, Adjaye, & Bakhshi, 1995; Lee, 2012; Lee & Oh, 2012).

As depicted in Table 2.5, presence of catalyst is necessary for deoxygenation and aromatics production. Non-catalytic pyrolysis leads to an oxygenated organic fraction with low aromatics content. Table 2.5 illustrates that in catalytic cracking, oxygen is removed through decarboxylation, decarbonylation and dehydration resulting in higher yields of gas and aqueous fractions and lower yield of organic fraction compared to thermal cracking. Use of suitable catalyst also increases the aromatics content of the produced oil. However, high selectivity of catalyst towards aromatics is not the only considerable factor for selection of a proper catalyst. The potential of catalyst for production of high yield of organic fraction is also a significant factor in designing an economically feasible process for aromatics production. For instance, as shown in Table 2.5, in an in-situ catalytic upgrading of beech wood fast pyrolysis vapors performed in a packed-bed reactor, the activity of catalysts on basis of aromatics selectivity was as the following order: alumina > zirconia/titania > ZSM-5 (Stefanidis, Kalogiannis, Iliopoulou, Lappas, & Pilavachi, 2011). However, alumina and zirconia/titania are not efficient catalysts since they led to low yields of organic fraction (5.46 and 13.98 wt%, respectively). ZSM-5 seems to be the most suitable catalyst with a good selectivity towards aromatic compounds and acceptable yield of organic fraction (20.82 wt%).

Table 2.5: Comparison between catalytic and non-catalytic pyrolysis of lignocellulosic biomass.

Feedstock	Catalyst	Water	Oil	Aromatics	Gas	CO	CO_2	Solids	Oxygen	Ref
Corncob	Non-catalytic	22.9 wt% of feed	33.9 wt% of feed	7.62 wt.% of oil	14 wt% of feed	4.3 wt% of feed	8.6 wt% of feed	25.2 wt% of feed	40.28 wt% of oil	(Zhang et al., 2009)
	HZSM-5	25.6	13.7	74.22	26	10.4	11.5	28.5	14.69	
Wood waste shavings	Non-catalytic	27.0	11.80	5010 mg kg^{-1} oil	25.3	14.5	8.2	17.8	46.4	(Williams & Horne, 1995b)
	HZSM-5	19.3	6.01	362421	37.8	16.7	13.4	29	5.5	
	Na/ZSM-5	18.0	5.47	390671	36.9	15.9	12.3	29.3	4.6	
	Y-zeolite	23.9	1.13	450079	29.6	13.3	9.1	36.6	8.4	
	Alumina	23.0	3.12	228368	28.2	12.7	9.7	35.5	9.2	
Lignocellulosic biomass originated from beech wood	Non-catalytic	21.38	37.37	0.1 GC-MS peak area %	18.35	6.54	10.02	22.89	41.68	(Stefanidis et al., 2011)
	Alumina (S_{BET}:215 m^2/g)	32.47	5.46	10.8	28.23	11.12	12.93	33.85	-	
	Zirconia/titania (S_{BET}:85 m^2/g)	28.25	13.98	7.3	29.61	10.10	15.33	28.17	29.02	
	ZSM-5[a] (S_{BET}:138 m^2/g)	27.70	20.82	5.7	25.86	11.43	11.10	25.70	30.98	
Lignin	Non-catalytic	7.9	15.7	-	18.2	4.2 C% of gas	6.0 C% of gas	48.7	-	(Huang et al., 2012)
	La/HZSM-5	14.4	7.7	-	34.2	8.3	7.0	39.9	-	

[a] Commercial equilibrium ZSM-5 catalyst diluted with silica-alumina (contains 30 wt% crystalline zeolite)

Among the three major lignocellulosic components (cellulose, hemicellulose and lignin), lignin is the most difficult one to be decomposed which results in highest solid residues production (Ben & Ragauskas, 2011; Li et al., 2012; Mullen & Boateng, 2010). Meanwhile, pyrolytic lignin has high theoretical potential to be converted to aromatics (Zhao et al., 2010). Therefore, lignin is an attractive compound to be studied as biomass model compound. In catalytic cracking of pyrolytic lignin separated from rice husk derived bio-oil, the activity of catalysts on basis of production of more liquid fraction and less coke was determined as the following order: ZSM-5 > HZSM-5 > MCM-41 ~ SBA-15 > Beta (Zhao et al., 2010). In addition, aromatics yield decreased in the order ZSM-5 > HZSM-5 ~ Beta > MCM-41 > SBA-15, showing that microporous zeolites produced more aromatics. The selectivity for aromatics and poly aromatic hydrocarbons was more than 85% in the presence of ZSM-5. It was also shown that phenols were considerably deoxygenated and converted to aromatics over this catalyst. Toluene, naphthalene and benzene were the most abundant aromatics produced by ZSM-5. In non-catalytic pyrolysis, the selectivity towards phenol, 4-ethylphenol, 4-methylbenzaldehyde, benzene, toluene and naphthalene were 12, 17, 13, 0, 3, 0% which, by addition of ZSM-5 as catalyst, were changed to 7, 2, 0, 9, 32, 13%, respectively. This great change in selectivity caused by using ZSM-5 shows unambiguously the significant contribution of catalyst in the reaction. In another study for pyrolytic conversion of lignin at 600 °C over sand and five different catalysts (HZSM-5, KZSM-5, Al-MCM-41, solid phosphoric acid and a hydrotreating catalyst ($Co/Mo/Al_2O_3$)), HZSM-5 was found to be the most effective catalyst (Jackson et al., 2009). Although use of catalysts did not result in remarkable change in yields of produced gas, liquid and char fractions compared to non-catalytic pyrolysis using sand, aromatics selectivity was a strong function of catalyst type. HZSM-5 had maximum rate of deoxygenation and resulted in less oxygenated aromatics (phenolics, diols and dihydrobenzofuran), but high amount of naphthalenics which are

carcinogenic was obtained using this catalyst. Solid phosphoric acid was not effective for deoxygenation of lignin and produced a liquid fraction containing 98% phenolics. Al-MCM-41 was less effective than HZSM-5 for deoxygenation and led to significant production of naphthalenics. KZSM-5 and $Co/Mo/Al_2O_3$ were also not efficient for deoxygenation of lignin, but resulted in low amounts of naphthalenics. Kraft lignin can also be pyrolyzed to produce aromatics. However, its sulfur content has negative impact on catalytic pyrolysis and reduces aromatics yield (Li et al., 2012; Zhao et al., 2010). Li et al. (2012) pyrolyzed Kraft lignin with and without HZSM-5. In the absence of zeolite, fast pyrolysis of lignin mainly led to phenolic and guaiacol compounds. However, use of HZSM-5 totally changed product distribution and considerable yield of aromatics was obtained (see Table 2.4, entries 27 and 28). Product distribution was also shown to be a great function of the acidity of HZSM-5; the decrease of Si/Al ratio of zeolite (increase of acidity) reduced the yields of phenols and other oxygenate compounds and increased aromatics yield.

Scheme 2.2 presents a proposed reaction pathway for catalytic fast pyrolysis of cellulose over solid acid catalyst. In the first step, cellulose is pyrolyzed and converted into volatile organics, gases and coke. The volatile organics are dehydrated in heterogeneous catalyst or in homogeneous gas phase. Then the dehydrated species (furans) diffuse into zeolite and are converted into aromatics, CO, CO_2 and H_2O through a series of reactions such as dehydration, decarbonylation, decarboxylation, isomerization, oligomerization and dehydrogenation. In conversion of furans into aromatics, olefins act as intermediate compounds (Cheng, Jae, et al., 2012). In fact, furans are converted to allene through decarbonylation. Then, the allene undergoes oligomerization and forms a series of olefins which react with furans to form aromatics. As shown in Scheme 2.2, coke can be produced from biomass feedstock, volatile oxygenates, dehydrated species or aromatic

compounds. Coke is formed through both thermal decomposition of homogeneous gas phase and heterogeneous reactions occurred over catalyst.

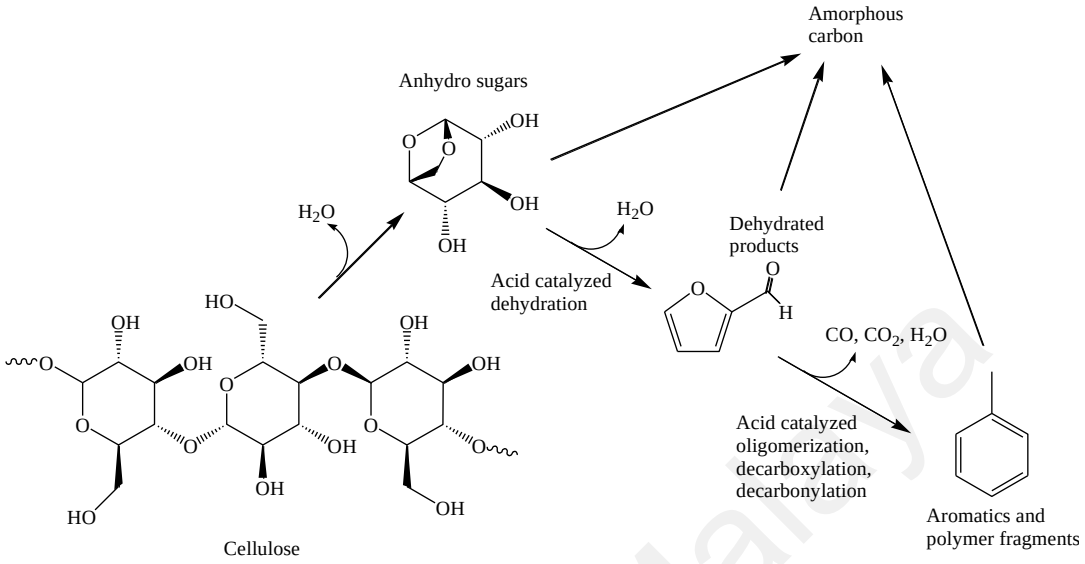

Scheme 2.2: Reaction pathway for catalytic fast pyrolysis of cellulose over solid acid catalyst (Carlson et al., 2009).

2.2.2 Dependency of aromatics selectivity on catalyst properties

Both catalyst porosity and acidity are essential for conversion of biomass derived oxygenates to aromatics. In catalytic fast pyrolysis of lignin performed in a platinum coil pyrolyzer at 650 °C, aromatic yields of silicalite and HZSM-5 were compared (Ma et al., 2012). As shown in Scheme 2.3, coke is the major product in non-catalytic fast pyrolysis. In the case of using porous catalyst without acid sites like silicalite, intermediates are adsorbed and stabilized. Therefore, they are not repolymerized to coke and higher yield of liquid is achieved. However, composition of liquid fraction is not considerably affected by silicalite. Use of HZSM-5 instead of silicalite increases aromatic yield and decreases the yields of phenol alkoxy and aromatic alkoxy compounds. Alkoxy aromatics and alkoxy phenols are dealkoxylated and converted to aromatics and phenols, respectively. Phenols are also deoxygenated into aromatics, but this step requires high content of HZSM-5. The transformations occurred over HZSM-5 are acid catalyzed reactions and cannot be performed by silicalite. Therefore, apart from porosity, catalyst needs to contain

acid sites in order to produce high yield of aromatics. In fact, introduction of acid sites into catalyst leads to the cleavage of C-O and C-C bonds and catalytic transformation of intermediates through reactions like dehydration, decarboxylation, aromatization, isomerization, cracking, dealkylation and oligomerization. Considering the fact that acid sites are responsible for formation of both aromatics and coke, catalyst acidity should be optimized in a way to achieve high yield of aromatization while the possibility for further polymerization of aromatics and coke formation is reduced. Both density and strength of acid sites should be taken into account in order to optimize catalyst acidity. For instance, in catalytic fast pyrolysis of lignocellulosic biomass (beech wood), silicalite with Si/Al ratio of >1000 which contains very few number of acid sites showed to have higher selectivity towards aromatics compared to mesoporous aluminosilicate Al-MCM-4 (Si/Al ratio of 30) with significantly higher number of acid sites (Stephanidis et al., 2011). The reason for this is that silicalite contained strong Brønsted acid sites while the acid sites of Al-MCM-4 were weak. Therefore, it is clearly concluded that number of acid sites present in a proper porous structure as well as their strength distribution should be simultaneously modified for enhanced aromatization. The need for both catalyst acidity (Brønsted acid sites) and pore structure was also shown to be essential in catalytic conversion of glucose into aromatics (Carlson et al., 2008). ZSM-5 had the aromatic selectivity of 31%, but both silicalite and silica-alumina produced mainly coke with aromatic yields of only 6.5 and 0.6%, respectively. The reason for low aromatic yield of silicalite and silica-alumina is that these zeolites do not have both Brønsted acid sites and pore structure. Although pore structure of silicalite is the same as that of ZSM-5, but this zeolite does not contain Brønsted acid sites. Silica-alumina contains Brønsted acid sites but has amorphous structure with no shape-selectivity effects. Similarly, the dependency of aromatization on both catalyst acidity and shape selectivity was shown in conversion of maple wood derived bio-oil over mixtures of silica-alumina and HZSM-5 (Adjaye et al., 1996). Silica-

alumina produced an organic liquid fraction mainly composed of aliphatic hydrocarbons. When a small amount of HZSM-5 (below 10 wt%) was mixed with silica-alumina, catalytic cracking activity was enhanced, and more olefins and paraffins were formed as end products. This increase of cracking activity is due to the increase of acid strength caused by HZSM-5 addition. By increase of the fraction of HZSM-5 (above 10 wt%), reaction pathway was affected by shape-selectivity effects of this catalyst; the produced olefins became as intermediate compounds and were converted to aromatics through aromatization.

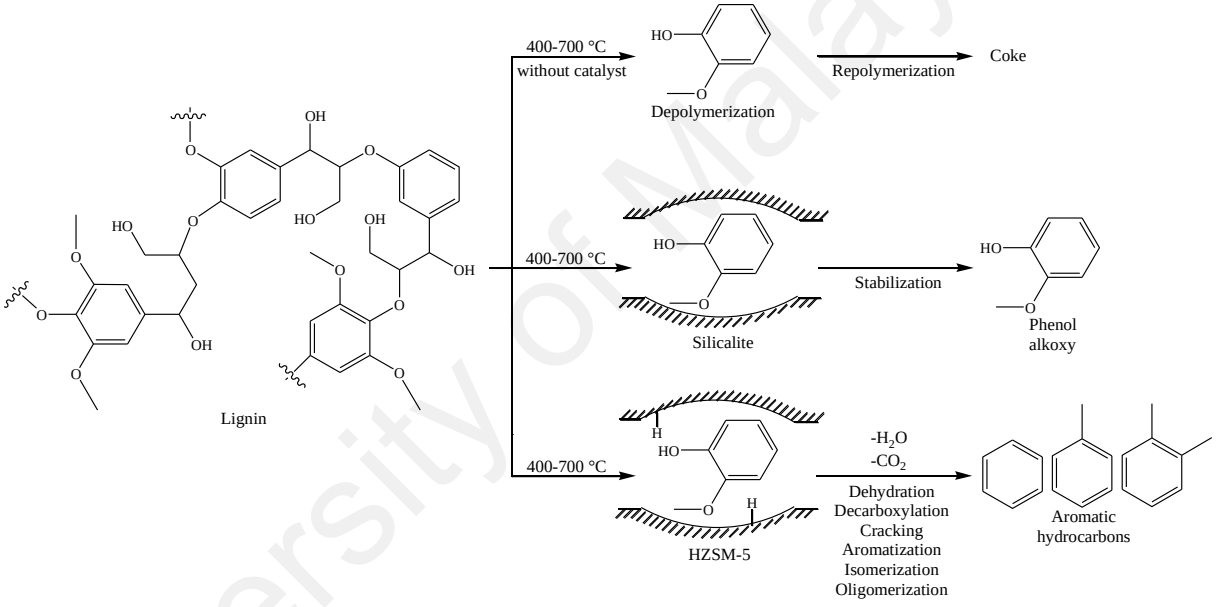

Scheme 2.3: Reaction mechanism for non-catalytic/catalytic fast pyrolysis of lignin (Ma et al., 2012).

Catalyst pore-opening size is a crucial factor in selection of a proper catalyst for enhanced aromatics production. Pore-opening size affects mass transfer and can restrict the diffusion of large molecules into catalyst. In catalytic fast pyrolysis of lignin, it was shown that the catalysts with larger pore size produced more liquid and less coke (Ma et al., 2012). It was explained that larger pore size allows larger molecules to penetrate into catalyst and react. This was in agreement with the results obtained from thermogravimetric analysis (TGA) of HZSM-5 and H-USY showing that H-USY (7.4 Å) which has larger pore size produced less thermal coke compared to HZSM-5 (5.5 Å).

However, in catalytic cracking of some other bio-oil model compounds, it was concluded that smaller pore size leads to less coke and higher aromatics yield. For instance, in catalytic cracking of glycerol conducted in a microactivity test (MAT) reactor at temperature range of 500-700 °C, six catalysts (fresh commercial FCC catalyst containing Y zeolite in a silica–alumina matrix (FCC), commercial equilibrium FCC catalyst with V and Ni impurities (ECat), ZSM-5 FCC additive, Al_2O_3, Y zeolite and low-surface area inert silicon carbide (SiC)) were tested, and the aromatic yield was shown to decrease in the order ZSM-5 >> Al_2O_3 > FCC > ECat > Y >> SiC (Corma, Huber, Sauvanaud, & Oconnor, 2007). Meanwhile, ZSM-5 led to the lowest coke yield, while maximum coke production was obtained using Y zeolite. The less coke and more aromatics obtained by ZSM-5 was attributed to smaller pore size of this catalyst preventing from formation of polyaromatic compounds which act as coke precursors. In catalytic pyrolysis of γ-valerolactone, it was revealed that aromatics yield was increased with decrease of catalyst pore diameter (Zhao, Fu, & Guo, 2012). The average pore diameters of MCM-41, Beta zeolite and ZSM-5 were 3.8, 0.7 and 0.5 nm, and carbon yields of produced aromatic hydrocarbons were 1.74, 7.50 and 28.48%, respectively. Different effects of catalyst pore size observed in these experiments could be due to the difference in the molecular size of intermediate compounds formed from pyrolysis of different feedstocks. In a catalytic fast pyrolysis conducted in semi-batch pyroprobe reactor, microporous and mesoporous HZSM-5 were tested for catalytic conversion of glucose and maple wood (Foster et al., 2012). In the case of using maple wood, mesoporous HZSM-5 resulted in much lower polyaromatics selectivity compared to microporous HZSM-5. However, when glucose was used as feedstock, the polyaromatics selectivities obtained from both zeolites were approximately the same. This difference is due to the size of initial intermediate compounds formed from these two feedstocks. The intermediates produced from maple wood are larger and cannot easily diffuse into microporous HZSM-5. Therefore, they are

converted to thermal coke by non-catalytic transformation outside catalyst. But, the intermediates formed from glucose are small enough to enter the pores of microporous zeolite and reach Brønsted acid sites.

Shape selectivity effect of catalyst is not limited to its pore size, and shape of catalyst pores could also affect reaction selectivity and product yield. In fact, the confined space inside pores influences reaction pathway by restricting the formation of certain transition states. Various zeolites with pores of different size and shape were used in a study for production of aromatics from glucose in a pyroprobe-GC-MS system under following conditions: weight ratio of catalyst to feed 19, temperature 600 °C and reaction time 240 s (see Table 2.4, entries 10-20) (Jae et al., 2011). Maximum aromatic yield was observed in the pore size range of 5.3-5.5 Å. Aromatic compounds were formed largely in the medium pore zeolites such as MCM-22, ZSM-23, SSZ-20, ZSM-11, ZSM-5, IM-5 and TNU-9. The use of small pore zeolites like ZK-5 and SAPO-34 mainly resulted in oxygenated species as well as char, CO and CO_2. Also, the main product by the use of large pore zeolites like Beta zeolite, SSZ-55 and Y zeolite was coke. The highest aromatic selectivity of 35% was obtained using ZSM-5, a zeolite with an intersecting 10-membered ring pore system containing straight (5.3×5.6 Å) and sinusoidal (5.1×5.5 Å) channels. ZSM-11 composed of two intersecting straight channels (5.3×5.4 Å) led to aromatic yield of 25%. Although, MCM-22, TNU-9, and IM-5 are similar to ZSM-5 and ZSM-11 in pore size, pore dimensionality and silica to alumina ratio, they showed considerably low aromatic selectivity. The reason for this is that these zeolites have high mesopore volumes formed by inter-crystalline spaces in comparison with ZSM-5 and ZSM-11. The high mesopore volume was recognized suitable for coke production which is the main competing reaction with aromatic formation. Therefore, it can be concluded that product selectivity in this reaction is dependent on both the transition state effects within catalyst like the steric hindrance of reacting molecules inside zeolite pores and mass transfer

which is a function of pore-opening size. The main aromatics produced from all zeolites were naphthalenes, toluene, xylenes, and benzene. Aromatic distribution was also shown to be dependent on both internal pore architecture of catalyst and pore size. For instance, naphthalene selectivity was increased with the increase of pore size of one-dimensional zeolites such as ZSM-23, SSZ-20, and SSZ-55 (24.9%, 38.3% and 47.2%) while 2 and 3 dimensional zeolites showed the opposite trend. Furthermore, although large pores can facilitate the formation of larger aromatic compounds, zeolites with large pore size like Beta and Y zeolite produced relatively low naphthalene and high benzene, toluene, xylene selectivity compared to medium pore zeolites. In addition, aromatic distribution of medium pore TNU-9 and large pore zeolites was the same. This study clearly shows that shape selectivity is a result of both mass transfer effects (pore-opening size) and transition state effects (internal void space). Shape selectivity imposed by pore-opening size can also affect product selectivity by allowing only small molecules to diffuse out of catalyst pores. In catalytic fast pyrolysis of furan and 2-methylfuran over HZSM-5, it was found that reduction of catalyst pore-opening size increased selectivity towards *p*-xylene over its isomers since *o*- and *m*-xylenes were not small enough to diffuse out of the catalyst with reduced pore openings and were isomerized to *p*-xylene (Cheng, Wang, Gilbert, Fan, & Huber, 2012).

Crystallite size of catalyst is another property of catalyst which affects product yield. Hoang et al. (2010) investigated the effect of HZSM-5 (Si/Al ratio of 45) crystallite size on alkyl-aromatics yield and catalyst stability. Propanal was used as model compound for bio-oil. Reactions were performed at 400 °C and atmospheric pressure in a packed-bed reactor. Two zeolites with different crystallite size were tested: a small crystallite HZSM-5 with the average crystallite size of 0.2-0.5 μm and a large crystallite HZSM-5 with an average crystallite size of 2-5 μm. It was shown that for an identical space time, small crystallite zeolite resulted in higher propanal conversion compared to large crystallite

HZSM-5. In addition, the propanal conversion obtained at different values of time on stream revealed that the zeolite with small crystallite size had more stability than large crystallite zeolite. It was also observed that at similar levels of propanal conversion, both zeolites resulted in the same yield of alkyl aromatics. However, the distribution of alkyl aromatics was greatly affected by zeolite crystallite size. The ratio of *p*-xylene to the sum of *o*- and *m*-xylenes [p/(o+m)] of large crystallite zeolite was significantly higher compared to that of small one. The reason for this is that *p*-xylene has higher diffusion coefficient and can diffuse out of large crystallite zeolite in a shorter time than *ortho*- and *meta*- isomers. *O*- and *m*-xylenes stay longer inside large crystallite zeolite and their chance of being isomerized to *p*-xylene is increased. But, in small crystallite zeolite that diffusion path length is short, all the products can diffuse out of catalyst rapidly resulting in a low p/(m+o) ratio. Also, the ratio of $C_9/(C_8+C_7)$ aromatics obtained by small crystallite zeolite was much higher than that observed for the zeolite with large crystallite size. In fact, C_9 aromatics have a low chance of being cracked to smaller secondary aromatics in small crystallite zeolite due to short diffusion path length.

The pathway for aromatics formation is strongly dependent on catalyst type. This was clearly shown by comparison of HZSM-5 and a mixed metal oxide catalyst (CoO/MoO_3) used for pyrolysis of lignin in a pyroprobe reactor at 650 °C (Mullen & Boateng, 2010). Four lignin samples obtained from different sources were used in this study. Three of them were pure lignins and the forth one was a mixture of cellulose and lignin (~1:1). Based on the amounts of phenols, guaiacols and syringol obtained from non-catalytic conversion of the four lignins, the relative H-lignin (*p*-hydroxyphenyl subunits), G-lignin (guaiacyl subunits) and S-lignin (syringyl subunits) compositions of the samples were determined. Both HZSM-5 and CoO/MoO_3 catalysts led to aromatics production with the highest selectivity towards toluene. However, the pathways for aromatics formation over these catalysts were shown to be different. HZSM-5 resulted in approximately the same

yield of aromatics using both pure lignin samples and the sample containing lignin and cellulose. This illustrates that the aromatic structure of lignin do not affect aromatic yield and cellulose has also high potential to be converted to aromatics over HZSM-5. Therefore, the pathway shown in Scheme 2.4 can be proposed for the final step in conversion of cellulose over HZSM-5. Light organics derived from pyrolysis of cellulose like acids, alcohols, esters and ketones are firstly cracked to olefins and then these intermediate olefins undergo aromatization to produce aromatics. The aromatization of olefinic compounds is named Diels-Alder reaction which has been studied by several researchers (Chang & Silvestri, 1977; Cypres, 1987; Depeyre, Flicoteaux, & Chardaire, 1985; Williams & Taylor, 1993). Unlike HZSM-5, CoO/MoO_3 produced lower aromatics from the sample containing cellulose compared to pure lignins. This implies that aromatic structure of lignin is effective for aromatics production over CoO/MoO_3. Therefore, as presented in Scheme 2.5, the pathway for formation of aromatics over CoO/MoO_3 seems to be more likely a direct deoxygenation reaction. It was also shown that CoO/MoO_3 catalyst produced less aromatics from the lignin sample with the most S-lignin suggesting that S-lignin is less potential than G- and H-lignin to produce aromatics over this catalyst. This can be attributed to the pathway presented in Scheme 2.5 since this type of lignin needs more deoxygenation than G- or H-lignin.

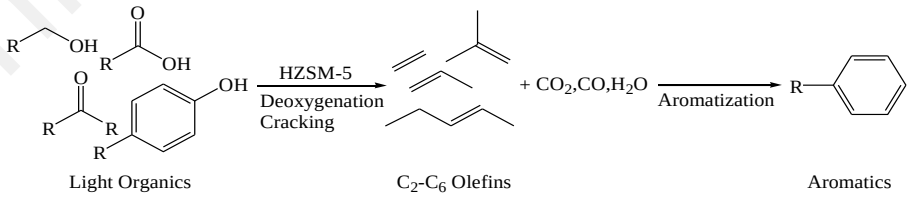

Scheme 2.4: Reaction mechanism for production of aromatics from cellulose-derived light organics over HZSM-5 (Mullen & Boateng, 2010).

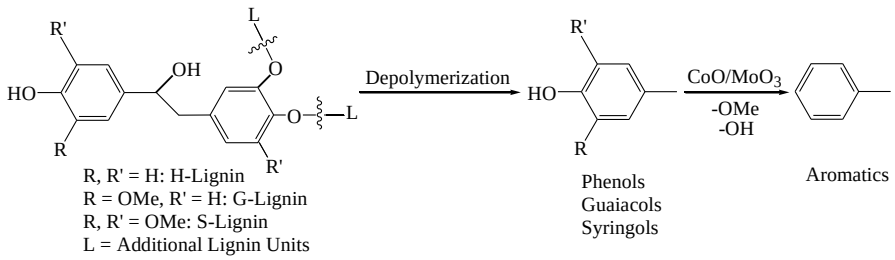

Scheme 2.5: Reaction mechanism for production of aromatics from lignin over CoO/MoO_3 (Mullen & Boateng, 2010).

2.2.3 Metal-modified zeolites

Zeolite could be modified by incorporation of metals as promoter. Use of bifunctional catalysts in which the incorporated metal promotes aromatization is an effective method for enhanced selectivity towards aromatic compounds. Table 2.6 shows some yields of aromatics produced by metal-modified zeolites. This section is a review on performance of metal-modified zeolites in catalytic cracking of biomass pyrolysis vapors/bio-oil and bio-oil model compounds.

Table 2.6: Aromatic selectivity obtained by catalytic cracking of biomass pyrolysis vapors/bio-oil and bio-oil model compounds over metal-modified zeolite.

entry	Catalyst (Si/Al ratio)	Feed	Conv. (%)	Reactor	T (°C)	feed/cat ratio	Aromatic yield	Aromatic distribution			Ref
								Benzene	Toluene	Xylene	
1	Co/HZSM-5 (50)[a] Co content: 5.0 wt%	Pine wood	-	Pyroprobe	650	0.11 g feed/g cat	39.8 C% of feed	8.0 C% of feed	11.1 C% of feed	9.6 C% of feed	(Thangalazhy-Gopakumar, Adhikari, & Gupta, 2012)
2	Ni/HZSM-5 (50) [a] Ni content: 5.0 wt%	Pine wood	-	Pyroprobe	650	0.11	41.3	7.4	10.6	10.0	
3	Mo/HZSM-5 (50) [a] Mo content: 5.0 wt%	Pine wood	-	Pyroprobe	650	0.11	42.5	6.4	11.5	11.0	
4	Pt/HZSM-5 (50) [a] Pt content: 0.5 wt%	Pine wood	-	Pyroprobe	650	0.11	46.4	6.7	12.0	11.9	
5	Ga/Meso-MFI (17.5) Ga content: 1.0 wt%	Radiata pine sawdust	-	Packed-bed	500	10	-	2.3 wt% of OLP[b]	7.8 wt% of OLP	11.8 wt% of OLP	(Park et al., 2010)
6	Ga/Meso-MFI (17.5) Ga content: 5.0 wt%	Radiata pine sawdust	-	Packed-bed	500	10	-	0.4	2.1	5.1	
7	La/HZSM-5 (23) La content: 6.0 wt%	Lignin	-	Packed-bed	600	0.33	-	0.58 wt% of feed	1.65 wt% of feed	1.29 wt% of feed	(Huang et al., 2012)
8	Ga/HZSM-5[c] (30)	Furan	47	Packed-bed	600	10.4 g feed/g cat.h	43.5 wt% of feed	33.7 wt% of aromatics	15.1 wt% of aromatics	1.5 wt% of aromatics	(Cheng, Jae, et al., 2012)
9	Ga/HZSM-5[d] (30)	Furan	50	Packed-bed	600	10.4	39.7	35.6	17.5	1.9	
10	Ni/HZSM-5 (30) Ni content: 1.0 wt%	40 wt% pine sawdust bio-oil + 60 wt% methanol	81	Fluidized-bed[e]	500	2.7	42	-	-	-	(Valle, Gayubo, Alonso, et al., 2010)

[a] At 400 psi hydrogen pressure
[b] OLP: organic liquid product
[c] Synthesized by ion exchange method
[d] Synthesized by incipient-wetness method
[e] Catalytic upgrading was performed after thermal treatment

Incorporation of 1-10 wt% transition metals like nickel and cobalt into ZSM-5 catalyst increased the production of aromatics from lignocellulosic biomass (Iliopoulou et al., 2012). The increase of aromatics yield was attributed to the effect of these transition metals in promoting dehydrogenation reactions. Valle et al. (2010) showed that aromatics yield was increased from 35 to 42 wt% by addition of 1.0 wt% Ni into HZSM-5 (see Table 2.3, entry 24 and Table 2.6, entry 10). Impregnation of Ga on mesoporous MFI increased its aromatics yield from radiata pine derived pyrolytic vapors due to enhancement of dehydrogenation (Park et al., 2010). Addition of Pt into HZSM-5 and mesoporous MFI was shown to increase aromatics production from miscanthus derived pyrolytic vapors due to participation of Pt in cracking, hydrogenolysis, hydrocracking and dehydrogenation reactions (Park et al., 2012). In catalytic pyrolysis of particle board, it was shown that impregnation of HZSM-5 by 1.0 wt% Ga through incipient-wetness method increased aromatics production due to involvement of Ga in dehydrocyclization of reaction intermediates (Choi et al., 2013).

Cruz-Cabeza et al. (2012) studied catalytic activity of metal-exchanged Beta zeolites for conversion of acetone. Beta zeolite was impregnated by several metals (Cr, Mn, Fe, Co, Ni, Cu, Zn, Al and Pb). Incorporation of all metals reduced surface area as well as both micropore and mesopore volumes of this zeolite. It was also reported that ion exchange decreased Brønsted acidity and generated new Lewis acid sites. The effect of these metals on acetone conversion was reported as the following order: Al > Mn ~ Cr ~ Zn > Cu > Pb ~ Ni ~ Co ~ Fe. It was revealed that acetone conversion and reaction selectivity was not solely dependent on density of Brønsted acid sites, and Lewis acid sites also affected the reaction. Among the metal-exchanged Beta zeolites, Al-Beta and Cu-Beta led to maximum and minimum aromatics selectivity, respectively. Mn-Beta was the only zeolite which did not produce naphthalene derivatives, and H-, Al-, Cr- and Zn-Beta resulted in

more production of naphthalene derivatives in comparison with other metal-exchanged Beta zeolites.

The method of metal incorporation have great effect on catalytic activity and selectivity. In catalytic upgrading of furan with bifunctional Ga/ZSM-5 performed in a packed-bed reactor at temperature of 600 °C and WHSV of 10.4 h^{-1}, it was found that Ga-promoted catalysts prepared by ion-exchange and incipient-wetness methods resulted in higher catalytic activity and aromatics selectivity compared to HZSM-5, while direct incorporation of Ga into ZSM-5 framework reduced its catalytic activity and aromatics selectivity (see Table 2.4, entry 26 and Table 2.6, entries 8 and 9) (Cheng, Jae, et al., 2012). Ga-framework catalyst also led to high coke yield indicating that framework Ga is not suitable for aromatics production. Ga-promoted ZSM-5 synthesized by all methods resulted in higher benzene production and lower yields of toluene and xylenes in comparison with unpromoted HZSM-5. Ga/HZSM-5 prepared by ion-exchange method was shown to have maximum aromatics selectivity. Using this method of incorporation, aromatics selectivity of catalyst was enhanced from 31 to 44% while coke selectivity was decreased from 34 to 24%. Moreover, olefin yield was decreased and selectivity towards CO and allene was increased. These results indicate higher rates of decarbonylation (higher formation of CO and allene) and olefin aromatization (more conversion of olefins into aromatics) caused by Ga incorporation through ion exchange method.

In deoxygenation of benzaldehyde over Ga/HZSM-5, it was revealed that hydrogenation/hydrogenolysis required for conversion of benzaldehyde to toluene only occurs in the presence of Ga, and Brønsted acid sites only support decarbonylation through which benzene is produced (Ausavasukhi, Sooknoi, & Resasco, 2009). In the case of using helium as carrier gas in a continuous flow reactor, no toluene was produced from HZSM-5 and Ga/HZSM-5, and benzaldehyde was converted to benzene through decarbonylation. When carrier gas was changed to hydrogen with the flow rate of 30

ml/min under atmospheric pressure, only Ga/HZSM-5 could produce toluene in addition to benzene. By addition of Ga into HZSM-5, the carbonyl group of benzaldehyde is hydrogenated to benzyl alcohol which is converted to toluene and water through hydrogenolysis. Increase in the Ga loading of HZSM-5 leads to increase in hydrogenation/hydrogenolysis activity and causes increase in toluene selectivity and in turn decrease in benzene production.

Although addition of special metals into zeolite can enhance reaction selectivity towards aromatics, it might also cause some negative effects. One major challenge in metal incorporation could be reduction in amount of catalyst acid sites. For instance, in catalytic pyrolysis of radiata pine sawdust, performance of HZSM-5 (Si/Al ratio of 26) was compared with that of 1.0 wt% Ga/HZSM-5 (Park et al., 2007). The selectivity of HZSM-5 towards aromatics production was shown to be increased by incorporation of Ga. However, Ga/HZSM-5 resulted in a lower degree of deoxygenation compared to HZSM-5. This was explained as being the result of decrease in amount of strong acid sites of HZSM-5 *via* Ga impregnation. Moreover, selectivity towards benzene derivatives like toluene and xylenes was increased by Ga impregnation. The positive impact of Ga on benzene alkylation was mentioned as the reason for increase of benzene derivatives selectivity.

The effect of incorporation of metal into catalyst can be a function of operational conditions. For example, in catalytic pyrolysis of pine wood performed in a pyroprobe reactor under hydrogen pressure, it was shown that hydrogenation effect of Mo as promoter was enhanced by increase of pressure (Thangalazhy-Gopakumar et al., 2012). Using HZSM-5 as catalyst, change of pressure in the range of 100-400 psi did not significantly affect aromatics yield (36-40 C%). But when molybdenum-impregnated HZSM-5 (5.0 wt%) was used, the increase of pressure increased aromatics yield. Below 300 psi, Mo/ZSM-5 produced less aromatics compared to HZSM-5 probably due to

reduction in number of catalyst acid sites which were occupied by Mo. But at 400 psi, Mo/ZSM-5 led to higher aromatics yield than HZSM-5. At this pressure, the promotion of hydrogenation reactions caused by Mo was more effective than the reduction of zeolite acid sites and led to higher aromatics yield.

2.2.4 Dependency of aromatics selectivity on reaction conditions

Aromatics yield obtained from catalytic cracking of biomass pyrolysis vapors/bio-oil could be enhanced by reduction in selectivity towards coke formation. One way to reduce coke formation is to increase carbon effective ratio (H/C_{eff}) of feedstock through co-feeding of hydrogen or hydrogen containing compounds. Zhang et al. (2012) increased H/C_{eff} ratio of feedstock by addition of alcohol and studied the effect of this ratio on the yield of petrochemicals produced by catalytic fast pyrolysis process. Pine wood sawdust with H/C_{eff} ratio of 0.11 was used as biomass. The H/C_{eff} ratio was increased by addition of different alcohols like methanol, 1-propanol, 1-butanol and 2-butanol. The experiments were performed in a fluidized-bed reactor and ZSM-5 was implemented as catalyst. The addition of each of these alcohols at H/C_{eff} ratio of 1.25 increased the yield of aromatic compounds (see Table 2.3, entries 2-7). The carbon yield of aromatics produced from pine wood at 450 °C was 5.9% which was increased to 21.1% by addition of methanol at H/C_{eff} ratio of 1.25. The aromatic distribution achieved by addition of methanol was significantly different from that obtained by addition of other alcohols. The selectivities of xylene, benzene and toluene produced from catalytic pyrolysis of mixture of pine wood and methanol were 62.9%, 5.8% and 16.9%, respectively. However, co-feeding other alcohols with pine wood resulted in selectivities of 39.2-40.2%, 10.4-11.0% and 38.6-39.3% for xylene, benzene and toluene, respectively. This was explained by higher production of methyl radicals from methanol compared to other alcohols leading to higher alkylation of benzene and toluene molecules to xylene molecules. Furthermore, isotopic

labelling study of catalytic pyrolysis of pine wood and methanol revealed that production of toluene and xylene from methanol was more than that from pine wood. But, naphthalene was shown to be mostly formed from pine wood, and benzene seemed to be random mixture of the carbons of both methanol and pine wood. The result of isotopic labelling study indicates that methanol is efficiently involved in catalytic reactions and aromatics production, and is a suitable compound to be used in order to supply hydrogen to the hydrocarbon pool inside zeolite. The potential of light alcohols to be converted to aromatics over HZSM-5 is also confirmed by other researchers (Gujar et al., 2009; Le Van Mao & McLaughlin, 1989). Using Ni/HZSM-5 as catalyst, it was observed that addition of methanol into bio-oil caused a slight reduction in bio-oil conversion which is due to the fact that water formed by dehydration of methanol acts as competitor with oxygenate compounds to be adsorbed on acid sites of catalyst (Valle, Gayubo, Aguayo, Olazar, & Bilbao, 2010). In addition, methanol changes reaction pathway from decarbonylation and decarboxylation to reactions for hydrocarbons production. As a result of this fact, by addition of 20 wt% methanol, aromatics selectivity increased from 0.4 to 0.48. However, further addition of methanol slightly reduced aromatics production, and aromatics selectivity was less than 0.4 for the feed containing 80 wt% methanol. Considering the positive effect of methanol in attenuating catalyst deactivation, methanol content of 60 wt% was determined as the optimum methanol content in order to achieve a high yield of aromatics. Aromatics selectivity of 40% and benzene, toluene, xylene selectivity of 25% was achieved from the feed with 60 wt% methanol. Hydrogenation using hydrogen gas can also be implemented for enhancement of H/C_{eff} ratio of feedstock and increase of aromatics yield (see Table 2.3, entries 8-12) (Vispute et al., 2010).

Recycle of undesired products which can be as intermediates for aromatics production is an economic technique for increase of aromatics yield. Torren R. Carlson et al. (2011) proposed olefin recycle to achieve enhanced aromatics yield. They studied the effect of

olefin co-feed by addition of ethylene and propylene into pine wood sawdust and furan. Propylene was found to be more reactive than ethylene. Due to the higher stability of carbocation of propylene compared to ethylene, propylene is more easily converted to aromatics and can be recycled to reactor to obtain higher yield of aromatics. Propylene co-fed with pine sawdust at the propylene/wood carbon ratio of 0.3 increased aromatics carbon yield from 11.0 to 12.4%. Also, the addition of propylene greatly affected aromatics distribution. Among aromatic products, indene and benzofuran selectivities were strongly influenced by addition of propylene. By increase of propylene/wood carbon ratio up to 0.3, the selectivity of indene decreased from 7.1 to 0.3 C% and benzofuran selectivity increased from 1.6 to 11.0 C%. Meanwhile, co-feeding propylene with furan significantly increased the selectivities of toluene and xylenes, and decreased the selectivities of benzene, styrene, indene, benzofuran and naphthalene.

Reaction selectivity towards aromatics could be increased by optimization of operational parameters such as heating rate, catalyst to feed ratio and reaction temperature. High heating rate and high ratio of catalyst to feed can remarkably enhance aromatics yield through reducing coke formation. For instance, it was shown that by increase of ZSM-5 to glucose weight ratio from 1.5 to 19, carbon yield of aromatics increased from 13 to 31%, and carbon yield of coke decreased from 44 to 33% (Carlson et al., 2008). Temperature is another reaction parameter with significant effect on aromatics yield. In conversion of glucose to aromatics over HZSM-5, the increase of temperature from 400 to 600 °C increased carbon yield of aromatics from 10% up to 30% (Carlson, Jae, Lin, Tompsett, & Huber, 2010). Also, coke formation was remarkably reduced by increase of reaction temperature. In addition, temperature was effective on aromatics distribution. For instance, the selectivity to benzene was increased from 10 C% up to 30 C% when temperature was raised from 400 to 800 °C. However, in selecting a proper temperature, it should be considered that reactions for aromatics formation like oligomerization and

hydrogen transfer are exothermic and could be restricted at high temperatures. For example, in catalytic cracking of glycerol over ZSM-5, it was observed that at 500 °C, the aromatics yield had increase with conversion but at 600 and 700 °C, it decreased with increase of conversion (Corma et al., 2007). The dependency of reaction pathway on temperature and heating rate is illustrated in Scheme 2.6 which shows reaction chemistry proposed for catalytic fast pyrolysis of glucose over ZSM-5. The process includes two steps. At first, glucose undergoes a rapid thermal decomposition (less than one second) which could be performed through two different pathways. At low temperatures or low heating rates, glucose is decomposed to small oxygenates by retro-aldol condensation reactions. At high temperatures or high heating rates, glucose undergoes dehydration and forms anhydrosugars and furans. The second step is diffusion of the oxygenates into ZSM-5 pores and formation of aromatics through decarbonylation, decarboxylation, dehydration and oligomerization reactions. This step is much slower than the thermal decomposition of glucose and takes about 2 min. As shown in Scheme 2.6, the major competing reaction with production of aromatic compounds is coke formation. Coke is expected to be produced by decomposition of the resins which are formed through polymerization of the intermediate furans.

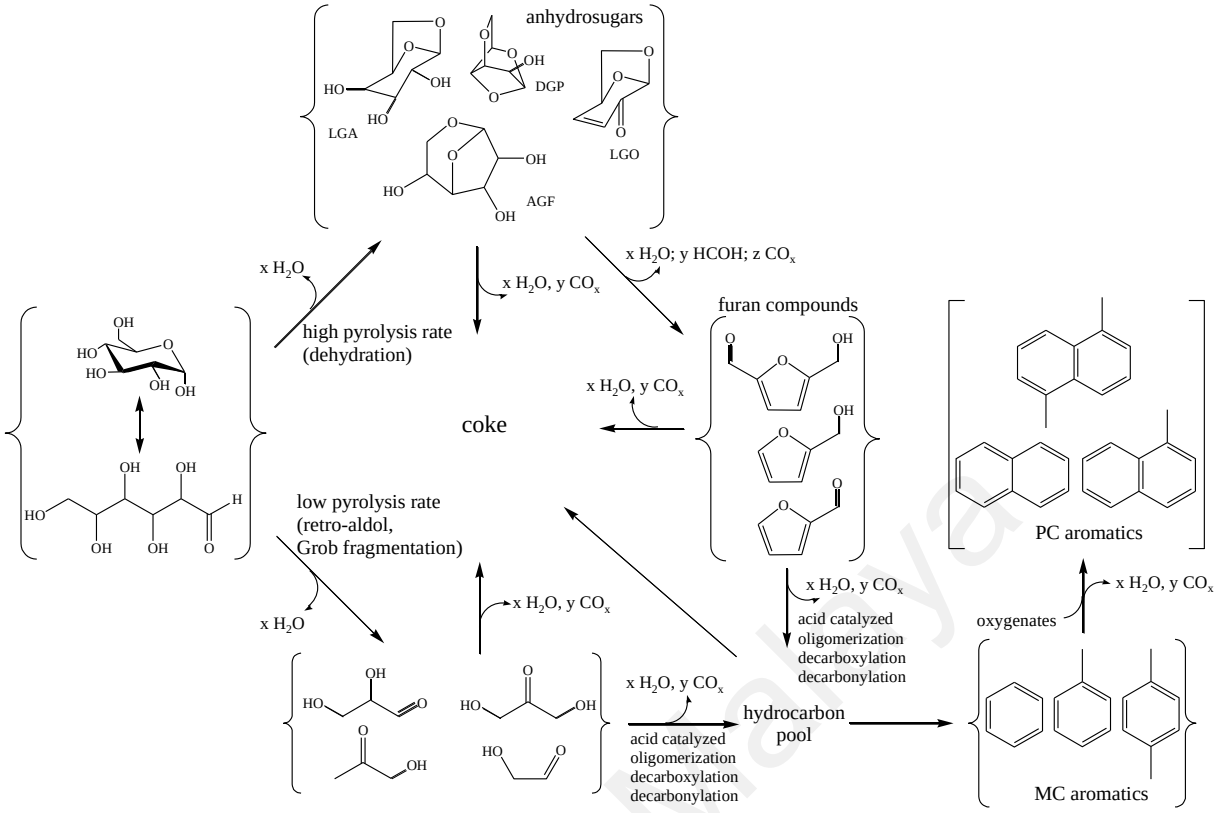

Scheme 2.6: Reaction pathway for catalytic fast pyrolysis of glucose over ZSM-5 (Carlson et al., 2010).

Reactor configuration is another factor which has impact on product selectivity by influencing mass transfer. Carlson et al. (2011) conducted catalytic fast pyrolysis of pine wood sawdust and furan in three different reactor types: bubbling fluidized-bed reactor, packed-bed reactor and semi-batch pyroprobe reactor. HZSM-5 was used as catalyst. Pyroprobe reactor resulted in higher aromatics yield and more naphthalene selectivity compared to continuous reactors. However, no olefins were obtained using pyroprobe reactor. These differences between different reactor configurations were attributed to the difference in mass transfer. Mass transfer is higher in continuous reactors due to high gas flux in catalyst bed. Also, since there is no gas flow in pyroprobe reactor, this reactor has longer gas residence time resulting in higher selectivity towards the compounds like naphthalene which are produced through secondary reactions. Moreover, low mass transfer in pyroprobe reactor favors the oligomerization of olefins to aromatics.

2.3 Coke formation and catalyst deactivation

One of the main challenges in catalytic cracking of biomass pyrolysis vapors/bio-oil is undesired formation and retention of carbonaceous deposits, called coke. Coke can be produced through gas phase thermal decomposition, homogeneous reactions in gas phase and heterogeneous reactions over catalyst (Carlson et al., 2008; Jae et al., 2011). Catalytic cracking of biomass pyrolysis vapors/bio-oil results in two fractions of coke deposited over catalyst: one of thermal origin and the other of catalytic origin. Thermal coke is mostly caused by polymerization of phenolic compounds and is mainly deposited on outside of catalyst particles. Catalytic coke is formed in the internal channels of catalyst due to transformation of oxygenate compounds over catalyst acid sites through reactions of oligomerization, cyclization, aromatization and condensation (Gayubo, Aguayo, Atutxa, Prieto, et al., 2004; Gayubo, Valle, Aguayo, Olazar, & Bilbao, 2010; Gayubo, Valle, Aguayo, Olazar, & Bilbao, 2009; Gayubo et al., 2010). In catalytic cracking of bio-oil over HZSM-5, it was shown that precursors of coke deposited on outside of the catalyst particle are saturated aliphatic hydrocarbons with the boiling point below 200 °C, and precursors of coke deposited inside catalyst particle are mostly aromatic compounds with the boiling point in the range of 350-650 °C (Guo, Zheng, Zhang, & Chen, 2009). Coke causes catalyst deactivation through poisoning catalyst acid sites and/or pore blockage. Apart from reducing catalyst lifetime, coke formation results in lower yields of desired products; in catalytic conversion of biomass derived oxygenates, coke formation is the major competing reaction with production of aromatics. Therefore, it seems essential to change reaction pathway in order to lower coke formation. Coke yields reported in previous studies of catalytic cracking of biomass pyrolysis vapors/bio-oil and some bio-oil model compounds are presented in Table 2.7. Catalyst properties, reaction conditions and chemical composition of feedstock are known as the factors influential on the yield and composition of coke which are reviewed in this section.

Table 2.7: Coke selectivity obtained by catalytic cracking of biomass pyrolysis vapors/bio-oil and bio-oil model compounds.

entry	Catalyst (Si/Al ratio)	Feed	Conv. (%)	Reactor	T (°C)	feed/cat ratio	Coke yield	Ref
1	HZSM-5 (50)	Methanol	100	Packed-bed	500	4 g feed/g cat.h	1.95 wt% of feed	(Horne & Williams, 1996)
2	HZSM-5 (50)	Furfural	91.8	Packed-bed	500	4	8.26	
3	HZSM-5 (50)	Anisole	69.1	Packed-bed	500	4	7.52	
4	HZSM-5 (50)	Cyclopentanone	80.8	Packed-bed	500	4	3.95	
5	HZSM-5 (30)	Furan	48	Packed-bed	600	10.4	33.8	(Cheng, Jae, et al., 2012)
6	Ga/HZSM-5[a] (30)	Furan	47	Packed-bed	600	10.4	23.8	
7	HZSM-5	Propanoic acid	99.9	Packed-bed	410	3.6	26.7	(Adjaye & Bakhshi, 1995a)
8	HZSM-5	4-Methylcyclohexanol	98.2	Packed-bed	410	3.6	7.8	
9	HZSM-5	2-Methylcyclopentanone	94.8	Packed-bed	410	3.6	5.0	
10	HZSM-5	Ethoxybenzene	49.9	Packed-bed	410	3.6	2.8	
11	HZSM-5	Eugenol	60	Packed-bed	410	3.6	4.0	
12	HZSM-5	Aspen poplar wood bio-oil	-	Packed-bed	410	3.6	12.3	
13	Al-MCM-41 (30)	Beech wood	-	Packed-bed	500	2.1 g feed/g cat	38.08	(Iliopoulou et al., 2007)
14	HZSM-5 (25)	Kraft lignin (Sulfur content: 4.10 %)	-	Curie-point pyrolyzer	650	0.05	65.5	(Li et al., 2012)
15	HZSM-5 (25)	Kraft lignin (Sulfur content: 1.49 %)	-	Curie-point pyrolyzer	650	0.05	39.7	
16	Al-MCM-41 (34.2)	Miscanthus	-	Packed-bed	500	2.1	40.90	(Antonakou, Lappas, Nilsen, Bouzga, & Stöcker, 2006)
17	Cu/Al-MCM-41 (24)	Miscanthus	-	Packed-bed	500	2.1	28.95	
18	Fe/Al-MCM-41 (23)	Miscanthus	-	Packed-bed	500	2.1	34.76	
19	Zn/Al-MCM-41 (49)	Miscanthus	-	Packed-bed	500	2.1	39.72	

‘Table 2.7, continued’

entry	Catalyst (Si/Al ratio)	Feed	Conv. (%)	Reactor	T (°C)	feed/cat ratio	Coke yield	Ref
20	HZSM-5 (30)	Pine wood sawdust	-	Fluidized-bed	600	0.2	30.2 C% of feed	(Carlson et al., 2011)
21	HZSM-5 (30)	Furan	-	Packed-bed	600	10.4	32.5	
22	ZK-5 (5.5)	Glucose	-	Pyroprobe	600	0.05	55.1	(Jae et al., 2011)
23	SAPO-34 (0.56)	Glucose	-	Pyroprobe	600	0.05	34.7	
24	Ferrierite (20)	Glucose	-	Pyroprobe	600	0.05	48.0	
25	ZSM-23 (160)	Glucose	-	Pyroprobe	600	0.05	40.8	
26	MCM-22 (30)	Glucose	-	Pyroprobe	600	0.05	63	
27	SSZ-20 (90)	Glucose	-	Pyroprobe	600	0.05	43.1	
28	ZSM-11 (30)	Glucose	-	Pyroprobe	600	0.05	44.7	
29	HZSM-5 (30)	Glucose	-	Pyroprobe	600	0.05	30.4	
30	IM-5 (40)	Glucose	-	Pyroprobe	600	0.05	48.5	
31	TNU-9 (40)	Glucose	-	Pyroprobe	600	0.05	66.8	
32	Beta zeolite (38)	Glucose	-	Pyroprobe	600	0.05	67.0	
33	SSZ-55 (54)	Glucose	-	Pyroprobe	600	0.05	83.7	
34	Y zeolite (5.2)	Glucose	-	Pyroprobe	600	0.05	84.9	
35	ZSM-5	Pine wood	-	Fluidized-bed	450	0.35 g feed/g cat.h	41.6	(Zhang et al., 2012)
36	ZSM-5	Pine wood (36 wt%) + Methanol (64 wt%)	-	Fluidized-bed	450	0.56	14.5	
37	ZSM-5	Pine wood (41 wt%) + 1-Propanol (59 wt%)	-	Fluidized-bed	450	0.58	10.7	
38	ZSM-5	Pine wood (47 wt%) + 1-Butanol (53 wt%)	-	Fluidized-bed	450	0.64	14.3	
39	ZSM-5	Pine wood (45 wt%) + 2-Butanol (55 wt%)	-	Fluidized-bed	450	0.64	12.8	

'Table 2.7, continued'

entry	Catalyst (Si/Al ratio)	Feed	Conv. (%)	Reactor	T (°C)	feed/cat ratio	Coke yield	Ref
40	HZSM-5 (30)	Furan	60	Packed-bed	650	10.4	26.9	(Cheng & Huber, 2011)
41	HZSM-5 (30)	White oak bio-oil	-	-	600	11.7	49.5	(Vispute et al., 2010)
42	HZSM-5 (30)	White oak bio-oil hydrogenated over Ru/C	-	-	600	11.7	34.6	
43	HZSM-5 (30)	WSBO[b]	-	-	600	11.7	32.3	
44	HZSM-5 (30)	WSBO hydrogenated over Ru/C	-	-	600	11.7	17.4	
45	HZSM-5 (30)	WSBO hydrogenated over Ru/C and Pt/C	-	-	600	11.7	12.6	
46	HZSM-5 (24)	1-Propanol	-	Packed-bed	400	9.7	1.55 wt% of catalyst (TOS[c]: 6 h)	(Gayubo, Aguayo, Atutxa, Aguado, & Bilbao, 2004)
47	HZSM-5 (24)	1-Butanol	-	Packed-bed	400	19.6	1.66 (TOS: 6 h)	
48	HZSM-5 (24)	Phenol+Water (Water/Phenol mass ratio: 13.28)	-	Packed-bed	400	0.84	0.87 (TOS: 2.4 h)	
49	HZSM-5 (24)	Acetic acid+Water (Water/Acetic acid mass ratio: 0.952)	-	Packed-bed	400	6.3	1.91 (TOS: 6 h)	(Gayubo, Aguayo, Atutxa, Aguado, Olazar, et al., 2004)
50	HZSM-5 (24)	Acetone+Water (Water/Acetone mass ratio: 1.26)	-	Packed-bed	400	2.4	1.75 (TOS: 6 h)	

'Table 2.7, continued'

entry	Catalyst (Si/Al ratio)	Feed	Conv. (%)	Reactor	T (°C)	feed/cat ratio	Coke yield	Ref
51	HZSM-5 (24)	Acetaldehyde	-	Packed-bed	400	9.3	4.21 (TOS: 4 h)	
52	HZSM-5 (30)	Furan	64	Packed-bed	600	5.9	23.0 C% of products	(Cheng & Huber, 2012)
53	HZSM-5 (30)	2-Methylfuran	98	Packed-bed	600	5.7	16.6	
54	HZSM-5 (30)	Furfural	100	Packed-bed	600	9.0	16.6	
55	HZSM-5 (30)	Furfuryl alcohol	100	Packed-bed	600	3.3	25.8	
56	HZSM-5 (30) V_{meso}:0.054 cm^3/g	Furan	35.9	Packed-bed	600	10.4	17.4	(Foster et al., 2012)
57	HZSM-5 (30) V_{meso}:0.550 cm^3/g	Furan	36.3	Packed-bed	600	10.4	29.0	
58	L-tartaric acid treated HZSM-5 (30) V_{meso}:0.062 cm^3/g	Furan	40.3	Packed-bed	600	10.4	24.6	
59	L-tartaric acid treated HZSM-5 (30) V_{meso}:0.709 cm^3/g	Furan	29.5	Packed-bed	600	10.4	28.1	

[a] HZSM-5 modified by Ga through ion exchange method
[b] WSBO: water-soluble fraction of pine wood bio-oil
[c] TOS: time on stream

2.3.1 Dependency of coke formation on catalyst properties

Catalyst properties like pore size and shape as well as catalyst particle size are greatly influential on the amount of coke formation. In catalytic upgrading of pine wood pyrolysis vapors conducted in a dual fluidized-bed reactor, it was shown that catalyst with small pore size led to less coke formation (Aho et al., 2010). Among Beta, Y and Ferrierite zeolites used in this study, Ferrierite zeolite which had too narrow pores resulted in less cokefication. In another work for catalytic pyrolysis of wood biomass, higher coke yields were obtained from catalysts with larger pore size; Y zeolite and activated alumina which had larger pore size produced more coke compared to ZSM-5 (Williams & Horne, 1995b). This was explained by diffusion of larger coke precursors into pore structure of catalyst and their involvement in coke formation. Similarly, Jae et al. (2011) reported that zeolites with low pore size result in less coke formation (see Table 2.7, entries 22-34). ZSM-5 and ZSM-11 with medium pore size resulted in the least formation of coke. Also, Beta zeolite, SSZ-55 and Y zeolite which had the largest pores produced highest coke amounts. It was also observed that apart from pore-opening size which controls diffusion rate of molecules, the space inside zeolite channels have a great effect on coke formation; MCM-22, TNU-9 and IM-5 which had medium pore size produced more amounts of coke due to their high mesoporosity which provides enough space for coke formation. Furthermore, in catalytic pyrolysis of pine wood performed in a fluidized-bed reactor at 450 °C, it was concluded that large cavities in zeolite structure causes high yield of coke (Aho et al., 2008). Among the four zeolites (HZSM-5, H-Beta, H-Y and H-Mordenite) used as catalyst, H-Y zeolite had the highest coke content. This was attributed to its highest initial surface area and large cavities in the structure of H-Y allowing larger molecules to diffuse into catalyst. Coke content of spent zeolites decreased in the order H-Y > H-Beta > H-Mordenite > HZSM-5. However, in contrast with what is mentioned above, Ma et al. (2012) concluded that larger pore size leads to less coke by allowing larger molecules to

enter catalyst and react and not to be converted to thermal coke. Coke formation and catalyst deactivation was also shown to be affected by catalyst crystallite size; in catalytic conversion of propanal over HZSM-5, small crystallites showed more stability and were less deactivated in comparison with large crystallites (Hoang et al., 2010). This was attributed to the longer diffusion path length of larger crystallites; in larger crystallites, products need to take longer path to diffuse out of zeolite channels and have more time to be converted to coke precursors.

Metal impregnation can lead to either positive or negative results in term of coke formation. In catalytic conversion of bio-oil, addition of 6.0 wt% La into HZSM-5 caused a remarkable decrease in coke formation and catalyst deactivation (Gong et al., 2011). Similarly, impregnation of HZSM-5 by Mg led to less coke deposition and catalyst deactivation (Hong et al., 2013). In catalytic conversion of bio-oil for 45 h at 600 °C and WHSV of 0.4 h^{-1}, the rates of coke deposition over HZSM-5 and Mg/HZSM-5 were 3.3 and 1.7 mg coke $(g_{catalyst}\ h)^{-1}$, respectively. The reduction of coke formation by La and Mg impregnation may be due to the effect of these metals in increasing the density of catalyst medium acid sites. However, in another attempt for modification of HZSM-5, it was concluded that impregnation of HZSM-5 by 1.0 wt% Ni increased coke formation and catalyst deactivation due to the dehydrogenating activity of Ni which leads to higher condensation of coke precursors (Valle, Gayubo, Alonso, et al., 2010).

In catalytic conversion of acetone/n-butanol mixture over dealuminated HZSM-5, it was illustrated that catalyst deactivation is not only affected by the amount of coke deposited on catalyst but also by composition and location of the coke (de Lucas, Canizares, Durán, & Carrero, 1997). HZSM-5 was dealuminated through steaming followed by HCl leaching. Dealumination showed to be effective in reducing coke deposition and catalyst deactivation. The coke contents deposited on non-treated HZSM-5, steam-treated HZSM-5 (steamed at 550 °C) and steam-HCl treated HZSM-5 (steamed at 550 °C, followed by

leaching in HCl) were 6.57, 3.30 and 5.20 wt%, respectively. Although steam-treated HZSM-5 had the lowest coke content, but steam-HCl treated HZSM-5 underwent lower deactivation. This shows that amount of coke deposition is not the only factor which determines the level of catalyst deactivation. The effect of catalyst steaming on reduction of coke deposition was also observed in fluid catalytic cracking of hybrid poplar wood over commercial FCC catalyst containing Y zeolite (Mante, Agblevor, & McClung, 2011).

One problem in using zeolites for catalytic cracking of biomass pyrolysis vapors/bio-oil is that catalyst regeneration performed under high temperature can itself result in irreversible deactivation. Vitolo et al. (2001) studied the performance of HZSM-5 zeolite in repeated upgrading-regenerating cycles. Regeneration was done in a furnace at 500 °C in the presence of air for 12 h in order to remove the coke deposited on catalyst. However, the combustion of coke during regeneration treatment increased catalyst temperature and led to dehydroxylation of Brønsted acid sites making catalyst less effective. Each upgrading run was prolonged till the catalyst was completely deactivated and then a regeneration treatment was performed. The fresh catalyst was deactivated after 90 min run. The catalyst regenerated two times showed to be active for 60 min and the catalyst regenerated four times deoxygenated bio-oil for less than 30 min. Deactivation was reported to be irreversible by the fifth regeneration treatment.

2.3.2 Dependency of coke formation on reaction conditions

Coke yield can be remarkably reduced by optimizing operational parameters such as residence time, reaction temperature, heating rate and catalyst to feed ratio. In catalytic upgrading of wood pyrolysis oils using zeolites, it was inferred that less coke is formed at lower residence times (Vitolo, Seggiani, Frediani, Ambrosini, & Politi, 1999). This was explained by the fact that condensation and polymerization reactions are reduced at low

residence times. However, the degree of deoxygenation is also significantly decreased by reduction of residence time leading to the oil with high oxygen content. Higher values of heating rate and catalyst to feed ratio were also shown to result in less coke formation in catalytic fast pyrolysis of biomass derived compounds; increase of these two factors are supposed to decrease the probability of thermal decomposition of organic compounds before they enter catalyst (Carlson et al., 2009; Carlson et al., 2008). In catalytic upgrading of bio-oil over nickel modified HZSM-5, temperature and space time were shown to be influential on coke formation (Valle, Gayubo, Aguayo, et al., 2010). By increase of space time, the yield of catalytic coke was increased due to the involvement of catalyst acid sites in coke production. However, the yield of thermal coke was constant. Therefore, total yield of coke was increased. But, total coke content in catalyst was decreased due to decrease in both thermal and catalytic coke contents. Furthermore, by increase of reaction temperature from 400 to 500 °C, catalyst coke content increased from 3.18 to 4.67 wt%. This increase of coke content was due to the increase of thermal coke while catalytic coke was almost constant. Higher deposition of thermal coke by rising temperature can be due to the increase in polymerization of lignin pyrolysis phenol derivatives present in bio-oil. However, in a study for catalytic transformation of a mixture of model components (acetone, acetic acid, methanol, 2-butanol, phenol and acetaldehyde) over HZSM-5, it was shown that by increase of temperature from 400 to 450 °C, the amount of catalytic coke deposited on HZSM-5 was increased while thermal coke content was remained constant (Gayubo, Aguayo, Atutxa, Valle, & Bilbao, 2005). In catalytic transformation of bio-oil model compounds such as alcohols, phenols, aldehydes, ketones and acids over HZSM-5, it was shown that coke deposition is a strong function of operating conditions like temperature, water content in reaction medium and space time (Gayubo, Aguayo, Atutxa, Aguado, & Bilbao, 2004; Gayubo, Aguayo, Atutxa, Aguado, Olazar, et al., 2004). The effect of these factors on coke deposition is depicted

in Table 2.8. Coke deposition was decreased by increase of space time and water content. Less coke contents were achieved at lower temperatures and it was recommended to upgrade pyrolysis-derived bio-oil below 400 °C in order to prevent from irreversible deactivation of catalyst.

Table 2.8: Coke content in HZSM-5 for different reactants and reaction conditions (Gayubo, Aguayo, Atutxa, Aguado, & Bilbao, 2004; Gayubo, Aguayo, Atutxa, Aguado, Olazar, et al., 2004).

Water/oxygenate mass ratio	**T (°C)**	**Space time [(g catalyst) h (g oxygenate)$^{-1}$]**	**Time on stream (h)**	**Coke content (wt%)**
1-Propanol				
1.23	300	0.026	6	1.31
1.23	300	0.103	6	1.26
1.23	300	0.411	6	1.17
0	400	0.103	6	1.55
1.23	400	0.026	6	1.58
1.23	400	0.103	6	1.46
1.23	400	0.411	6	1.36
2-Propanol				
1.27	300	0.425	6	0.33
1.27	400	0.425	6	1.01
1-Butanol				
0	300	0.051	6	0.56
0	400	0.051	6	1.66
2-Butanol				
0	300	0.013	6	0.64
0	400	0.013	6	1.74
Phenol				
13.28	400	1.19	2.4	0.87
13.28	450	1.19	6.8	1.43
2-Methoxyphenol				
0	200-450	0.03	4.2	10.58
0	200-450	0.06	4.2	3.98
Acetic Acid				
0.952	400	0.159	6	1.91
0.952	450	0.317	6	2.93
Acetaldehyde				
0	400	0.053	4	4.74
0	400	0.107	4	4.21
Acetone				
1.26	300	0.844	6	2.50
1.26	400	0.421	6	1.75

One solution for reduction of coke formation in catalytic cracking of biomass pyrolysis vapors/bio-oil is to co-feed hydrogen or hydrogen containing compounds in order to

increase H/C_{eff} ratio of feed. In catalytic upgrading of bio-oil over nickel modified HZSM-5, increase of methanol content in feed was shown to reduce both thermal and catalytic coke contents of Ni/HZSM-5, and no thermal coke was formed in the case of feeding pure methanol (Gayubo et al., 2009; Gayubo et al., 2010; Valle et al., 2012; Valle, Gayubo, Aguayo, et al., 2010). Table 2.9 shows the effect of methanol addition on coke deposition. The reduction of coke deposition by addition of methanol can be explained by the effect of methanol in increasing H/C_{eff} ratio of feed. The positive effect of increasing H/C_{eff} ratio of feedstock in attenuating coke formation and catalyst deactivation is reported in several studies (Chen, Walsh, & Koenig, 1988; French & Czernik, 2010; Li et al., 2012; Zhang et al., 2011). As an approach to enhance H/C_{eff} ratio of bio-oil, Vispute et al. (2010) conducted a hydrogenation step prior to zeolite catalysis. They found that increasing the hydrogen content of zeolite feed improved its thermal stability through conversion of thermally unstable carbonyl functionalities of bio-oil to thermally stable corresponding alcohols. This increase of thermal stability reduced coke yield of zeolite upgrading (see Table 2.7, entries 41-45). In another work for transformation of anisole over H-Y, coke deposition and catalyst deactivation were decreased by co-feeding a hydrogen donor like tetralin (Prasomsri, To, Crossley, Alvarez, & Resasco, 2011). The amount of carbon deposited on H-Y in conversion of pure anisole for 3 h was 11.8 wt% which was declined to 8.8 and 6.0 wt% when tetralin was co-fed at concentrations of 35 and 50%, respectively. Promoting the desorption of surface species and lowering the rate of H-transfer from coke precursors were proposed as the two possible ways through which tetralin reduces coke deposition.

Table 2.9: Content of total coke, thermal coke and catalytic coke (C_{CT}, C_{C1}, C_{C2}, respectively) and fraction of thermal coke (f_{C1}) obtained in transformation of bio-oil/methanol mixtures at space time of 0.12 (g catalyst) h (g oxygenate)$^{-1}$ and temperatures of 450 and 500 °C (Gayubo et al., 2009).

Feed bio-oil/methanol mass ratio	**C_{CT} (wt %)**	**f_{C1}**	**C_{C1} (wt %)**	**C_{C2} (wt %)**
450 °C				
100/0	11.45	0.362	4.15	7.31
80/20	10.81	0.358	3.87	6.94
60/40	9.67	0.345	3.34	6.33
40/60	8.68	0.279	2.42	6.26
20/80	5.54	0.155	0.86	4.68
0/100	3.98			3.98
500 °C				
100/0	17.09	0.497	8.49	8.60
80/20	16.89	0.478	8.07	8.82
60/40	13.05	0.422	5.49	7.54
40/60	11.01	0.386	3.96	7.05
20/80	8.42	0.245	2.06	6.36
0/100	4.72			4.72

2.3.3 Dependency of coke formation on chemical composition of feedstock

Coke formation in catalytic cracking of biomass pyrolysis vapors/bio-oil is mostly caused by lignin pyrolysis phenol derivatives. In catalytic conversion of various biomass feedstocks with different contents of cellulose, hemicellulose and lignin over La/HZSM-5, it was revealed that lignin or feedstocks with more lignin content result in higher coke formation (Huang et al., 2012). In another study for catalytic pyrolysis of different lignin samples over HZSM-5, it was found that H-lignin component leads to highest deactivation of catalyst in comparison with G- and S-lignin components (Mullen & Boateng, 2010). The reason for this is that through primary pyrolysis of these lignin components, H-lignin produces the highest concentration of simple phenolics which are tightly bound to acid sites of HZSM-5 resulting in coke formation and catalyst deactivation. However, it was reported in literature that it is possible to reduce adsorption of phenol on catalyst acid sites by increase of temperature. The transformation of methylcyclohexane and n-heptane over H-Y zeolite in the absence and presence of phenol revealed that phenol addition increases catalyst deactivation due to adsorption of phenol molecules on both Brønsted and Lewis acid sites (Graça, Comparot, et al., 2009; Graça

et al., 2010). By increase of reaction temperature from 350 to 450 °C, the phenol deactivating effect was shown to be reduced which should be due to less adsorption of phenol on catalyst acid sites. Faster diffusion of phenol molecules, decrease in the number of acid sites which can hold the adsorbed phenol molecules and exothermic nature of adsorption can be explained as reasons for reduction of phenol adsorption by increase of temperature. Phenol was also shown to be adsorbed on both Brønsted and Lewis acid sites of HZSM-5 in methylcyclohexane transformation (Graça et al., 2009). However, increase of reaction temperature did not reduce the adsorption of phenol on HZSM-5 because of the narrow channels in structure of this type of zeolite which prevent fast diffusion of phenol molecules even at high temperatures. Slow rate of diffusion facilitates the adsorption and retention of phenol molecules on zeolite acid sites. The yields of catalytic and thermal coke are also dependent on reactivity of the compounds present in feedstock. For instance, in catalytic transformation of some bio-oil model compounds over HZSM-5, it was shown that acetone, acetic acid, propanol and butanol resulted in catalytic coke and in turn catalyst deactivation (Gayubo, Aguayo, Atutxa, Aguado, & Bilbao, 2004; Gayubo, Aguayo, Atutxa, Aguado, Olazar, et al., 2004). However, 2-methoxyphenol and acetaldehyde had low reactivity and underwent thermal degradation and polycondensation resulting in high thermal coke (about 50 wt%). Although, the coke produced from these compounds is not of catalytic origin and does not lead to catalyst deactivation, high amount of thermal coke formed due to their low reactivity can create problems such as reactor plugging. Removal of such low reactive compounds from feedstock prior to catalytic upgrading of bio-oil could be implemented in order to reduce thermal coke formation. Furthermore, the yield of thermal coke could be affected by molecular size of feedstock components; diffusion rate of the components with high molecular size into catalyst pores is low and their possibility of being converted to thermal coke is higher than that of those with low molecular size.

2.4 Summary of literature review

Pyrolysis derived bio-oil is highly oxygenated and needs to be upgraded in order to be used as a fuel source. In catalytic cracking of biomass pyrolysis vapors/bio-oil, reactions of decarbonylation, decarboxylation, dehydration, oligomerization, isomerization and dehydrogenation are taken place, and oxygen is removed in the form of CO, CO_2 and H_2O. Since coke formation is the major competing reaction with production of aromatic hydrocarbons, it is of great importance to change reaction pathway in order to lower coke formation. The product distribution obtained from catalytic cracking of biomass pyrolysis vapors/bio-oil is a strong function of acidity and shape selectivity of catalyst. Shape selectivity effects are mainly imposed by pore-opening size, pore shape and crystallite size of catalyst. Catalyst pore size greatly influences reaction selectivity by affecting mass transfer of reactants and products into and out of catalyst; smaller pore size reduces mass transfer and restricts the diffusion of large molecules. Several researchers concluded that this mass transfer difficulty prevents production of polyaromatic compounds which act as coke precursors and leads to formation of less coke and more aromatics. However, it was also reported in the literature that the catalysts with larger pore size allows larger molecules to penetrate into catalyst and react resulting in less production of thermal coke. Apart from pore size, internal pore structure also significantly affects product distribution. For instance, confined space inside catalyst pores influences reaction pathway by restricting the formation of certain transition states. Product selectivity can also be controlled by catalyst crystallite size which determines diffusion path length and in turn the contact time between different molecules and catalyst. For instance, in larger crystallites, products need to take longer path to diffuse out of catalyst channels and their chance of being converted to coke precursors is higher. It was also revealed that Brønsted acid sites are necessary for cracking and aromatics production. Both density and strength of acid sites are needed to be optimized in order to achieve maximum yield of aromatics

and minimum coke formation. Zeolites contains both Brønsted and Lewis acid sites and have molecular size dimensions which make them suitable for shape selective catalysis. Thus, zeolites are of great potential to be modified for enhanced conversion of biomass derived feedstocks to aromatic hydrocarbons. Use of multifunctional catalyst by incorporation of the metals which promote the desired reactions can be considered as an effective approach for high production of aromatic hydrocarbons. The content of metal loading and the method of incorporation are influential on final product selectivity. Product selectivity is also highly dependent on reaction conditions like temperature, reaction time and catalyst to feed ratio. These factors greatly influence reaction pathway, and their effect on product selectivity can be varied by change of catalyst type and feedstock composition. Low reactive compounds such as 2-methoxyphenol and acetaldehyde which undergo thermal degradation and polycondensation and produce high thermal coke as well as those (such as phenol) which are tightly bound to catalyst acid sites and result in catalyst deactivation can be removed from bio-oil prior to catalytic upgrading. Pyrolysis derived bio-oil has low H/C_{eff} ratio and its upgrading leads to high yield of catalytic coke. This problem can be solved by co-feeding a hydrogen donor like tetralin in order to supply hydrogen to the hydrocarbon pool inside catalyst. From this study, it is inferred that catalytic cracking of biomass pyrolysis vapors/bio-oil is a potential technique for production of aromatic hydrocarbons. However, there are some challenges which should be solved for an enhanced yield of aromatic hydrocarbons. As mentioned in this literature review, lignin is the most difficult fraction of biomass to be deoxygenated. So far, studies of catalytic pyrolysis of lignin have been conducted at reaction temperatures above 600 °C with low yield of aromatic hydrocarbons. One novelty of this research is to study the deactivating effect of lignin derived phenolics on zeolite, and to design an efficient catalyst for enhanced conversion of lignin fraction of biomass into aromatic hydrocarbons at temperatures below 600 °C. Meanwhile, the

interactive effects of pore structure and acidity of catalyst has not been noticeably discussed in the literature. The interaction between different catalyst characteristics is supposed to have a strong effect on the amount of coke formation in conversion of biomass materials over zeolites used as catalyst. The other novelty of this work is to optimize the interaction between zeolite pore structure and density of acid sites for suppression of formation of both catalytic and thermal coke, and in turn, enhanced yield of aromatic hydrocarbons.

CHAPTER 3: MATERIALS AND METHODS

3.1 Materials

Phenol (C_6H_6O, ≥99%), *m*-cresol (C_7H_8O, ≥98%) and lignin were purchased from Sigma-Aldrich. Cellulose was provided by Acros Organics. Methanol (CH_4O, ≥99.9%) was procured from Merck. Ethyl acetate was purchased from R&M Chemicals. The chemicals were used as received without further purification. Purified hydrogen and nitrogen were supplied from Linde Malaysia Sdn. Bhd. Palm kernel shell (PKS) was obtained from Szetech Engineering Sdn. Bhd. in Selangor, Malaysia. The biomass was ground with high-speed rotary cutting mill and sieved to obtain particle sizes below 300 μm. Then, the biomass was dried at 100 °C for 24 h and kept in screw cap plastic bottles.

3.2 Biomass proximate and ultimate analysis

Proximate analysis was performed by thermogravimetric analysis. Volatile matter, fixed carbon and moisture contents were determined based on ASTM D-5142-02a using TGA/Q500 manufactured by TA Instruments. Ash content of the biomass was measured by its ignition in a muffle furnace at 575 °C for 24 h based on ASTM E-1755-01 standard method. Ash content (wt. %) was calculated by dividing ash weight to initial weight of biomass sample dried at 105 °C. The basic elemental composition of the biomass was determined by ultimate analysis. Biomass ultimate analysis was carried out using a Perkin-Elmer model 2400, Series II CHNS/O analyzer to measure carbon, hydrogen, nitrogen and sulfur contents. Oxygen content was calculated by difference.

3.3 Catalyst preparation

HZSM-5, HY, dealuminated HY, mixtures of HZSM-5 and dealuminated HY, HBeta and 1 wt% Fe/HBeta were used for catalytic reactions in this work. HY was provided by

Zeolyst International (CBV 720, SiO_2/Al_2O_3 molar ratio: 30). The dealuminated HY was obtained by treatment of HY in 2 M aqueous HCl solution at 80 °C for 12 h using 15 ml acid solution/$g_{zeolite}$. Then, the sample was filtered, washed with distilled water, and dried in oven at 100 °C for 12 h. Afterward, the dealuminated sample was converted to the protonic form by ion exchange in 0.1 M aqueous NH_4Cl solution at 60 °C for 12 h using 50 ml NH_4Cl solution/$g_{zeolite}$. Then, the sample was filtered, washed with distilled water and dried at 100° C for 12 h, followed by calcination under static air in a muffle furnace at 550 °C (with heating rate of 3 °C/min) for 12 h. HBeta and HZSM-5 were obtained by calcination of the ammonium form of Beta zeolite (Zeolyst, CP814C, SiO_2/Al_2O_3 molar ratio: 38) and ZSM-5 (Zeolyst, CBV 3024E, SiO_2/Al_2O_3 molar ratio: 30; Zeolyst, CBV 5524G, SiO_2/Al_2O_3 molar ratio: 50), respectively. Calcination was carried out at 550 °C (with heating rate of 3 °C/min) for 12 h. The iron impregnated HBeta was prepared by incipient wetness impregnation of HBeta with an aqueous solution of $Fe(NO_3)_3.9H_2O$ (Sigma-Aldrich). Afterwards, Fe/HBeta was dried at 100 °C for 12 h, followed by calcination at 550 °C for 12 h.

3.4 Catalyst characterization

3.4.1 X-ray fluorescence (XRF) analysis

The chemical composition of the catalysts was determined by X-ray fluorescence (XRF) instrument (PANalytical Axios^{mAX}).

3.4.2 X-ray diffraction (XRD)

The crystalline phase of zeolites was verified by X-ray diffraction (XRD) on a Rigaku Miniflex diffractometer using Cu Kα radiation (λ = 1.54443 Å) at 45 kV and 40 mA. The XRD patterns were recorded in the 2θ range of 5-80° with a step size of 0.026° and scan rate of 0.05°/s.

3.4.3 Surface area and porosity analysis

The surface area and pore size distribution of the catalysts were measured by N_2 isothermal (-196 °C) adsorption-desorption using Micromeritics ASAP 2020 surface area and porosity analyzer. The samples were degassed at 180 °C under vacuum for 4 h prior to the analysis.

3.4.4 Temperature-programmed desorption of ammonia (NH_3-TPD)

Temperature-programmed desorption of ammonia (NH_3-TPD) using Micromeritics ChemiSorb 2720 instrument was implemented for characterization of acid site distribution of the catalysts. 200 mg of each sample was set in TPD cell. In a stream of He gas (20 ml/min), the sample was heated from ambient temperature to 510 °C (close to the pyrolysis temperature of 500 °C) at a heating rate of 20 °C/min and was held at this temperature for 1 h. Afterward, the sample temperature was brought down to 170 °C and ammonia was introduced into the cell in a stream of 10%NH_3/90%He (20 ml/min) for 30 min. After being flushed with He gas for 30 min for elimination of physisorbed NH_3, the sample was cooled down to 50 °C. When the thermal conductivity detector (TCD) signal was stable, ammonia desorption measurement was performed by heating the sample to 800 °C with a rate of 10 °C/min under He flow (20 ml/min).

3.4.5 Hydrogen temperature-programmed reduction (H_2-TPR)

Hydrogen temperature-programmed reduction (H_2-TPR) was carried out using the same apparatus as with NH_3-TPD. Before analysis, 100 mg of sample was heated at 20 °C/min up to 510 °C in a stream of He (20 ml/min), and held at this temperature for 1 h. Afterward, the sample was cooled down to 30 °C and exposed to a stream of 5%H_2/95%N_2 (20 ml/min). Subsequently, the sample was heated to 800 °C at a heating rate of 10 °C/min. The amount of hydrogen uptake was recorded by a TCD.

3.4.6 FTIR spectroscopy

Fourier transform infrared spectroscopy (FTIR; model: BRUKER TENSOR 27) was used for qualitative analysis of the functional groups of the chemical components present in the coke deposited on spent catalysts. The IR spectra of the catalysts were recorded in the range from 600 to 4000 cm^{-1} with a resolution of 4 cm^{-1}.

3.4.7 Coke analysis

The amount of coke deposited on catalysts was measured by thermogravimetric analysis using a PerkinElmer STA 6000 Simultaneous Thermal Analyzer. In the flow of synthetic air at 100 ml/min, samples were heated from 30 to 750 °C with the rate of 5 °C/min and kept at final temperature for 30 min. The weight loss in temperature range of 300-750 °C was considered as the amount of coke deposited on catalyst, and the weight loss below 300 °C was assigned to desorption of water and volatile components.

3.5 Catalyst regeneration

The spent catalyst was washed with acetone and dried in oven at 100 °C for 12 h. Then, it was regenerated in a muffle furnace at 550 °C (with heating rate of 3 °C/min) in the presence of air for 12 h.

3.6 Catalytic activity measurement

3.6.1 Catalytic conversion of liquid feed

The catalytic reactions for conversion of methanol, *m*-cresol and mixtures of methanol/*m*-cresol (90:10 wt%), methanol/phenol (90:10 wt%) and *m*-cresol/phenol (90:10 wt%) were conducted in a continuous, down-flow, fixed-bed tubular reactor (ID: 6 cm; height: 60 cm) made of stainless steel 316L which was heated by a two-zone furnace. All runs were carried out at atmospheric pressure. In each run, 5 g calcined catalyst was loaded in a

stainless steel cylindrical cup (ID: 3 cm; height: 10 cm) with screen of 400 mesh at the bottom side. The cup was placed inside the reactor. The activity of catalysts was studied at reaction temperatures of 350 or 450 °C. The temperature of catalyst bed was measured by a K-type thermocouple inserted into the catalyst bed. Feed was pumped to the reactor using a syringe pump (Fisher, KDS100). In the case of using pure HBeta zeolite, catalyst bed was heated to reaction temperature and nitrogen was purged to the reactor at flow rate of 2 L/min for 30 min. Afterward, 10 g feed was introduced into the reactor with weight hourly space velocity (WHSV) of 2 h^{-1} and N_2 flow rate was kept at 2 L/min. When Fe/HBeta was used as catalyst, catalyst bed was heated to 300 °C in a stream of N_2 (2 L/min). At this temperature, gas was changed to H_2 (0.4 L/min) for in situ reduction of catalyst for 2 h. Subsequently, temperature was raised to 350 or 450 °C for reaction. Then, H_2 flow rate was increased to 2 L/min and 10 g feed was injected with WHSV of 2 h^{-1}. The liquid products were collected by two condensers maintained at -10 °C. All lines were heated to avoid any condensation. After each run, the catalyst bed was exposed to N_2 flow (2 L/min) at the reaction temperature for 30 min in order to remove the components which might remain on the catalyst.

3.6.2 Catalytic pyrolysis of solid feed

Catalytic pyrolysis was conducted in a continuous, down-flow, fixed-bed tubular reactor (ID: 7.5 cm; height: 60 cm) made of stainless steel 316L which was heated by a two-zone furnace. A stainless steel cylindrical cup with screen of 400 mesh at the bottom side was set in each zone of the reactor. In each run, 5 g calcined catalyst was loaded in the second cup, and feedstock was introduced into the first cup through a feed hopper on the top of the reactor. The first zone was used as pylolyzer, and the pyrolysis vapors were conducted to the second zone which was a fixed-bed reactor for catalytic upgrading. The feedstocks used in this study were cellulose, lignin and palm kernel shell (PKS). All runs were carried

out at atmospheric pressure. Temperature of each zone was measured by a K-type thermocouple. In the case of using pure zeolite, both zones were heated to 500 °C and nitrogen was purged to the reactor at flow rate of 2 L/min for 30 min. Afterward, the feed was introduced into the reactor with weight hourly space velocity (WHSV) of 6 h^{-1} and N_2 flow rate was kept at 2 L/min. When Fe/HBeta was used as catalyst, reactor was heated to 450 °C in a stream of N_2 (2 L/min). At this temperature, gas was changed to H_2 (0.4 L/min) for in situ reduction of catalyst for 2 h. Subsequently, temperature was raised to 500 °C for reaction. Then, H_2 flow rate was increased to 2 L/min, and feed was introduced with WHSV of 6 h^{-1}. In the case of using N_2 as carrier gas during the reaction, H_2 was changed to N_2 (2 L/min) after the catalyst reduction is completed. Then, temperature was increased to 500 °C, and feed was introduced at this temperature. The liquid products were collected by two condensers maintained at -10 °C. All lines were heated to avoid any condensation. After each run, the catalyst bed was purged by N_2 flow (2 L/min) at the reaction temperature for 30 min in order to remove the components which might remain on the catalyst. The reaction conditions applied in the experiments are shown in Table 3.1.

Table 3.1: Reaction conditions applied in the experiments.

Parameter	Value
Reaction temperature	350, 450, 500 °C
Reaction Pressure	1 atm
Weight hourly space velocity	2, 6 h^{-1}
Time on stream	60 min
Carrier gas flow rate	2 L/min
Reducing gas flow rate	0.4 L/min
Product condensation temperature	-10 °C
Catalyst calcination temperature	550 °C

3.7 GC-MS analysis

Qualitative and quantitative analysis of liquid products was performed by GC/MS (Shimadzu QP 2010, DB-5 30 m × 0.25 mm × 0.25 μm), equipped with flame ionization and mass spectrometry detection. The GC oven temperature program was as follows: temperature was held at 50 °C for 5 min, ramped to 300 °C at 10 °C/min, and kept at 300

°C for 10 min. The injector temperature was 290 °C and a split ratio of 50:1 was employed. Helium (Linde Malaysia Sdn. Bhd.) was used as carrier gas with flow rate of 1.26 ml/min. Peak identification was done using the NIST (National Institute of Standards and Technology) mass spectrum library. The organic phase of liquid product was separated from the aqueous phase with ethyl acetate (R&M Chemicals) before injection to GC/MS. 2-Isopropylphenol (Sigma-Aldrich) was used as internal standard for quantitative analysis of products. Yield and selectivity of products were calculated as follows: yield = (weight of a certain product/total weight of feed) × 100; selectivity = (weight of a certain product/total weight of organic phase in liquid product) × 100.

CHAPTER 4: RESULTS AND DISCUSSION

4.1 Origin of zeolite deactivation in conversion of lignin-derived phenolics

4.1.1 Physicochemical characteristics of catalysts

The XRD data show that there is no distinct difference in crystallinity between HBeta and Fe/HBeta indicating that crystalline structure of HBeta was relatively unchanged by addition of Fe (Figure 4.1). No iron species were detected in Fe/HBeta signifying that Fe is well dispersed on HBeta surface. HBeta is a zeolite with three-dimensional framework formed of 12-membered ring pores with dimensions of 0.66 × 0.67 and 0.56 × 0.56 nm which are suitable for diffusion of relatively large phenolic compounds (Jae et al., 2011). Textural properties of fresh HBeta and Fe/HBeta as well as HBeta used in different reactant systems evaluated from nitrogen isothermal adsorption-desorption are presented in Table 4.1. The fresh catalysts are mostly microporous since the surface area and volume of micropores are larger than those of mesopores. BET surface area of 1 wt% Fe/HBeta was 6% lower than that of pure HBeta, and this reduction in surface area only occurred in micropores. As shown in Figure 4.2, both zeolites displayed type IV isotherm with H4-type hysteresis loop which indicates the predominance of microporous structure in these catalysts. The BJH desorption pore size distribution showed that most of the mesoporosity of both zeolites was in the range below 4 nm. The acidity of fresh HBeta and Fe/HBeta determined by NH_3-TPD analysis is depicted in Figure 4.3. HBeta exhibited two ammonia desorption peaks at 232 and 328 °C, while desorption peak temperatures for Fe/HBeta were 248 and 322 °C. The peak area of iron incorporated HBeta was lower than that of HBeta demonstrating the reduction in the density of free acid sites as a result of Fe loading.

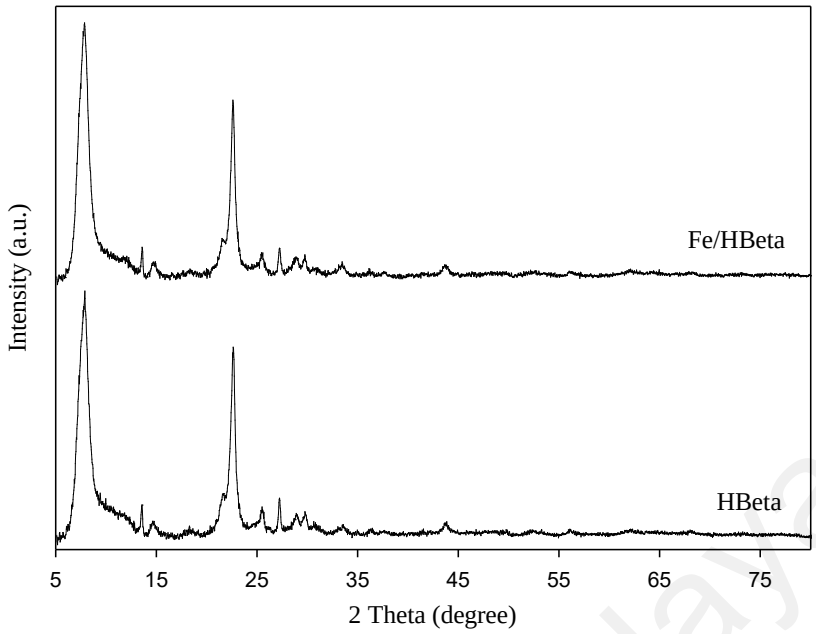

Figure 4.1: X-ray diffraction patterns of HBeta and Fe/HBeta.

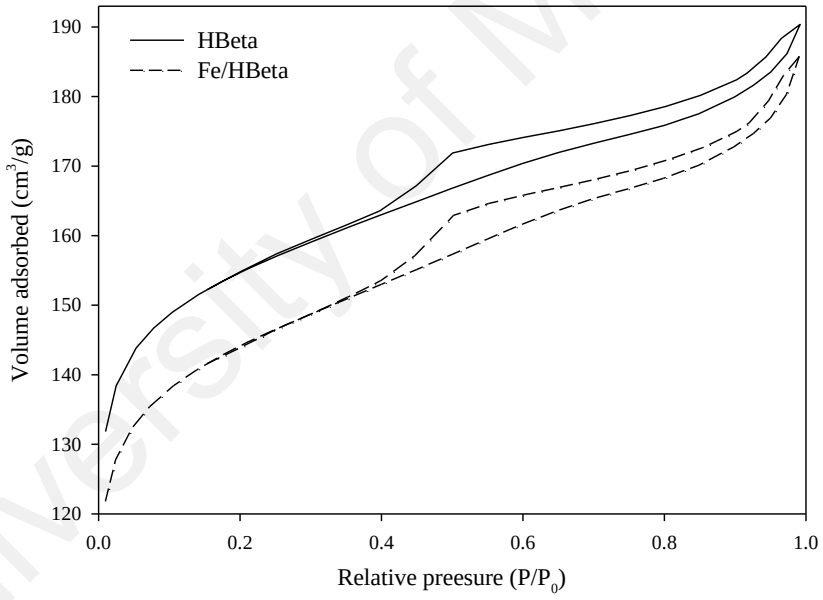

Figure 4.2: Nitrogen adsorption-desorption isotherms of HBeta and Fe/HBeta.

Table 4.1: Textural properties of HBeta and Fe/HBeta.

Sample	S_{BET}[a] ($m^2 g^{-1}$)	S_{meso}[b] ($m^2 g^{-1}$)	S_{BET}/S_{meso}	V_{total}[c] ($cm^3 g^{-1}$)	V_{micro}[d] ($cm^3 g^{-1}$)	V_{meso}[e] ($cm^3 g^{-1}$)	d[f] (nm)
HBeta	502	118	4.25	0.294	0.188	0.106	6.672
Fe/HBeta	471	123	3.83	0.287	0.169	0.118	6.815
HBeta[g] (MeOH[h]-450 °C)	497	120	4.14	0.291	0.177	0.114	6.586
HBeta[g] (MeOH-350 °C)	494	122	4.05	0.282	0.173	0.109	6.611
HBeta[g] (MeOH/Cresol-450 °C)	465	131	3.55	0.258	0.136	0.122	6.457
HBeta[g] (MeOH/Phenol-450 °C)	436	128	3.41	0.243	0.111	0.132	6.348
HBeta[g] (MeOH/Cresol-350 °C)	397	134	2.96	0.223	0.096	0.127	6.112
HBeta[g] (MeOH/Phenol-350 °C)	355	137	2.59	0.211	0.073	0.138	5.819

[a] Calculated in the range of relative pressure (P/P_0) = 0.05-0.25.
[b] Evaluated by t-plot method.
[c] Total pore volume evaluated at $P/P_0 = 0.99$.
[d] Evaluated by t-plot method.
[e] $V_{meso} = V_{total} - V_{micro}$.
[f] BJH adsorption average pore width.
[g] Used HBeta (WHSV, 2 h^{-1}; time on stream: 60 min; carrier gas, N_2)
[h] MeOH: methanol.

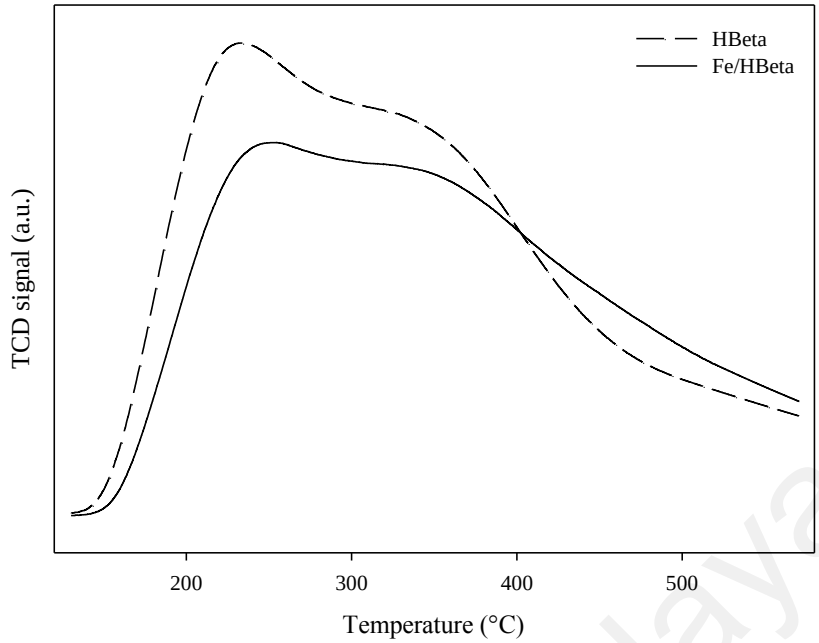

Figure 4.3: NH_3-TPD profiles of HBeta and Fe/HBeta.

4.1.2 Catalytic activity

The yields and selectivities of the products obtained from catalytic reactions at 350 °C are presented in Table 4.2. HBeta zeolite was efficient for transformation of methanol to aromatic hydrocarbons, and aromatics yield of 59.6 wt% was achieved using this catalyst. The main aromatic hydrocarbons detected in liquid product were xylene, trimethylbenzene, ethyl-methylbenzene and tetramethylbenzene. When *m*-cresol was co-fed with methanol at low amount of 10 wt%, aromatics yield was 24.3 wt% which was 59% lower than that obtained from pure methanol. Cresol, phenol, xylenol, ethylphenol, trimethylphenol and some other oxygenate compounds were also detected in the liquid product from conversion of mixture of methanol/*m*-cresol over HBeta. Compered to *m*-cresol, addition of 10 wt% phenol to methanol caused much more negative effect on catalytic performance of HBeta, and the aromatics yield achieved from mixture of methanol/phenol was only 6.2 wt%. Furthermore, as shown in Table 4.3, the amount of coke deposited on HBeta in the conversion of methanol at 350 °C was 0.22 wt% which was increased to 2.61 and 3.48 wt% in the conversion of mixtures of methanol/*m*-cresol and methanol/phenol, respectively. The data in Table 4.3 are given by TGA results

presented in Figure 4.4. Meanwhile in transformation of pure *m*-cresol over HBeta under hydrogen atmosphere, low yield of aromatics (2.6 wt%) was obtained. Iron incorporated HBeta showed to be effective for deoxygenation of *m*-cresol through hydrogenolysis. In the transformation of *m*-cresol over Fe/HBeta, aromatics yield of 17.5 wt% was achieved. At temperature of 350 °C, WHSV of 2 h^{-1} and under hydrogen atmosphere, 58.5 wt% of *m*-cresol was converted mostly to phenol, trimethylbenzene, xylene and ethyl-methylbenzene. However, when 10 wt% phenol was co-fed with *m*-cresol, cresol conversion and aromatics yield were reduced to 30.1 and 3.2 wt%, respectively. This clearly shows the significance of negative effect of phenol on catalytic performance of Fe/HBeta. In another experiment under similar reaction conditions, Fe/HBeta was used for conversion of pure phenol, but the yield of hydrocarbons detected in liquid product was very low (below 0.3 wt%).

Table 4.2: Product yields and selectivities (wt%) obtained from catalytic conversion of different reactants over HBeta and Fe/HBeta. Reaction conditions: WHSV, 2 h^{-1}; reaction temperature, 350 °C; pressure, 1 atm.

Feed **Catalyst** **Gas**	**MeOH**[a] **HBeta** **N_2**	**MeOH-Cresol** **HBeta** **N_2**	**MeOH-Phenol** **HBeta** **N_2**	**Cresol** **HBeta** **H_2**	**Cresol** **Fe/HBeta** **H_2**	**Cresol-Phenol** **Fe/HBeta** **H_2**
% Yield of organic phase						
	59.62	32.58	13.96	87.29	83.34	81.50
% Selectivity in organic phase						
Toluene				0.23	1.53	0.22
Xylene	41.68	32.47	19.91	0.64	5.00	0.85
Ethyl-methylbenzene	15.93	12.12	7.59	0.34	4.24	1.09
Trimethylbenzene	28.65	20.35	10.96	0.57	5.51	0.89
Tetramethylbenzene	6.81	3.68	1.72	0.18	1.19	0.16
Naphthalenes				0.30	1.31	0.20
Other hydrocarbons	6.93	5.89	3.94	0.70	2.21	0.47
Phenol		8.48	42.34	25.83	11.43	17.97
Cresol		13.57	8.88	60.72	49.82	73.48
Other oxygenates		3.44	4.66	10.49	17.76	4.67

[a] MeOH: methanol.

Table 4.3: Coke deposition on HBeta and Fe/HBeta for different reactants at reaction temperatures of 350 and 450 °C. Reaction conditions: WHSV, 2 h^{-1}; time on stream: 60 min; pressure, 1 atm.

Feed **Catalyst** **Gas**	**MeOH**[a] **HBeta** **N_2**	**MeOH-Cresol** **HBeta** **N_2**	**MeOH-Phenol** **HBeta** **N_2**	**Cresol** **Fe/HBeta** **H_2**	**Cresol-Phenol** **Fe/HBeta** **H_2**
% $g_{coke}/g_{catalyst}$					
350 °C	0.22	2.61	3.48	9.33	11.86
450 °C	0.28	1.52	1.94	6.11	7.02

[a] MeOH: methanol.

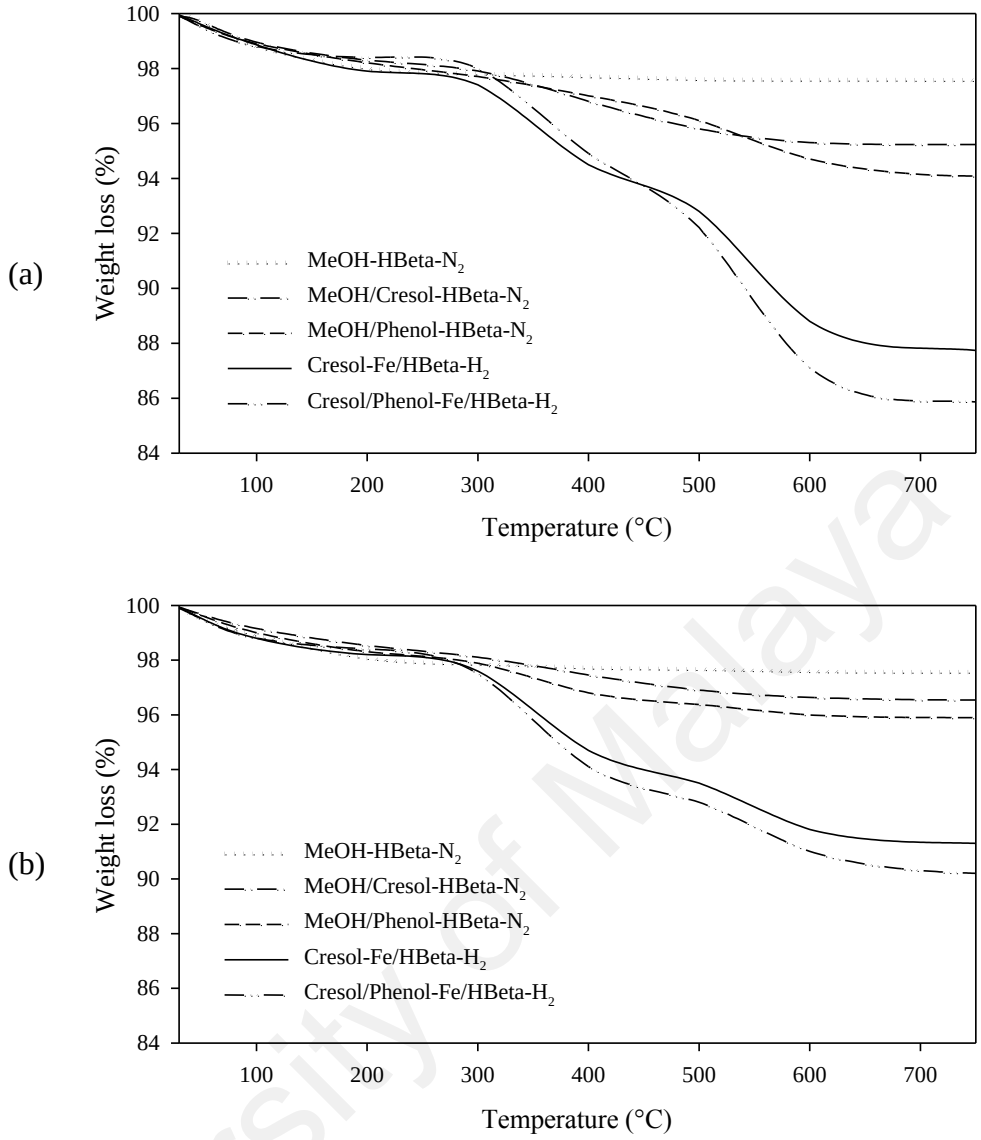

Figure 4.4: TGA curve of the spent catalysts used in different reactant systems at 350 °C (a) and 450 °C (b) (WHSV, 2 h^{-1}; time on stream: 60 min; pressure, 1 atm).

Methanol could be considered as representative for that part of biomass which has high potential to be deoxygenated at atmospheric pressure; methanol is easily transformed into aromatics with small amount of coke deposited on zeolite. It is well described in literature that lignin derived phenolic compounds have very low reactivity over zeolite acid sites. Mullen and Boateng (2010) revealed that phenols derived from *p*-hydroxyphenyl units of lignin are more difficult than other lignin derived phenols like guaiacols and syringols to be reacted over zeolite, and cause higher deactivation of catalyst. The reason for higher reactivity of guaiacols and syringols was mentioned to be the steric hindrance caused by the methoxy groups on the benzene ring of these compounds which prevents from tight

bond with zeolite acid sites leading to less coke formation and catalyst deactivation. As it was observed in this work, when 10 wt% *m*-cresol or phenol which are derivatives of *p*-hydroxyphenyl units of lignin was co-fed with methanol, aromatics yield of HBeta zeolite had a significant decrease. TPD profiles of fresh HBeta and HBeta used in different reactant systems shown in Figure 4.5 demonstrate that methanol transformation caused a slight reduction in the number of free acid sites. However TPD results for HBeta exposed to mixtures of methanol/*m*-cresol and methanol/phenol reveal that the number of zeolite acid sites occupied by catalytic coke significantly increased by co-feeding *m*-cresol or phenol. Furthermore, the data from nitrogen isothermal adsorption-desorption presented in Table 4.1 illustrate that mixtures of methanol/*m*-cresol and methanol/phenol led to much more reduction in surface area and volume of micropores of HBeta compared to pure methanol. These results are in agreement with the TGA data given in Table 4.3 showing that the amount of coke deposited on HBeta had a noticeable increase by addition of *m*-cresol or phenol to methanol. Therefore, the presence of these phenolic compounds result in high zeolite deactivation and in turn less aromatization of methanol. It is also clear from the data in Figure 4.5 and Table 4.1 that phenol caused a higher reduction in number of free acid sites and surface area of HBeta compered to *m*-cresol. This clearly indicates that phenol has more negative effect than *m*-cresol on catalytic performance of zeolite. The reason for this is the interaction between hydroxyl of phenol molecules and zeolite framework oxygen atoms producing phenolate ions which are strongly adsorbed on the oxygen atoms linked to framework aluminium (Graça et al., 2009). Meanwhile, the phenol molecules tightly bound to zeolite acid sites act as coke precursor and result in rapid formation of coke which is deposited on catalyst surface causing fast deactivation. But, *m*-cresol might have less potential to form a tight bond with acid sites due to the steric hindrance caused by the methyl group present on the phenolic ring of *m*-cresol. In fact, the steric bulk around the hydroxyl of *m*-cresol provided by the methyl

group prevents from the interaction between the hydroxyl and zeolite framework oxygen atoms. The significant effect of this steric hindrance is due to the confined space inside the micropores of HBeta where the reaction occurs. Furthermore, one other reason for lower aromatization of methanol in the presence of *m*-cresol or phenol could be some competing reactions which might occur by addition of these phenols. Since methanol could be used as alkylating agent for alkylation of phenolic compounds over zeolite, a fraction of methanol might be involved in alkylation reactions and not undergo deoxygenation and aromatization (Sad, Padró, & Apesteguía, 2008; Wang et al., 2004). Besides, transalkylation of aromatics produced from methanol with the co-fed phenols or the compounds produced from transformation of phenols could vary product distribution (Zhu, Lobban, Mallinson, & Resasco, 2011; Zhu, Mallinson, & Resasco, 2010). However, considering the significant reduction in number of free acid sites and surface area of HBeta exposed to *m*-cresol or phenol, it seems that catalyst deactivation is the main cause for less aromatization of methanol in the presence of these phenols.

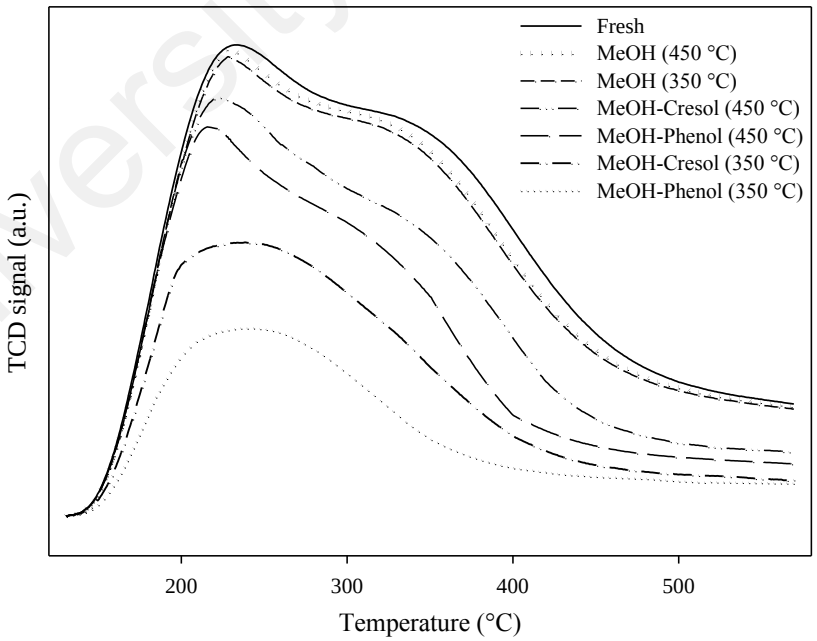

Figure 4.5: NH_3-TPD profiles of fresh HBeta and HBeta used in different reactant systems (WHSV, 2 h^{-1}; time on stream: 60 min; carrier gas, N_2).

It was shown in this study that bifunctional catalyst of HBeta impregnated with iron which promotes hydrogenolysis reaction was effective for cleavage of C-O bond of *m*-cresol under hydrogen atmosphere; *m*-cresol was transformed into aromatics with a noticeable yield of 17.5 wt% over Fe/HBeta. However, this catalyst was not efficient for deoxygenation of simple phenol molecule which, as mentioned above, is tightly bound to zeolite acid sites. It can be inferred that in transformation of *m*-cresol, the main source of catalyst deactivation is the adsorption of phenol molecules which are produced through demethylation of *m*-cresol. Therefore, reduction of reaction selectivity toward phenol production could increase lifetime of zeolite and its catalytic activity. Consequently, Fe/HBeta is expected to exhibit higher catalytic lifetime compared to HBeta when exposed to phenolic compounds; over Fe/HBeta and under hydrogen atmosphere, phenolic compounds could undergo hydrogenolysis and lower amount of phenol is produced and subsequently less adsorption of phenol on zeolite acid sites occurs compared to the case of using pure HBeta zeolite as catalyst. This study clearly demonstrates the undesired effect of phenol molecule on catalytic performance of zeolite in deoxygenation of biomass derived feedstocks; phenolic compounds not only have low reactivity over zeolite but also high potential of phenol molecule to be tightly bound to zeolite acid sites causes rapid catalyst deactivation. Therefore, it seems to be essential to use modified zeolites for catalytic conversion of feedstocks derived from biomass with high content of lignin.

Table 4.4 demonstrates the catalytic activity of HBeta and Fe/HBeta at reaction temperature of 450 °C. In conversion of methanol at this temperature, the aromatics yield of HBeta was 51.3 wt% while it was 59.6 wt% at 350 °C. Comparison of the data presented in Tables 4.2 and 4.4 reveals that negative effect of co-feeding phenol or *m*-cresol is reduced by increase of reaction temperature, and aromatics yield is less decreased by addition of these phenols at higher temperature of 450 °C. By co-feeding

m-cresol or phenol with methanol at 350 °C, the aromatics yield of HBeta was decreased from 59.6 to 24.3 and 6.2 wt%, respectively. However at 450 °C, the presence of *m*-cresol or phenol in feed mixture caused less influence on HBeta performance and aromatics yield decreased from 51.3 to 36.7 and 12.3 wt%, respectively. As can be seen from TPD profiles in Figure 4.5, in the transformation of mixtures of methanol/*m*-cresol and methanol/phenol over HBeta, the reduction in the number of zeolite free acid sites at reaction temperature of 450 °C was lower than that at 350 °C. Meanwhile, the data in Table 4.1 indicate that surface area and pore volume of HBeta were less affected in the presence of *m*-cresol or phenol at 450 °C compared to 350 °C. Also as shown in Table 4.3, the coke content of spent HBeta was decreased at elevated temperature. Similarly, the increase of temperature attenuated the negative effect of phenol on catalytic activity of Fe/HBeta; in transformation of *m*-cresol over Fe/HBeta, phenol addition led to reduction of *m*-cresol conversion and aromatics yield from 58.5 and 17.5 to 30.1 and 3.2 wt% at 350 °C, and from 74.7 and 30.3 to 42.0 and 10.6 wt% at 450 °C, respectively. As can be observed in Table 4.3, the amount of coke deposited on catalyst is less increased by addition of phenol or *m*-cresol at reaction temperature of 450 °C compared to 350 °C. For instance, addition of 10 wt% phenol to *m*-cresol at 350 °C caused an increase of 2.53 wt% in the coke content of Fe/HBeta (from 9.33 to 11.86 wt%). However, presence of phenol led to less increase of 0.91 wt% of coke content (from 6.11 to 7.02 wt%) at 450 °C. Therefore, it can be inferred that increase of temperature led to lower adsorption of phenolic compounds on zeolite acid sites causing less catalyst deactivation. One reason for this is that increase of temperature leads to increase in diffusion rate of phenol molecules in the pores of catalyst and reduces the possibility of phenol adsorption on zeolite acid sites. Graça et al. (2009) revealed that increase of temperature did not result in less adsorption of phenol on HZSM-5 zeolite in transformation of mixture of methylcyclohexane/phenol. They concluded that the 10-membered ring channels of

HZSM-5 are too narrow which cause slow diffusion of phenol molecules even at higher temperature of 450 °C. However, HBeta zeolite used in this work contains 12-membered ring channels (0.66 × 0.67 and 0.56 × 0.56 nm) which are larger than HZSM-5 channels (0.51 × 0.55 and 0.53 × 0.56 nm) (Jae et al., 2011). Therefore, increase of reaction temperature might cause faster diffusion of phenol molecules in at least the larger channel (0.66 × 0.67) of HBeta resulting in less adsorption of phenol on zeolite acid sites and in turn lower formation of coke and catalyst deactivation. The other reason for the positive effect of temperature increase is the exothermic nature of phenol adsorption. Therefore at higher temperature, less phenol molecules can be tightly bound to acid sites. In fact, less number of zeolite acid sites, only those with high acidic strength, can adsorb and retain phenol molecules at elevated temperature. As can be seen from the TPD profiles shown in Figure 4.3, desorption peak temperatures for HBeta and Fe/HBeta were below 350 °C illustrating that the majority of acid sites of HBeta or Fe/HBeta are not of high acidic strength. Therefore by increase of reaction temperature, the number of acid sites of these zeolites which could adsorb and retain phenol molecules was noticeably decreased (Figure 4.5), resulting in less catalyst deactivation at 450 °C compared to 350 °C. This can be another reason why phenol adsorption on HZSM-5 was not decreased by increase of temperature in the study held by Graça et al. (2009). HZSM-5 mostly shows two TPD peaks with one at temperature above 400 °C (Kim, Choi, & Ryoo, 2010; Liu et al., 2014; Ni et al., 2011). Therefore, HZSM-5 contains considerable density of strong acid sites which probably could still adsorb phenol molecules at higher temperature of 450 °C. The dependency of phenol adsorption on strength of acid sites is also shown in Figure 4.5; it can be seen from TPD profiles that strong acid sites had higher reduction compared to weak acid sites, and the acid sites of very low strength were only affected at 350 °C. As a result, it can be concluded that higher reaction temperature as well as the use of zeolite

with larger pore size and lower density of strong acid sites could be efficient for atmospheric deoxygenation of phenolic compounds.

Table 4.4: Product yields and selectivities (wt%) obtained from catalytic conversion of different reactants over HBeta and Fe/HBeta. Reaction conditions: WHSV, 2 h^{-1}; reaction temperature, 450 °C; pressure, 1 atm.

Feed	**MeOH[a]**	**MeOH-Cresol**	**MeOH-Phenol**	**Cresol**	**Cresol-Phenol**
Catalyst	**HBeta**	**HBeta**	**HBeta**	**Fe/HBeta**	**Fe/HBeta**
Gas	**N_2**	**N_2**	**N_2**	**H_2**	**H_2**
% Yield of organic phase					
	51.27	45.48	20.69	85.27	83.19
% Selectivity in organic phase					
Toluene				3.39	1.11
Xylene	40.10	34.17	25.62	9.31	3.25
Ethyl-methylbenzene	22.12	19.81	15.51	7.49	3.32
Trimethylbenzene	24.52	16.14	10.97	9.17	2.86
Tetramethylbenzene	6.14	2.92	1.30	1.51	0.49
Naphthalenes				1.55	0.53
Other hydrocarbons	7.12	7.61	5.99	3.08	1.21
Phenol		8.14	30.98	15.80	20.87
Cresol		9.08	6.34	29.69	57.65
Other oxygenates		2.13	3.29	19.01	8.71

[a] MeOH: methanol.

4.2 Aromatic hydrocarbon production by catalytic pyrolysis of palm kernel shell waste using a bifunctional Fe/HBeta catalyst: effect of lignin-derived phenolics on zeolite deactivation

4.2.1 Biomass feedstock properties

On the dry basis, the approximate molecular formula of Palm kernel shell (PKS) was $C_{4.1}H_{5.5}O_{2.7}$. PKS has high content of lignin (50.7 wt%), and cellulose and hemicellulose constitute 20.8 and 22.7 wt% of PKS, respectively (Mohammed et al., 2011). The proximate analysis result is 2.8 wt% moisture, 67.9 wt% volatiles, 13.0 wt% fixed carbon and 16.3 wt% ash. The elemental analysis showed 49.05 wt% carbon, 5.59 wt% hydrogen, 44.22 wt% oxygen (by difference), 0.76 wt% nitrogen and 0.38 wt% sulfur. Nitrogen and sulfur containing compounds might cause poisoning effect on catalytic activity of metal and acid sites (Augusto, Zotin, & Faro, 2001; Thilakaratne, Wright, & Brown, 2014). In catalytic pyrolysis of Kraft lignin over HZSM-5, Li et al. (2012) showed that sulfur has negative effect, and increase in sulfur content of feedstock resulted in lower aromatic hydrocarbon yield and higher coke formation. However, the probable poisoning caused by nitrogen or sulfur containing compounds is expected to be negligible in this work due to the low content of nitrogen and sulfur in PKS.

4.2.2 Physicochemical characteristics of catalysts

Figure 4.6a presents the XRD patterns of HBeta and Fe/HBeta. No distinct difference in crystallinity between HBeta and Fe/HBeta indicates that crystalline structure of HBeta was relatively unchanged by incorporation of Fe. Fe is believed to be well dispersed on HBeta surface since no iron species were detected in XRD analysis of Fe/HBeta. The amount of Fe loading measured by XRF analysis was 1 wt%. Textural properties of HBeta, Fe/HBeta and HZSM-5 (SiO_2/Al_2O_3 molar ratio: 50) evaluated from nitrogen isothermal adsorption-desorption are shown in Table 4.5. Incorporation of 1 wt% Fe into

HBeta reduced 6% of its BET surface area, and this reduction was only occurred in micropores. As shown in Figure 4.6b, all zeolites displayed type IV isotherm with H4-type hysteresis loop indicating the predominance of microporous structure in these catalysts. As presented in Table 4.5, the surface area and volume of micropores are larger than those of meso- and macropores. The acidity of catalysts determined by NH_3-TPD analysis is depicted in Figure 4.6c. HBeta exhibited two ammonia desorption peaks at 232 and 328 °C, while desorption peak temperatures for Fe/HBeta were 248 and 322 °C. HZSM-5 also displayed two desorption peaks which were at 226 and 382 °C. The peak area of Fe/HBeta was lower than that of HBeta demonstrating the reduction in the density of acid sites caused by Fe loading. Quantitative analysis showed that the total amount of acid sites in HBeta, Fe/HBeta and HZSM-5 was 0.71, 0.62 and 0.67 mmol/g, respectively. H_2-TPR profile of Fe/HBeta shown in Figure 4.6d indicates the reducibility of catalyst below 450 °C which was selected as the temperature for reduction of Fe/HBeta used for catalytic pyrolysis. In a study held by Nie et al. (2014) for conversion of *m*-cresol to toluene, reduction of Fe/SiO_2 was carried out at similar temperature of 450 °C which was suitable for catalyst activation.

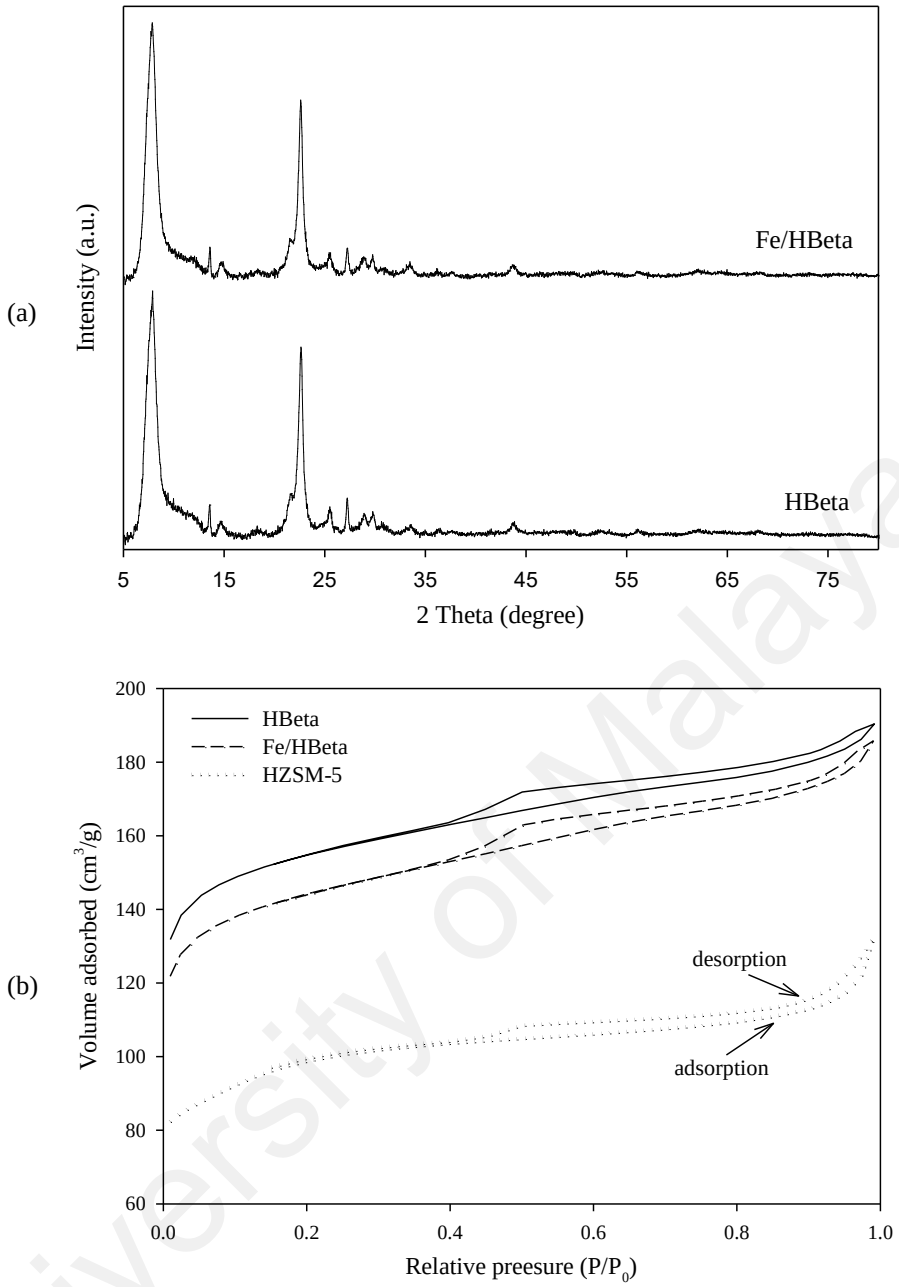

Figure 4.6: X-ray diffraction (a), nitrogen adsorption-desorption isotherm (b), NH_3-TPD (c) and H_2-TPR (d) profiles of catalysts.

(c)

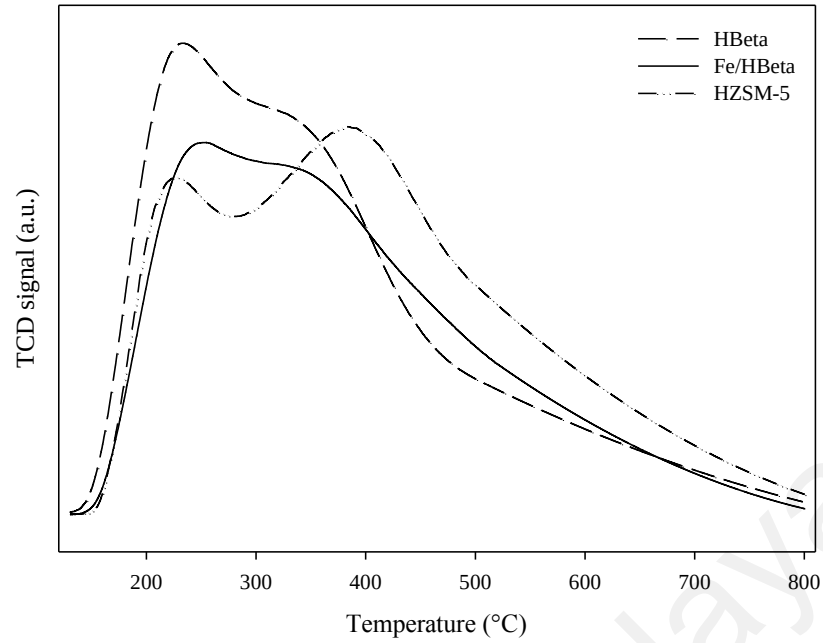

(d)

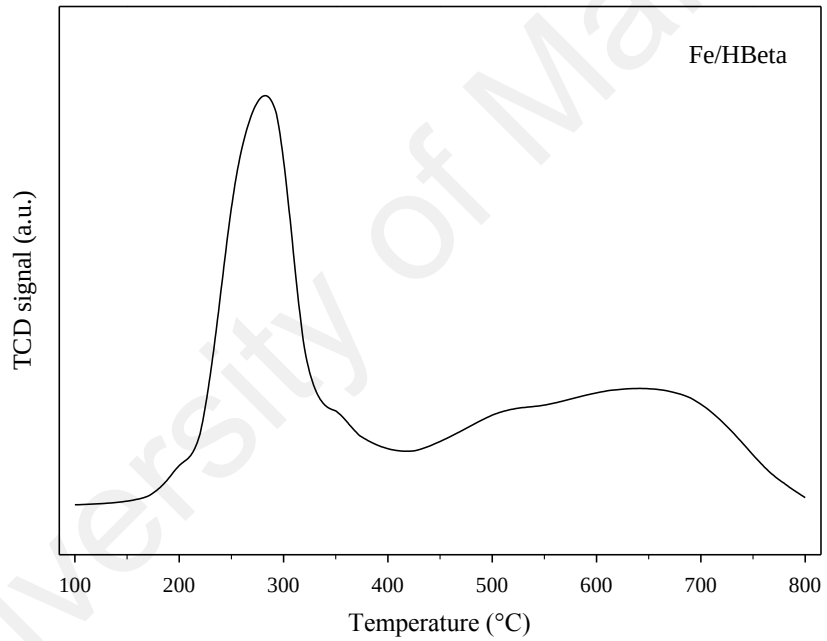

'Figure 4.6, continued'

Table 4.5: Textural properties of catalysts.

Sample	**S_{BET}[a] ($m^2 g^{-1}$)**	**S_{meso}[b] ($m^2 g^{-1}$)**	**S_{BET}/S_{meso}**	**V_{total}[c] ($cm^3 g^{-1}$)**	**V_{micro}[d] ($cm^3 g^{-1}$)**	**$V_{meso/macro}$[e] ($cm^3 g^{-1}$)**
HBeta	502	118	4.25	0.294	0.188	0.106
Fe/HBeta	471	123	3.83	0.287	0.169	0.118
HZSM-5	325	110	2.95	0.205	0.104	0.101
Fe/HBeta[f] (regenerated)	463	117	3.96	0.276	0.161	0.115

[a] Calculated in the range of relative pressure (P/P_0) = 0.05-0.25.
[b] Evaluated by t-plot method.
[c] Total pore volume evaluated at $P/P_0 = 0.99$.
[d] Evaluated by t-plot method.
[e] $V_{meso/macro} = V_{total} - V_{micro}$.
[f] Fe/HBeta regenerated after use for catalytic pyrolysis of PKS.

4.2.3 Catalytic activity

4.2.3.1 Catalytic pyrolysis of cellulose and lignin

Table 4.6 presents the yields of gas, liquid and solid products obtained from non-catalytic and catalytic pyrolysis of cellulose and lignin under different reaction conditions. It was observed that HBeta was efficient catalyst for deoxygenation of cellulose; over HBeta and under inert atmosphere of nitrogen, 21.38 wt% of cellulose was converted to the oil fraction with aromatic hydrocarbons selectivity of 87.1 wt%. Toluene, xylene, trimethylbenzene and ethyl-methylbenzene were the main aromatic hydrocarbons achieved from cellulose pyrolysis over HBeta. However, this catalyst was not effective for deoxygenation of lignin; the yield of oil produced from conversion of lignin over HBeta under nitrogen atmosphere was 27.41 wt% which its aromatic hydrocarbon content was only 3.5 wt%. Meanwhile, approximately similar yield of aromatic hydrocarbons was obtained from catalytic pyrolysis of lignin over HBeta using hydrogen as carrier gas. The lignin-derived oil was mostly composed of phenolic compounds such as phenol, cresol, xylenol, guaiacol, trimethylphenol and ethylphenol. As shown in Table 4.6, there is a great difference in catalytic performance of HBeta for deoxygenation of cellulose and lignin; this catalyst resulted in aromatic hydrocarbons yields of 18.62 and 0.95 wt% from pyrolysis of cellulose and lignin, respectively. This is caused by difference in the molecular structure of these polymers and different reaction pathways taken place for their conversion into aromatic hydrocarbons. Cellulose is an organic polymer consisting a linear chain made of β-D-glucose units. Cellulose pyrolysis results in production of volatile organics, gases and coke. The volatile organics are dehydrated in heterogeneous catalyst or in homogeneous gas phase. Over zeolite acid sites, the dehydrated species (furans) are converted into aromatics through decarbonylation of furans to allene followed by oligomerization of the allene to olefins which react with furans to form aromatics (Cheng, Jae, et al., 2012). Lignin is an irregular, three-dimensional polymer

made of coumaryl, coniferyl and sinapyl alcohols. Lignin is converted to phenolic compounds through catalytic cracking over zeolite acid sites or thermal cracking. It is well described in literature that phenolics have low reactivity over zeolite (Gayubo, Aguayo, Atutxa, Aguado, & Bilbao, 2004). This low reactivity causes low yield of aromatic hydrocarbons in atmospheric transformation of lignin over HBeta. The other reason for low conversion of lignin into aromatic hydrocarbons is rapid zeolite deactivation due to high potential of lignin-derived phenols to be tightly bound with zeolite acid sites (Graça, Comparot, et al., 2009; Graça et al., 2010; Graça et al., 2009; Mullen & Boateng, 2010). The reason for this tight bond is the interaction between the hydroxyl of phenolic ring and zeolite framework oxygen atoms producing phenolate ions which are strongly adsorbed on the oxygen atoms linked to framework aluminium (Graça et al., 2009). The strong adsorption of phenols leads to reduction in the number of free acid sites which can participate in reaction. Figure 4.7 depicts the TPD profiles of fresh HBeta and HBeta used in pyrolysis of cellulose, lignin and PKS. It can be seen from TPD results that lignin caused highest reduction in the number of zeolite free acid sites, and PKS with about 50 wt% lignin content led to higher occupation of acid sites compared to cellulose; the total amount of acid sites in the HBeta used for conversion of cellulose, PKS and lignin was 0.63, 0.40 and 0.30 mmol/g, respectively. This is due to strong adsorption of lignin-derived phenols which occupy zeolite acid sites and cause catalyst deactivation. Besides, the adsorbed phenols could act as coke precursor and cause high formation of coke which could block zeolite channels; as shown in Table 4.6, lignin resulted in higher yield of coke compared to cellulose. The adsorption of lignin-derived phenols is confirmed by the IR spectra of the coked HBeta used for catalytic pyrolysis of different feedstocks of lignin, cellulose and PKS (Figure 4.8). The two bands appeared at 1504 and 1593 cm^{-1} in the IR spectra of the HBeta exposed to lignin and PKS are characteristic of C-C stretching vibrations in phenol (Beutel, 1998; Graça, Comparot, et

al., 2009; Graça et al., 2010; Graça et al., 2009). However, no band attributed to phenol was displayed in the spectra of the catalyst exposed to cellulose. As mentioned above, strong adsorption of phenolics on acid sites causes catalyst deactivation since acid sites occupied by adsorbed phenolics are no longer involved in reaction. Meanwhile, adsorbed phenolics act as coke precursor and result in high yield of coke and catalyst deactivation; high deposition of coke on catalyst could cause pore blockage preventing from diffusion of large molecules into catalyst, and reduces the diffusion rate of reactants inside catalyst channels. Besides, coke deposits could cover catalyst active sites and reduce their accessibility for reactants. Among the three lignin monomers, phenols derived from coniferyl and sinapyl alcohols (guaiacols and syringols) have higher reactivity over zeolite acid sites compared to simple phenolics like phenol or cresol which are derived from coumaryl alcohol (Mullen & Boateng, 2010). The reason for this is that the methoxy groups on the benzene ring of guaiacols and syringols cause steric hindrance which prevents from tight bond with zeolite acid sites.

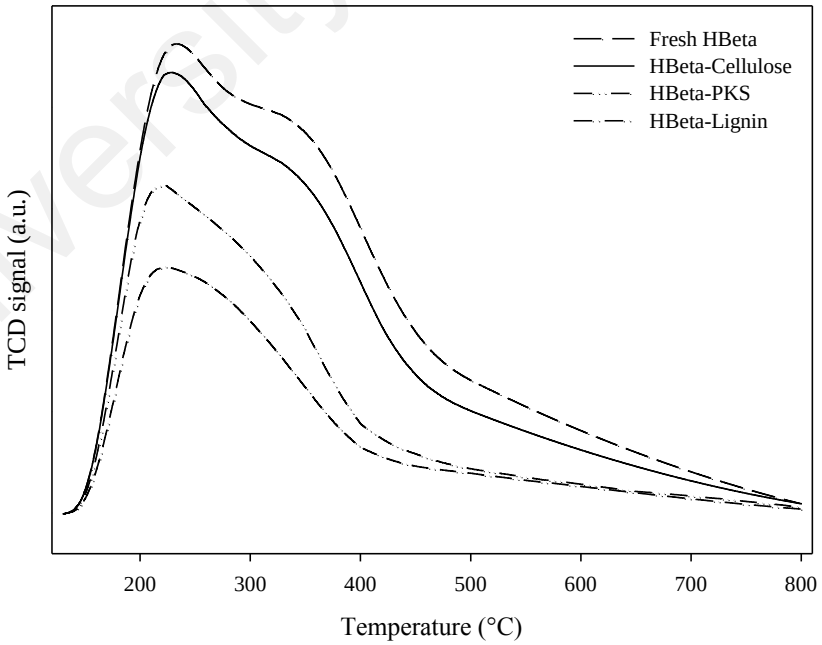

Figure 4.7: NH_3-TPD profiles of fresh HBeta and HBeta used in catalytic pyrolysis of cellulose, lignin and PKS (WHSV, 6 h^{-1}; time on stream, 60 min; carrier gas, N_2).

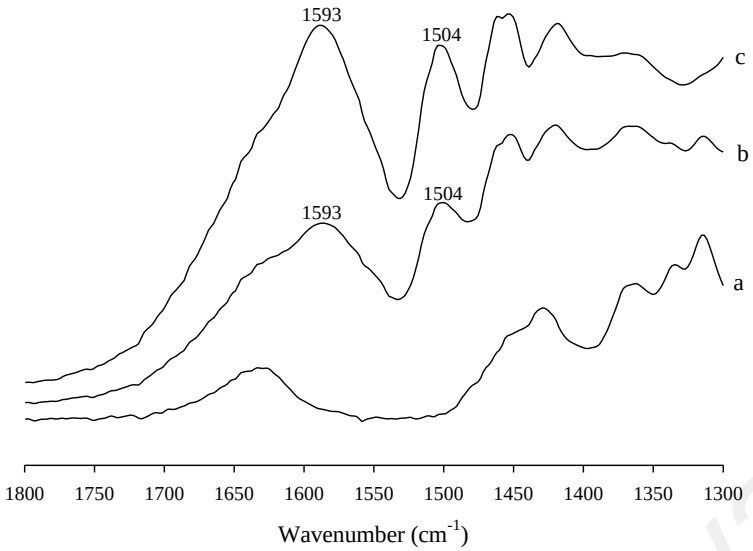

Figure 4.8: 1300-1800 cm^{-1} region of the FTIR spectra of the HBeta used in catalytic pyrolysis of cellulose (a), PKS (b) and lignin (c) (WHSV, 6 h^{-1}; time on stream, 60 min; carrier gas, N_2).

Table 4.6: Product yields (wt% on feed) and composition of organic phase of liquid product (wt% on organics) obtained from non-catalytic and catalytic pyrolysis of cellulose and lignin. Reaction conditions: WHSV, 6 h^{-1}; reaction temperature, 500 °C; pressure, 1 atm; time on stream, 60 min.

Feed	**Cellulose**	**Cellulose**	**Cellulose**	**Cellulose**	**Lignin**	**Lignin**	**Lignin**	**Lignin**
Catalyst	**non-catalytic**	**HBeta**	**Fe/HBeta**	**Fe/HBeta**	**non-catalytic**	**HBeta**	**Fe/HBeta**	**Fe/HBeta**
Carrier gas	**N_2**	**N_2**	**N_2**	**H_2**	**N_2**	**N_2**	**N_2**	**H_2**
% Yield								
Oil	30.42	21.38	21.19	20.85	31.30	27.41	24.76	15.90
Gas	33.50	39.16	39.41	39.77	13.24	13.53	14.49	17.83
Aqueous fraction	16.19	18.32	18.52	18.57	9.54	10.83	12.94	18.97
Char/Coke	19.89/0	19.71/1.43	19.48/1.40	20.04/0.77	45.92/0	46.10/2.13	45.74/2.07	45.53/1.77
% Yield of aromatic hydrocarbons								
	0.79	18.62	18.80	20.14	0.08	0.95	1.72	5.13
% Selectivity in organic phase of liquid product								
Benzene	0.14	0.73	1.28	2.92	0.02	0.07	0.16	0.89
Toluene	0.66	23.41	22.20	21.64	0.08	0.28	0.51	2.84
Xylene	0.61	20.86	19.33	19.37	0.06	0.95	1.90	8.33
Ethyl-methylbenzene	0.48	7.71	8.11	10.65		0.53	1.57	7.35
Trimethylbenzene		10.06	12.61	14.01		0.41	1.23	7.67
Tetramethylbenzene		1.69	2.14	3.12		0.20	0.36	1.14
Naphthalenes	0.46	15.88	16.02	16.46	0.05	0.39	0.42	1.76
Other hydrocarbons	0.25	6.75	7.03	8.41	0.05	0.64	0.80	2.28
Phenol	3.12	1.86	1.49	0.49	52.15	45.80	43.27	31.86
Cresol	1.89	1.56	1.17	0.25	20.59	22.39	19.44	13.31
Xylenol					5.30	8.84	9.02	7.88
Trimethylphenol					3.05	4.70	5.09	3.28
Ethylphenol					2.47	2.33	2.60	2.00
Guaiacol					9.96	8.34	8.95	6.41
Furfural	18.94	5.91	5.38	1.49				
Benzenediol	0.33				1.52	1.90	2.56	1.19
Other oxygenates	73.12	3.58	3.24	1.19	4.70	2.23	2.12	1.81

A bifunctional iron impregnated HBeta catalyst showed to be efficient for atmospheric deoxygenation of lignin. In the transformation of lignin over Fe/HBeta, catalytic cracking occurs over zeolite acid sites to produce phenolic compounds. Then, the produced phenols are deoxygenated to aromatic hydrocarbons mainly through hydrogenolysis reaction promoted by Fe active sites (Scheme 4.1). As shown in Table 4.6, use of Fe/HBeta in pyrolysis of lignin resulted in higher selectivity towards aromatic hydrocarbons compared to pure HBeta. Meanwhile, change of carrier gas from nitrogen to hydrogen led to increase of aromatic hydrocarbon production from lignin due to enhancement of hydrogenolysis reaction in the presence of H_2 gas. In lignin pyrolysis over Fe/HBeta under hydrogen atmosphere, aromatic hydrocarbons content of oil fraction and total yield of aromatic hydrocarbons were 32.3 and 5.13 wt%, respectively, which are considerably higher than those obtained from lignin conversion over HBeta using nitrogen as carrier gas. Meanwhile, use of Fe/HBeta and H_2 gas led to lower yield of oil fraction which is due to higher deoxygenation. From the yields of aromatic hydrocarbons produced over HBeta and Fe/HBeta, it could be inferred that turnover frequency of Fe active sites for conversion of phenolic compounds into aromatic hydrocarbons is higher than that of zeolite acid sites. One other reason for higher deoxygenation of lignin over Fe/HBeta could be less catalyst deactivation due to lower reaction selectivity towards simple phenolics like phenol and cresols; over iron incorporated zeolite, heavier phenolics especially those derived from coniferyl and sinapyl alcohols could be deoxygenated over Fe active sites through hydrogenolysis prior to being transformed to simple phenolics like phenol and cresols which have higher potential to form tight bond with zeolite acid sites. Therefore, by presence of Fe active sites in zeolite structure, the amount of adsorbed phenols which act as coke precursor is reduced leading to lower occupation of zeolite acid sites and less pore blockage. By comparison between TPD profiles of spent HBeta and Fe/HBeta used for conversion of lignin (shown in Figure 4.9), it can be seen that Fe/HBeta

had less occupied acid sites compared to HBeta; the total amount of acid sites of HBeta reduced from 0.71 to 0.30 mmol/g, while that of Fe/HBeta decreased from 0.62 to 0.35 mmol/g. This illustrates that presence of Fe active sites caused less adsorption of phenolics on zeolite acid sites. Meanwhile as shown in Table 4.6, the coke yield in catalytic pyrolysis of lignin was considerably reduced by replacement of HBeta and nitrogen gas with Fe/HBeta and hydrogen (from 2.13 to 1.77 wt%). However, Fe/HBeta under nitrogen atmosphere resulted in coke yield of 2.07 wt% which is approximately similar to that of HBeta. The reason for this is that hydrogenolysis is not effectively promoted by Fe active sites in the absence of H_2 gas. Furthermore, as presented in Table 4.6, no noticeable improvement was observed by the use of Fe/HBeta and H_2 gas in pyrolysis of cellulose demonstrating that deoxygenation of cellulose derived compounds could effectively occur over zeolite acid sites. Scheme 4.2 shows all the reactions carried out over Fe/HBeta catalyst for the conversion of lignin and cellulose fractions of biomass into aromatic hydrocarbons.

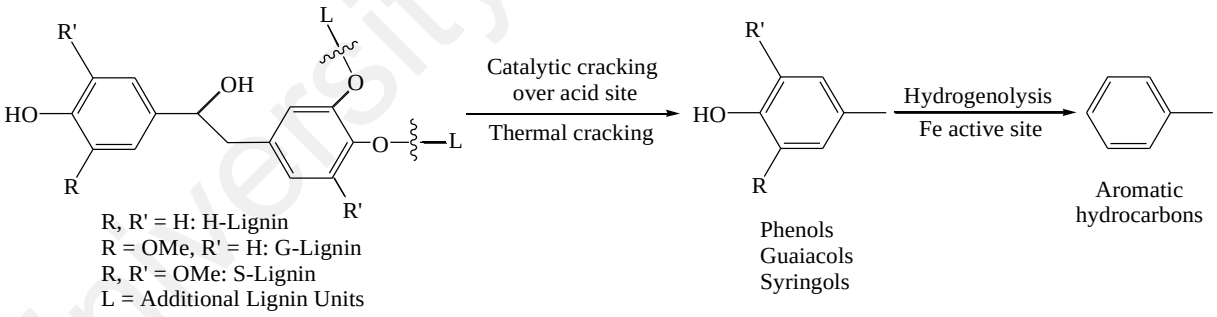

Scheme 4.1: Major reaction pathway for catalytic pyrolysis of lignin over Fe/HBeta. H-lignin, G-lignin and S-lignin represent for *p*-hydroxyphenyl, guaiacyl and syringyl subunits of lignin which are converted to phenols, guaiacols and syringols, respectively.

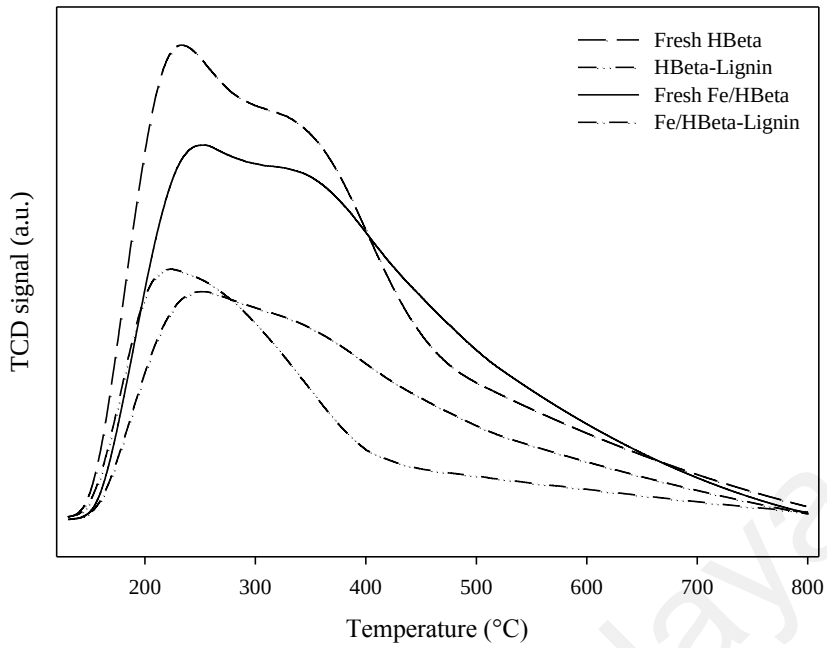

Figure 4.9: NH_3-TPD profiles of spent HBeta and Fe/HBeta used in catalytic pyrolysis of lignin (WHSV, 6 h^{-1}; time on stream, 60 min; carrier gas, N_2 for HBeta and H_2 for Fe/HBeta).

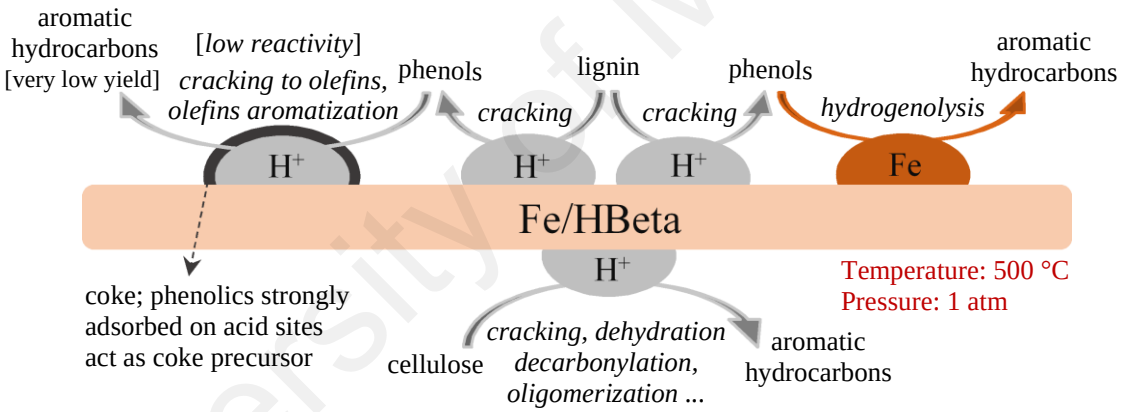

Scheme 4.2: Reactions carried out over Fe/HBeta catalyst for the conversion of lignin and cellulose fractions of biomass into aromatic hydrocarbons.

Metal-catalyzed hydrotreating of phenolic model compounds of lignin has been typically carried out using transition metals which are highly active for reactions involving hydrogen. Using bifunctional metal/zeolite catalyst, both metal and acid sites affect product distribution. Zeolite acid sites could influence product selectivity by promoting the reactions such as isomerization, transalkylation and alkylation (Zhu, Nie, Lobban, Mallinson, & Resasco, 2014). Two general pathways have been proposed in literature to illustrate the hydrodeoxygenation of phenolic model compounds of lignin: (i) hydrogenolysis (direct cleavage of $C_{aromatic}$-OH bonds of phenolic compounds) forming

aromatic hydrocarbons; (ii) hydrogenation of a phenolic ring forming cyclohexanones/cyclohexanols followed by dehydration of cyclohexanols to cyclohexenes and further hydrogenation of cyclohexenes to cyclohexanes (Chen et al., 2015; Zhu et al., 2011). No saturated cyclic compounds detected in the liquid product obtained using Fe/HBeta indicates that ring hydrogenation of phenolics did not occur over this catalyst, and hydrodeoxygenation proceeded through hydrogenolysis promoted by Fe active sites. This is in agreement with the studies held by Nie et al. (2014) and Olcese et al. (Olcese et al., 2012; Olcese, Francois, Bettahar, Petitjean, & Dufour, 2013) which reported that Fe is not a suitable metal for ring hydrogenation of phenolic model compounds of lignin. Therefore, Fe is a potential metal to be used for selective conversion of lignin into aromatic hydrocarbons. For ring hydrogenation of lignin model compounds, Ni and noble metals of Pt and Pd are the most commonly used metals reported in literature (Chen et al., 2015; Hellinger et al., 2015; Nie et al., 2014; Shin & Keane, 2000).

4.2.3.2 Catalytic pyrolysis of PKS

The yields of gas, liquid and solid products of non-catalytic and catalytic pyrolysis of PKS are presented in Table 4.7. Since in the pyrolyzer used in this study, biomass which is continuously fed to pyrolyzer is not in contact with catalyst bed (ex-situ pyrolysis), only thermal decomposition of biomass occurs and char yield is not affected by catalyst type and is almost constant in all runs. In this case, char yield is a function of pyrolysis temperature and heating rate, and could be reduced by increase of these operating parameters. As shown in Table 4.7, catalytic pyrolysis led to lower yield of oil as well as higher yields of gas and water compared to non-catalytic pyrolysis. This is due to higher amount of deoxygenation taken place in the presence of catalyst through reactions of decarbonylation, decarboxylation and dehydration as well as conversion to non-condensable compounds such as olefins. Furthermore, the use of bifunctional Fe/HBeta

catalyst and replacement of nitrogen with hydrogen as carrier gas resulted in higher reduction in the yield of produced oil due to promotion of hydrogenolysis reaction which, as mentioned before, results in deoxygenation of lignin-derived phenolic compounds. As shown in Table 4.7, almost no deoxygenation occurred in non-catalytic pyrolysis of PKS, and the hydrocarbon content of produced oil was about 0.5 wt%. The main compounds detected in the oil were phenol, cresol, furfural, xylenol, guaiacol and trimethylphenol. In pyrolysis of PKS using HBeta as catalyst, the yield of aromatic hydrocarbons was 1.86 wt%. These hydrocarbons are expected to be produced from conversion of cellulose and hemicellulose fractions of biomass, as it was observed in catalytic pyrolysis of lignin that HBeta is not a suitable catalyst for deoxygenation of lignin-derived phenolics. Fe/HBeta under nitrogen atmosphere resulted in relatively higher aromatic hydrocarbons yield of 3.21 wt% from conversion of PKS. By replacement of nitrogen with hydrogen, the aromatic hydrocarbons yield was remarkably increased to 9.37 wt%. The major aromatic hydrocarbons produced over Fe/HBeta under hydrogen atmosphere were xylene, toluene, trimethylbenzene and ethyl-methylbenzene. It is inferred from this study that pure zeolites are not efficient catalysts for deoxygenation of feedstocks derived from biomass with high content of lignin. Bifunctional catalysts containing promoter for hydrogenolysis could be useful for upgrading of such feedstocks.

Table 4.7: Product yields (wt% on feed) and composition of organic phase of liquid product (wt% on organics) obtained from non-catalytic and catalytic pyrolysis of PKS. Reaction conditions: WHSV, 6 h^{-1}; reaction temperature, 500 °C; pressure, 1 atm; time on stream, 60 min.

Catalyst **Carrier gas**	**HZSM-5** **N_2**	**HBeta** **N_2**	**Fe/HBeta** **N_2**	**Fe/HBeta** **H_2**	**Non-catalytic** **N_2**
% Yield					
Oil	22.56	23.22	22.40	14.76	30.73
Gas	25.70	25.12	24.92	28.69	20.51
Aqueous fraction	20.26	20.40	21.81	26.09	18.41
Char/Coke	29.68/1.80	29.56/1.70	29.24/1.63	29.29/1.17	30.35/0
% Yield of aromatic hydrocarbons					
	1.14	1.86	3.21	9.37	0.17
% Selectivity in organic phase of liquid product					
Benzene	0.09	0.17	0.31	2.95	0.03
Toluene	1.96	2.19	4.09	13.40	0.18
Xylene	1.52	1.80	3.31	15.71	0.09

'Table 4.7, continued'

Catalyst **Carrier gas**	**HZSM-5** **N_2**	**HBeta** **N_2**	**Fe/HBeta** **N_2**	**Fe/HBeta** **H_2**	**Non-catalytic** **N_2**
Trimethylbenzene	0.32	0.71	1.43	12.27	
Tetramethylbenzene	0.15	0.39	0.82	3.59	
Naphthalenes	0.43	1.20	2.18	6.39	0.15
Other hydrocarbons	0.20	0.99	1.07	2.06	0.10
Phenol	39.94	39.65	37.29	15.37	47.80
Cresol	19.27	18.13	16.33	7.40	16.09
Xylenol	9.44	9.11	8.60	3.28	6.01
Trimethylphenol	8.50	7.43	7.14	2.65	4.31
Ethylphenol	3.19	2.70	2.42	0.87	2.29
Guaiacol	4.16	4.02	3.70	1.73	5.27
Furfural	3.53	3.17	3.00	2.96	6.98
Benzenediol	2.03	2.25	1.93	0.49	1.43
Other oxygenates	4.89	5.53	5.26	1.77	9.27

4.2.3.3 Catalytic performance of HBeta *vs.* HZSM-5 in conversion of PKS

The results obtained from catalytic pyrolysis of PKS using HZSM-5 as catalyst are presented in Table 4.7. HZSM-5 resulted in low yield of aromatic hydrocarbons (1.14 wt%) approximately similar to the yield achieved by pure HBeta. However, HZSM-5 underwent higher deactivation compared to HBeta. As can be seen from TPD profiles in Figure 4.10, the reduction in the number of free acid sites of HZSM-5 was higher than that of HBeta; the total acid amount of HBeta reduced from 0.71 to 0.40 mmol/g, while that of HZSM-5 decreased from 0.67 to 0.20 mmol/g. As mentioned before, the origin of deactivation of zeolite acid sites in conversion of PKS is strong adsorption of lignin-derived phenolics on acid sites. Therefore, it could be inferred that lower adsorption of phenols occurred on HBeta compared to HZSM-5. This could be attributed to the difference in channel size of these zeolites. HZSM-5 contains 10-membered ring channels (0.51 × 0.55 and 0.53 × 0.56 nm), while the channels of HBeta are 12-membered ring (0.66 × 0.67 and 0.56 × 0.56 nm) (Jae et al., 2011). The larger channels of HBeta facilitate the diffusivity of phenolic molecules inside the catalyst channels, and diffusion rate is expected to be higher in HBeta compared to HZSM-5. Therefore, the possibility of adsorption of phenols on zeolite acid sites in HBeta is lower than that in HZSM-5, resulting in less deactivation of HBeta. Kinetic diameters of phenol, *o*-cresol, 2,3-xylenol

and anisole as some examples of the simplest lignin-derived phenolics with no methoxy group on the benzene ring are 0.55, 0.59, 0.60 and 0.61 nm, respectively ($\sigma = 2.44(T_c/P_c)^{1/3}$; σ: kinetic diameter (Å); T_c: critical temperature (K); P_c: critical pressure (atm)) (Jae et al., 2011). One other reason for higher adsorption of phenols on HZSM-5 could be higher percentage of strong acid sites of this zeolite compared to that of HBeta. The potential of zeolite acid sites to adsorb and retain phenolic molecules is enhanced by increase of their acidic strength. All the TPD profiles of spent catalysts in this work clearly indicate that strong acid sites were more occupied than weak acid sites illustrating the dependency of phenols adsorption on strength of acid sites. As can be seen from the distribution of strength of acid sites determined by TPD profiles of fresh HBeta and HZSM-5 shown in Figure 4.10, HZSM-5 contains higher percentage of strong acid sites, and the higher portion of acid sites of this zeolite could adsorb and retain phenolic molecules compared to HBeta, leading to higher deactivation of HZSM-5. Furthermore, higher adsorption of phenolics on HZSM-5 could also be due to the higher crystallite size of HZSM-5 used in this study compared to that of HBeta. Based on XRD data and Scherrer equation ($D = 0.9\lambda/\beta \cos\theta$; D: crystallite size; λ: X-ray wavelength; β: line broadening full width at half maximum (FWHM) after subtracting the instrumental line broadening (in radians); θ: Bragg angle), the average crystallite sizes of HBeta and HZSM-5 are 38.88 and 64.04 nm, respectively. In larger crystallites of HZSM-5 with longer diffusion path length, phenolics need to take longer path to diffuse out of zeolite channels and their chance of being adsorbed on acid sites is higher. It can be concluded that zeolites with larger pore size, smaller crystallites and lower percentage of strong acid sites could be more appropriate for atmospheric upgrading of biomass feedstocks with high content of lignin.

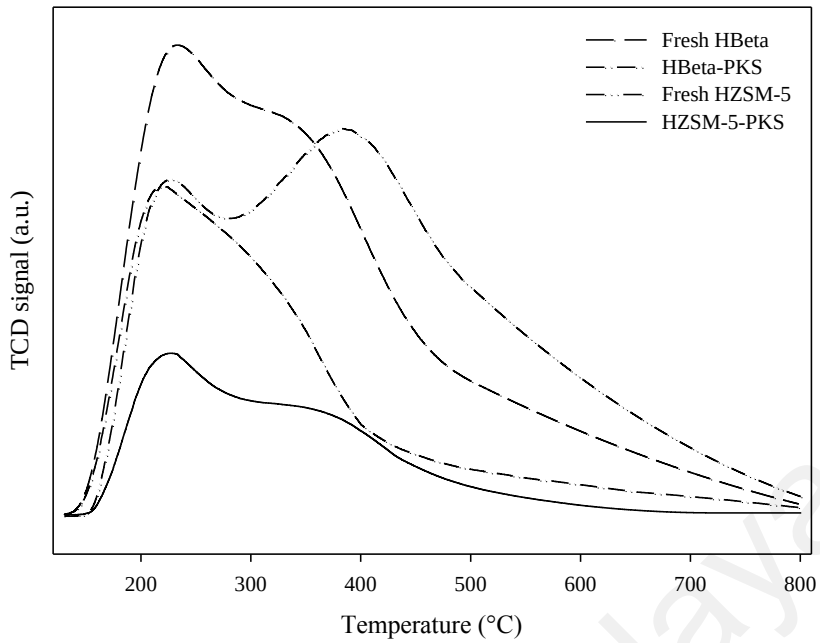

Figure 4.10: NH_3-TPD profiles of spent HBeta and HZSM-5 used in catalytic pyrolysis of PKS (WHSV, 6 h^{-1}; time on stream, 60 min; carrier gas, N_2).

4.2.3.4 Stability test of Fe/HBeta

Figure 4.11 shows the stability of Fe/HBeta in catalytic pyrolysis of cellulose, PKS and lignin under hydrogen atmosphere. This figure indicates that all feedstocks resulted in significant deactivation of catalyst. The yields of aromatic hydrocarbons obtained from cellulose, PKS and lignin in the first hour were 20.14, 9.37 and 5.13 wt% which were reduced to 15.23, 3.38 and 1.06 wt% in the fifth hour, respectively; the reduction in catalytic activity of Fe/HBeta exposed to cellulose, PKS and lignin for 5 h were 24.38, 63.93 and 79.34%, respectively. This indicates that catalyst lifetime is reduced by increase in lignin content of feedstock, which as mentioned before, is due to strong adsorption of lignin-derived phenolics on zeolite acid sites. Furthermore, catalyst regenerability was examined by regeneration of Fe/HBeta used for catalytic pyrolysis of PKS under hydrogen atmosphere. The catalyst was reactivated by regeneration, and the yield of aromatic hydrocarbons obtained from conversion of PKS over the regenerated Fe/HBeta was 9.16 wt% which is almost similar to the yield achieved by fresh Fe/HBeta.

Meanwhile, the data presented in Table 4.5 show that the initial surface area and textural properties of Fe/HBeta was recovered by regeneration.

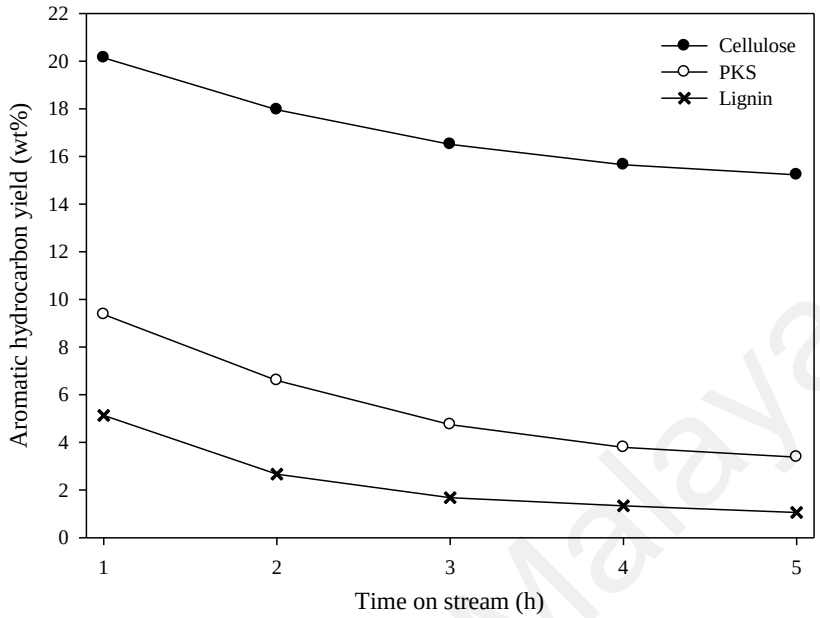

Figure 4.11: Effect of time on stream on aromatic hydrocarbon yield obtained from catalytic pyrolysis of cellulose, PKS and lignin over Fe/HBeta (WHSV, 6 h^{-1}; reaction temperature, 500 °C; carrier gas, H_2).

4.3 Suppression of coke formation and enhancement of aromatic hydrocarbon production in catalytic pyrolysis of cellulose over different zeolites: effects of pore structure and acidity

4.3.1 Physicochemical characteristics of catalysts

The acidity of catalysts determined by NH_3-TPD analysis is shown in Figure 4.12. The lower peak area of acid-treated HY compared to that of parent HY demonstrates the reduction in the number of acid sites caused by leaching of Al from zeolite structure. SiO_2/Al_2O_3 molar ratio of the parent and dealuminated forms of HY were 31.3 and 326.7, respectively. As depicted in Figure 4.13, both parent and dealuminated forms of HY displayed the typical diffraction lines of Y zeolite. It can be seen from XRD patterns that crystallinity of acid-treated HY had a slight reduction, and crystalline structure of HY was not significantly affected by dealumination. Table 4.8 presents the textural properties of catalysts evaluated from nitrogen isothermal adsorption-desorption. BET surface area of dealuminated HY was 13% lower than that of parent HY. Microporous surface area and volume of HY were reduced, while surface area and volume of mesopores were increased. This indicates that a portion of micropores was changed to mesopores due to extraction of aluminium from zeolite microporous channels and creation of mesoporous sapce. As shown in Figure 4.14, all zeolites displayed type IV isotherm. HZSM-5 and parent HY displayed H4-type hysteresis loop associated with narrow slit-shaped pores, and dealuminated HY exhibited H3-type hysteresis loop associated with slit-shaped pores (Xue, Huang, Zhan, Ma, & Shen, 2013).

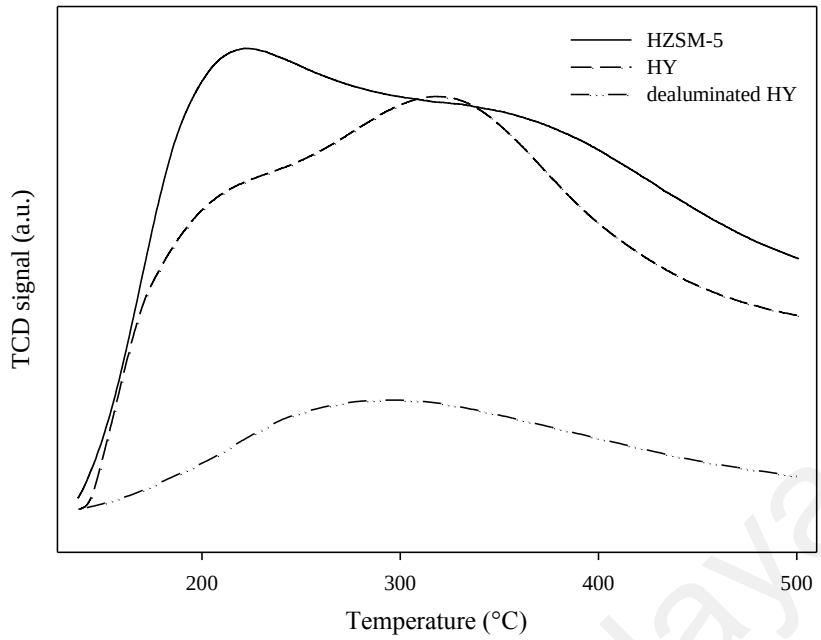

Figure 4.12: NH_3-TPD profiles of HZSM-5 and the parent and dealuminated forms of HY.

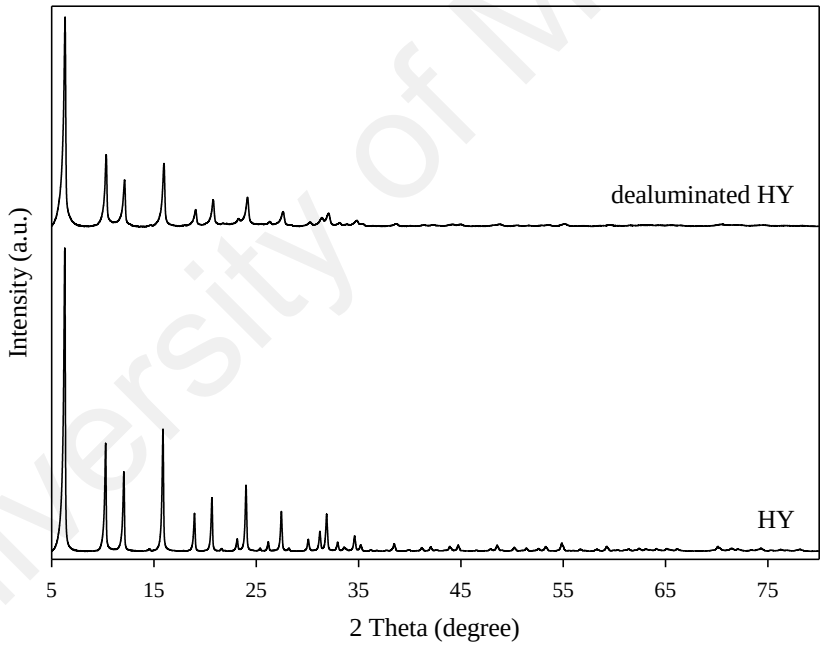

Figure 4.13: X-ray diffraction patterns of the parent and dealuminated forms of HY.

Table 4.8: Chemical and textural properties of catalysts.

Sample	SiO_2/Al_2O_3[a]	S_{BET}[b] ($m^2 g^{-1}$)	S_{meso}[c] ($m^2 g^{-1}$)	S_{BET}/S_{meso}	V_{total}[d] ($cm^3 g^{-1}$)	V_{micro}[e] ($cm^3 g^{-1}$)	V_{meso}[f] ($cm^3 g^{-1}$)
HZSM-5	32.3	291	99	2.94	0.191	0.094	0.097
parent HY	31.3	645	158	4.08	0.429	0.238	0.191
dealuminated HY	326.7	563	256	2.19	0.431	0.149	0.282

[a] Determined by XRF analysis.
[b] Calculated in the range of relative pressure (P/P_0) = 0.05-0.25.
[c] Evaluated by t-plot method.
[d] Total pore volume evaluated at P/P_0 = 0.99.
[e] Evaluated by t-plot method.
[f] $V_{meso} = V_{total} - V_{micro}$.

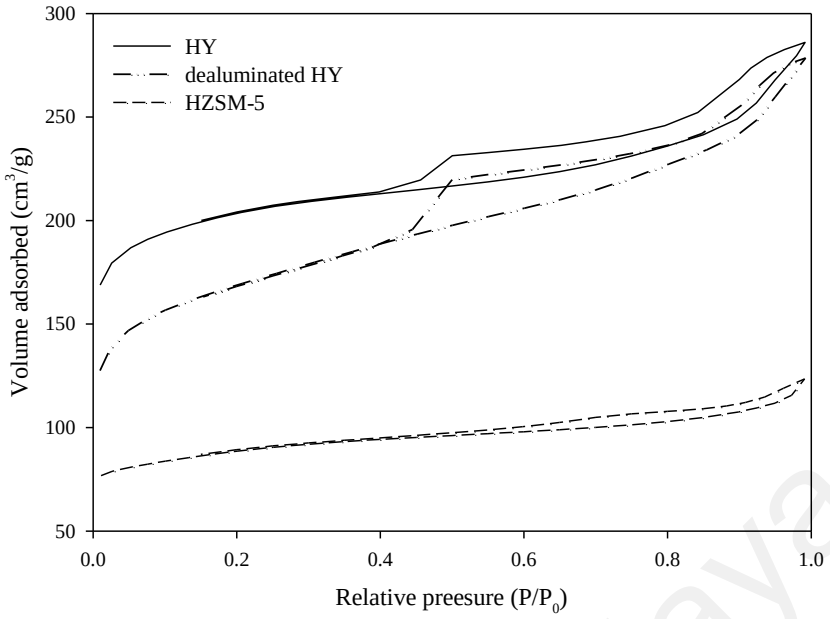

Figure 4.14: Nitrogen adsorption-desorption isotherms of HZSM-5 and the parent and dealuminated forms of HY.

4.3.2 Catalytic pyrolysis of cellulose over HZSM-5 and HY

The reason for using cellulose instead of biomass as the feedstock for the study of suppression of coke formation was that cellulose does not have phenolic structure, and the coke deposited on catalyst in transformation of cellulose is not caused by strong adsorption of phenolic compounds (as described in previous parts of this chapter), and the amount of coke formation could be explained by the diffusivity of pyrolysis-derived compounds inside catalyst and the interactive effects of pore structure and acidity of catalyst on the degree of polymerization of coke precursors. Table 4.9 presents the yields of gas, liquid and solid products obtained from catalytic pyrolysis of cellulose using different zeolites. HZSM-5 resulted in lower yield of oil as well as higher yields of gas and water compared to HY due to higher amount of deoxygenation taken place over HZSM-5. As shown in Table 4.9, the aromatic hydrocarbons yield achieved from catalytic pyrolysis of cellulose over HZSM-5 and HY were 20.31 and 8.91 wt%, respectively. The higher aromatic hydrocarbons yield of HZSM-5 compared to HY is due to the different pore structures of these catalysts. ZSM-5 is a zeolite with three-dimensional framework formed of 10-membered ring pores with dimensions of 0.51 ×

0.55 and 0.53 × 0.56 nm, while Y zeolite contains 12-membered ring channels of 0.74 × 0.74 nm (Jae et al., 2011). The smaller pore size of HZSM-5 prevents from formation of polyaromatic compounds which act as coke precursors, resulting in lower deposition of catalytic coke on HZSM-5 acid sites, and in turn, less deactivation of catalyst and higher yield of aromatic hydrocarbons (Corma et al., 2007). The main aromatic hydrocarbons produced from cellulose pyrolysis over HZSM-5 were toluene, xylene, trimethylbenzene and ethyl-methylbenzene. The dominant oxygenated compounds detected in the organic phase of liquid product obtained using HZSM-5 and HY were furfural, benzofuran, 5-hydroxymethyl furfural, phenol, cresol and benzenediol. The reaction pathway for conversion of cellulose into aromatic hydrocarbons is as follows: pyrolysis of cellulose to volatile organics which are dehydrated to furans, followed by decarbonylation of furans to allene, and subsequent oligomerization of the allene to olefins which react with furans to form aromatics (Carlson et al., 2009; Cheng, Jae, et al., 2012). In addition to lower yield of aromatic hydrocarbons, HY resulted in higher coke formation compared to HZSM-5; the content of coke deposited on HZSM-5 and HY were 7.01 and 11.47 wt%, respectively. Besides, the main cause of coke formation over these two zeolites was different. The results obtained by thermogravimetric analysis of spent catalysts shown in Figure 4.15a and Table 4.10 depict that the coke deposited on HZSM-5 is mostly of thermal origin and the coke formed over HY is mostly of catalytic origin; HZSM-5 and HY resulted in catalytic coke content of 2.28 and 10.21 wt%, and thermal coke content of 4.73 and 1.26 wt%, respectively. The two weight loss regions in temperature range of 300-500 and 500-750 °C were considered as the amounts of thermal and catalytic coke deposited on catalyst, respectively. The weight loss below 300 °C was assigned to desorption of water and volatile components (Ma et al., 2012). Differential thermogravimetry (DTG) shown in Figure 4.15b indicates that maximum combustion of thermal and catalytic coke occurred at 440 and 580 °C for HZSM-5, and 410 and 650 °C

for HY, respectively. The difference in catalytic and thermal coke contents of HZSM-5 and HY is caused by the different pore structures of these two zeolites. In fact, coke formation is a shape selective reaction. Large molecules formed by thermal cracking in homogeneous gas phase outside catalyst could not enter the narrow channels of HZSM-5 and undergo repolymerization and condensation outside catalyst, and are deposited on catalyst surface as thermal coke. However, HY which contains larger channels allows larger molecules enter the catalyst and react over zeolite acid sites inside catalyst channels. On the other hand, HY leads to higher yield of catalytic coke since this zeolite with larger pore diameter provides larger space for polymerization of coke precursors and formation of the intermediates and transition states which are involved in coke production resulting in higher amount of carbonaceous residues deposited on zeolite acid sites. In contrast to HY, smaller channels of HZSM-5 limit the degree of polymerization inside catalyst and cause lower yield of catalytic coke.

Table 4.9: Product yields and selectivities (wt%) obtained from catalytic pyrolysis of cellulose over different zeolites. Reaction conditions: WHSV, 6 h^{-1}; reaction temperature, 500 °C; pressure, 1 atm.

Catalyst	**HZSM-5**	**HY**	**dealuminated HY**	**HZSM-5/dealuminated HY**		
				70:30 wt%	**50:50 wt%**	**30:70 wt%**
% Yield						
Oil	27.96	31.85	37.59	28.98	30.28	31.22
Gas	33.74	29.73	27.17	33.46	32.86	32.26
Aqueous fraction	17.46	15.95	14.65	17.30	16.71	16.49
Char/Coke	19.57/1.27	20.30/2.17	19.86/0.73	19.43/0.83	19.38/0.77	19.30/0.73
% Yield of aromatic hydrocarbons						
	20.31	8.91	0.48	27.01	22.18	15.71
% Selectivity in organic phase of liquid product						
Benzene	1.36	0.30	0.09	2.01	1.17	0.71
Toluene	19.47	5.72	0.23	26.28	18.45	11.49
Xylene	17.08	6.82	0.27	24.8	16.85	10.65
Ethyl-methylbenzene	7.53	3.07	0.13	11.64	8.85	6.65
Trimethylbenzene	9.91	4.22	0.16	13.75	11.24	8.06
Tetramethylbenzene	2.86	1.46	0.11	1.97	2.18	1.21
Naphthalenes	9.24	4.84	0.19	8.40	9.68	6.5
Other hydrocarbons	5.19	1.54	0.10	4.35	4.83	5.05
Oxygenated compounds	27.36	72.03	98.72	6.80	26.75	49.68

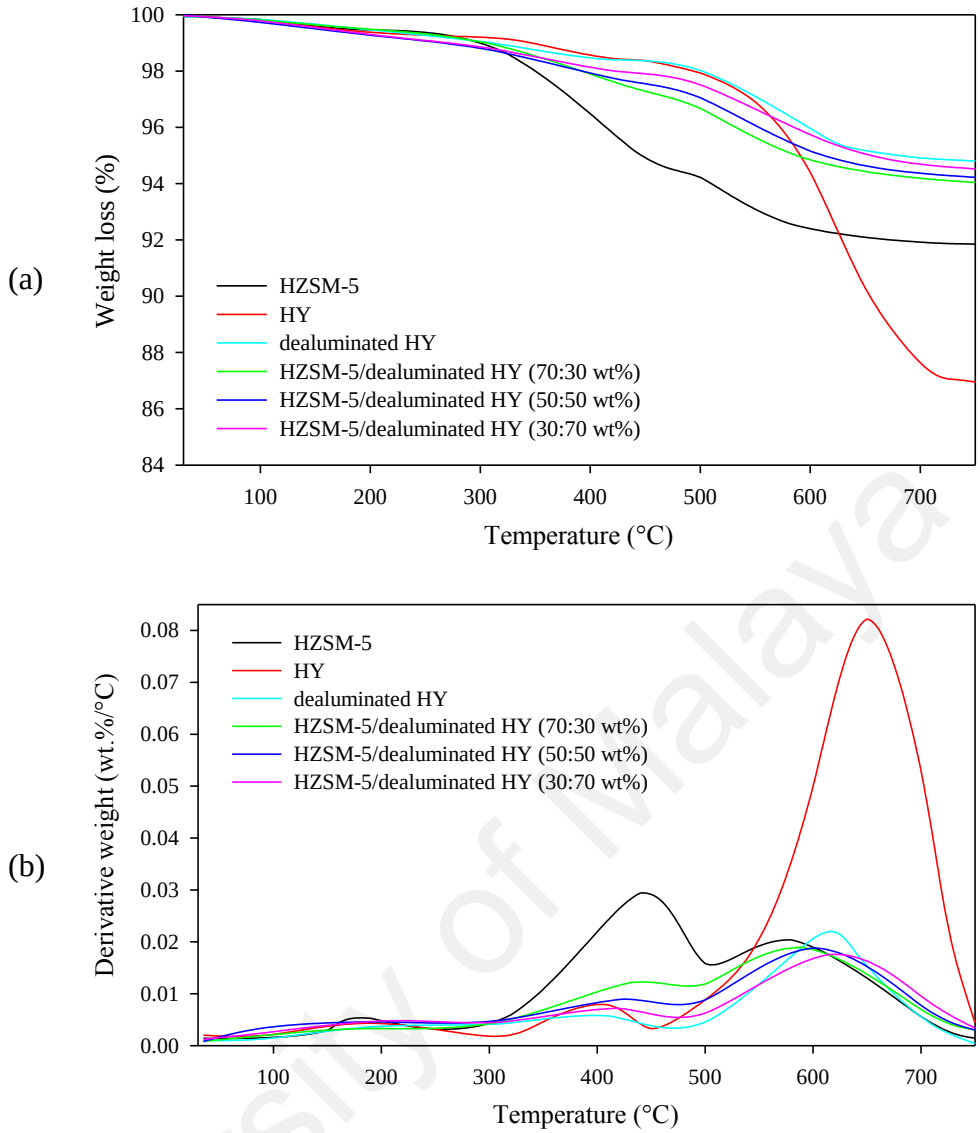

Figure 4.15: TGA (a) and DTG (b) of the spent catalysts used for cellulose pyrolysis (WHSV, 6 h^{-1}; time on stream, 60 min; reaction temperature, 500 °C).

Table 4.10: Content of total coke, thermal coke and catalytic coke deposited on the catalysts used for cellulose pyrolysis. Reaction conditions: WHSV, 6 h^{-1}; reaction temperature, 500 °C; pressure, 1 atm; time on stream, 60 min.

Catalyst	**HZSM-5**	**HY**	**dealuminated HY**	**HZSM-5/dealuminated HY**		
				70:30 wt%	**50:50 wt%**	**30:70 wt%**
% $g_{coke}/g_{catalyst}$						
Thermal coke	4.73	1.26	1.07	2.36	1.73	1.38
Catalytic coke	2.28	10.21	3.08	2.46	2.65	2.79
Total coke	7.01	11.47	4.15	4.82	4.38	4.17

4.3.3 Catalytic pyrolysis of cellulose over physically mixed catalysts of HZSM-5 and dealuminated HY

The amount of catalytic coke formed over HY was remarkably reduced by dealumination. The catalytic coke contents of HY and dealuminated HY were 10.21 and 3.08 wt%, respectively. Xue et al. (2013) also reported that dealumination resulted in less deposition of catalytic coke on mordenite zeolite. Dealuminated HY contains lower density of acid sites which leads to lower yield of catalytic coke. High molecular coke is formed through several reaction steps, and since lower density of acid sites leads to reduction in the number of acid sites which a reactant encounters, the possibility for converting into coke over dealuminated HY is attenuated. However, the aromatics yield achieved over dealuminated HY was very low (below 0.5 wt%). Use of mixtures of HZSM-5 and dealuminated HY showed to be efficient to achieve high yield of aromatic hydrocarbons with low content of coke deposited on catalyst. The coke contents of HZSM-5 and HY were 7.01 and 11.47 wt%, while the coke contents of mixtures of HZSM-5 and dealuminated HY with ratios of 70:30, 50:50 and 30:70 wt% were 4.82, 4.38 and 4.17 wt%, respectively. In the case of using HZSM-5 as catalyst, the compounds with molecular size larger than pore diameter of HZSM-5 could not enter catalyst and are converted to thermal coke and deposited on HZSM-5 outer surface. However, presence of HY with larger channels in catalyst mixture allows the compounds in wider range of molecular size to diffuse into catalyst and react over HY acid sites. In fact, the dealuminated HY showed to be a suitable catalyst for initial cracking of the compounds derived from pyrolysis of cellulose. Therefore, some compounds which could not enter HZSM-5 are firstly cracked over HY acid sites and converted to smaller compounds which could diffuse inside HZSM-5 channels and be transformed to aromatic hydrocarbons over HZSM-5 acid sites. Considering the thermal coke contents of the mixtures of HZSM-5 and dealuminated HY shown in Table 4.10 as well as the thermal

coke content of dealuminated HY which is 1.07 wt% (thermal coke content of dealuminated HY is supposed to be unchanged in presence of HZSM-5), the thermal coke content of HZSM-5 in mixtures of HZSM-5 and dealuminated HY with ratios of 70:30, 50:50 and 30:70 wt% are estimated to be 2.91, 2.39 and 2.10 wt%, respectively. This clearly shows that thermal coke content of HZSM-5 is reduced by increase in the amount of dealuminated HY in catalyst mixture. Meanwhile, dealuminated HY does not contain enough number of acid sites for high conversion of reactants to coke. Therefore, mixture of HZSM-5 and dealuminated HY results in less coke formation compared to HZSM-5 and HY due to the reduction in thermal coke deposited on HZSM-5 and the decrease in catalytic coke formed inside the channels of dealuminated HY. It could be inferred from the results obtained in this study that there is a significant interaction between pore space and density of zeolite acid sites which should be taken into account in designing an efficient catalyst. The steric constraints caused by limited space in the vicinity of acid sites could prevent from coke formation. Therefore, high density of acid sites located in small spaces could not lead to high formation of coke. However in larger channels, coke formation could be effectively suppressed by decrease in the density of acid sites which leads to reduction in the degree of polymerization and condensation. The aromatic hydrocarbons production is also improved over the physically mixed catalyst system. The aromatics yield achieved over HZSM-5 was 20.31 wt% which was enhanced to 22.18 and 27.01 wt% over mixtures of HZSM-5 and dealuminated HY with ratios of 50:50 and 70:30 wt%, respectively. This increase in aromatics yield is due to the possibility for a higher fraction of compounds to react over HZSM-5 since the compounds with molecular size larger than pore diameter of HZSM-5 could undergo cracking in larger channels of HY and diffuse inside HZSM-5 channels. However, the mixture of HZSM-5 and dealuminated HY with ratio of 30:70 wt% resulted in less aromatics yield compared to HZSM-5 illustrating that the amount of HZSM-5 in the catalyst mixture should be

adequate in order to proceed the reactions required for aromatics production; as mentioned in the previous section, formation of polyaromatic compounds as coke precursors is restricted by the steric constraints caused by smaller pore size of HZSM-5 resulting in higher catalytic activity of HZSM-5 and higher yield of aromatic hydrocarbons produced over this catalyst compared to HY. Therefore in the mixture of HZSM-5 and dealuminated HY, the amount of dealuminated HY should be sufficient for initial cracking of pyrolysis-derived compounds and effective reduction of thermal coke deposited on HZSM-5. Besides, the amount of HZSM-5 in the mixture should be high enough for efficient conversion of reactants. In the physically mixed catalyst system studied in this work, the lowest coke formation and the highest yield of aromatic hydrocarbons were observed at HZSM-5 to dealuminated HY ratios of 30:70 and 70:30 wt%, respectively.

It could be concluded from this study that formation of coke as an undesired product is a competing reaction with production of aromatic hydrocarbons in catalytic pyrolysis of biomass feedstocks. Therefore, catalyst properties should be optimized in order to have minimum selectivity towards coke and maximum selectivity towards desired products. Deposition of both types of coke is needed to be suppressed in an efficient catalyst system. Pore structure and location of acid sites in catalyst structure are the two significant properties which should be taken into account for reducing coke formation. Presence of channels with larger dimensions facilitates the diffusion of larger molecules inside catalyst leading to reduction in the yield of thermal coke. Meanwhile, acid sites with high density should be located in small spaces which restrict the degree of polymerization and catalytic coke deposition. However, there should be enough space in the vicinity of acid sites in order to allow formation of transition states for desired products.

CHAPTER 5: CONCLUSIONS AND RECOMMENDATIONS FOR FUTURE STUDIES

5.1 Conclusions

5.1.1 Origin of zeolite deactivation in conversion of lignin-derived phenolics

The composition of biomass and its amount of lignin content greatly affect the catalytic performance of zeolites in deoxygenation of biomass pyrolysis derived feedstocks. In this work, at reaction temperature of 350 °C, aromatics yield obtained from conversion of methanol over HBeta was 59.6 wt% which was decreased to 24.3 and 6.2 wt% by co-feeding 10 wt% *m*-cresol and phenol, respectively. Meanwhile, the coke content of HBeta used for conversion of pure methanol was 0.22 wt% which was increased to 2.61 and 3.48 wt% in the presence of *m*-cresol and phenol, respectively. It was revealed that atmospheric deoxygenation of *m*-cresol occurred over Fe/HBeta through hydrogenolysis under hydrogen atmosphere; aromatics yield of 17.5 wt% was achieved from conversion of *m*-cresol over Fe/HBeta. However, this yield was dramatically decreased to 3.2 wt% by addition of 10 wt% phenol since zeolite acid sites are rapidly occupied by phenol molecules due to high potential of phenol to be tightly bound with zeolite acid sites. But, the steric hindrance caused by the methyl group on the phenolic ring of *m*-cresol prevents from its strong adsorption on zeolite acid sites. Therefore, it could be concluded that the origin of zeolite deactivation in atmospheric conversion of pure *m*-cresol is the strong adsorption of simple phenol molecules which are produced from demethylation of *m*-cresol. Hydrogenolysis promoted by Fe active sites not only is effective for deoxygenation of *m*-cresol but also is a competing reaction with its demethylation on zeolite acid sites causing lower production of phenol and in turn less occupation of acid sites and catalyst deactivation. The negative effect of phenol on performance of zeolite showed to be attenuated at elevated temperature; addition of phenol to *m*-cresol reduced

the aromatics yield of Fe/HBeta from 17.5 to 3.2 wt% at 350 °C, and from 30.3 to 10.6 wt% at 450 °C. Meanwhile, the adsorption of phenol molecules on zeolite acid sites can be reduced by using a zeolite type with larger pore size and less density of strong acid sites. It could be inferred from this study that pure zeolite such as HBeta is not suitable for deoxygenation of feedstocks derived from biomass with high content of lignin due to low reactivity of lignin derived phenolic compounds over zeolite acid sites as well as strong adsorption of phenolics especially simple phenol molecules on the acid sites. Zeolite impregnated with the metals which could promote hydrogenolysis reaction is efficient for atmospheric deoxygenation of such feedstocks.

5.1.2 Aromatic hydrocarbon production by catalytic pyrolysis of palm kernel shell

The aromatic hydrocarbon yields achieved from catalytic pyrolysis of cellulose and lignin using HBeta zeolite were 18.62 and 0.95 wt%, respectively. The low deoxygenation of lignin was due to low reactivity of lignin-derived phenolics on zeolite acid sites as well as rapid catalyst deactivation caused by high potential of phenolic compounds to form tight bond with zeolite acid sites. It was shown in this work that Fe active sites incorporated into HBeta structure could remarkably enhance deoxygenation of lignin through hydrogenolysis reaction; conversion of lignin over Fe/HBeta using hydrogen as carrier gas resulted in aromatic hydrocarbons yield of 5.13 wt%. Bifunctional Fe/HBeta catalyst was efficient for production of aromatic hydrocarbons in catalytic pyrolysis of palm kernel shell waste with high lignin content of about 50 wt%. Aromatic hydrocarbons yield obtained from catalytic pyrolysis of palm kernel shell using HBeta as catalyst and nitrogen as carrier gas was 1.86 wt% which was enhanced to 9.37 wt% by replacement of HBeta and nitrogen gas with Fe/HBeta and hydrogen. It is concluded that catalysts which contain promoter for hydrogenolysis could be effective for atmospheric deoxygenation of the biomass feedstocks with high content of lignin. Furthermore, less

adsorption of phenolic molecules on zeolite acid sites was observed in HBeta compared to HZSM-5 due to larger pore size, smaller crystallites and lower percentage of strong acid sites in HBeta zeolite. Therefore, these zeolite characteristics could be taken into account in selection of a suitable catalyst for upgrading of the biomass feedstocks with high lignin content.

5.1.3 Suppression of coke formation: effects of zeolite pore structure and acidity

The results obtained in this study revealed that there is a significant interaction between zeolite pore structure (pore size and shape) and density of acid sites which greatly affects the amount of coke formation and deposition on zeolite in conversion of biomass feedstocks. It was also shown that these zeolite properties could be optimized in order to suppress coke formation and to enhance the yield of desired products. In catalytic pyrolysis of cellulose, lower formation of coke as well as higher yield of aromatic hydrocarbons were achieved over physically mixed catalysts of HZSM-5 and dealuminated HY compared to HZSM-5 and HY. Addition of HY to HZSM-5 results in lower deposition of thermal coke over HZSM-5 due to larger pores of HY which allow larger molecules diffuse into zeolite and react. Besides, formation of catalytic coke over the physically mixed catalysts was suppressed by small space inside HZSM-5 pores and low density of acid sites inside dealuminated HY pores which both restrict the degree of polymerization of coke precursors. The coke contents of HZSM-5 and HY were 7.01 and 11.47 wt%, respectively, while the coke content of physically mixed catalysts of HZSM-5 and dealuminated HY with ratio of 70:30 wt% was 4.82 wt%. Meanwhile, the aromatic hydrocarbons yield achieved over HZSM-5 and HY was 20.31 and 8.91 wt%, respectively, which was enhanced to 27.01 wt% over mixture of HZSM-5 and dealuminated HY (70:30 wt%).

5.2 Recommendations for future studies

The following suggestions are recommended for future research on modification of the process in terms of suppression of coke formation and enhanced production of high value added chemicals including aromatic hydrocarbons:

- Increase of hydrogen content in the hydrocarbon pool inside catalyst by:
    - Supplying hydrogen through co-feeding hydrogen donors with biomass/bio-oil.
    - Increasing the selectivity towards hydrogenation through incorporation of metals with high hydrogenation effect into catalyst.
    - Control of the fate of oxygen to be removed through decarboxylation and decarbonylation instead of dehydration; in this case, deoxygenation occurs without removal of hydrogen.
- Control of shape selectivity by modification of pore-opening size and pore shape of catalyst:
    - Pore-opening size is recommended to be large enough in order to allow large molecules to enter catalyst and react and not to be converted to thermal coke through non-catalytic transformation outside catalyst.
    - Catalyst mesoporosity should be low enough in order to restrict the degree of polymerization and to prevent catalytic coke formation.
- Optimization of catalyst acidity (strength distribution and number of acid sites) in order to have the maximum level of cracking with the minimum possibility for coke formation; optimum strength of acid sites depends on density of acid sites in catalyst structure, and the interactive effect of these two factors should be taken into account for optimization of catalyst acidity.
- Study of the interaction between acidity and pore shape; optimum density and strength of acid sites of small cavities is supposed to be different from that of those

located in large cavities. By understanding the interactive effect between acidity and mesoporosity, it would be possible to determine the proper location of acid sites in catalyst structure.

- Exploration of functionality of different metals for selective conversion of lignin-derived phenolic compounds into aromatic hydrocarbons.
- Optimization of the ratio of metal to acid sites in bifunctional metal/acid catalysts.

REFERENCES

Adjaye, J. D., & Bakhshi, N. N. (1995a). Catalytic conversion of a biomass-derived oil to fuels and chemicals I: Model compound studies and reaction pathways. *Biomass and Bioenergy, 8*(3), 131-149.

Adjaye, J. D., & Bakhshi, N. N. (1995b). Production of hydrocarbons by catalytic upgrading of a fast pyrolysis bio-oil. Part II: Comparative catalyst performance and reaction pathways. *Fuel Processing Technology, 45*(3), 185-202.

Adjaye, J. D., Katikaneni, S. P. R., & Bakhshi, N. N. (1996). Catalytic conversion of a biofuel to hydrocarbons: effect of mixtures of HZSM-5 and silica-alumina catalysts on product distribution. *Fuel Processing Technology, 48*(2), 115-143.

Aho, A., Kumar, N., Eränen, K., Salmi, T., Hupa, M., & Murzin, D. Y. (2008). Catalytic pyrolysis of woody biomass in a fluidized bed reactor: Influence of the zeolite structure. *Fuel, 87*(12), 2493-2501.

Aho, A., Kumar, N., Lashkul, A. V., Eränen, K., Ziolek, M., Decyk, P., . . . Murzin, D. Y. (2010). Catalytic upgrading of woody biomass derived pyrolysis vapours over iron modified zeolites in a dual-fluidized bed reactor. *Fuel, 89*(8), 1992-2000.

Antonakou, E., Lappas, A., Nilsen, M. H., Bouzga, A., & Stöcker, M. (2006). Evaluation of various types of Al-MCM-41 materials as catalysts in biomass pyrolysis for the production of bio-fuels and chemicals. *Fuel, 85*(14-15), 2202-2212.

Augusto, C., Zotin, J., & Faro, A., Jr. (2001). Effect of sulfur or nitrogen poisoning on the activity and selectivity of Y-zeolite-supported Pt–Pd catalysts in the hydrogenation of tetralin. *Catalysis Letters, 75*(1-2), 37-43.

Ausavasukhi, A., Sooknoi, T., & Resasco, D. E. (2009). Catalytic deoxygenation of benzaldehyde over gallium-modified ZSM-5 zeolite. *Journal of Catalysis, 268*(1), 68-78.

Ben, H., & Ragauskas, A. J. (2011). Pyrolysis of kraft lignin with additives. *Energy & Fuels, 25*(10), 4662-4668.

Beutel, T. (1998). Spectroscopic and kinetic study of the alkylation of phenol with dimethyl carbonate over NaX zeolite. *Journal of the Chemical Society, Faraday Transactions, 94*(7), 985-993.

Carlson, T. R., Cheng, Y.-T., Jae, J., & Huber, G. W. (2011). Production of green aromatics and olefins by catalytic fast pyrolysis of wood sawdust. *Energy & Environmental Science, 4*(1), 145-161.

Carlson, T. R., Jae, J., Lin, Y.-C., Tompsett, G. A., & Huber, G. W. (2010). Catalytic fast pyrolysis of glucose with HZSM-5: The combined homogeneous and heterogeneous reactions. *Journal of Catalysis, 270*(1), 110-124.

Carlson, T. R., Tompsett, G. A., Conner, W. C., & Huber, G. W. (2009). Aromatic production from catalytic fast pyrolysis of biomass-derived feedstocks. *Topics in Catalysis, 52*(3), 241-252.

Carlson, T. R., Vispute, T. P., & Huber, G. W. (2008). Green gasoline by catalytic fast pyrolysis of solid biomass derived compounds. *ChemSusChem, 1*(5), 397-400.

Chang, C. D., & Silvestri, A. J. (1977). The conversion of methanol and other O-compounds to hydrocarbons over zeolite catalysts. *Journal of Catalysis, 47*(2), 249-259.

Chen, C., Chen, G., Yang, F., Wang, H., Han, J., Ge, Q., & Zhu, X. (2015). Vapor phase hydrodeoxygenation and hydrogenation of m-cresol on silica supported Ni, Pd and Pt catalysts. *Chemical Engineering Science, 135*, 145-154.

Chen, N. Y., Walsh, D. E., & Koenig, L. R. (1988). Fluidized-bed upgrading of wood pyrolysis liquids and related compounds *Pyrolysis Oils from Biomass* (Vol. 376, pp. 277-289): American Chemical Society.

Chen, Y.-M. (2006). Recent advances in FCC technology. *Powder Technology, 163*(1-2), 2-8.

Cheng, Y.-T., & Huber, G. W. (2011). Chemistry of furan conversion into aromatics and olefins over HZSM-5: a model biomass conversion reaction. *ACS Catalysis, 1*(6), 611-628.

Cheng, Y.-T., & Huber, G. W. (2012). Production of targeted aromatics by using Diels–Alder classes of reactions with furans and olefins over ZSM-5. *Green Chemistry, 14*(11), 3114-3125.

Cheng, Y. T., Jae, J., Shi, J., Fan, W., & Huber, G. W. (2012). Production of renewable aromatic compounds by catalytic fast pyrolysis of lignocellulosic biomass with bifunctional Ga/ZSM-5 catalysts. *Angewandte Chemie International Edition, 51*(6), 1387-1390.

Cheng, Y. T., Wang, Z., Gilbert, C. J., Fan, W., & Huber, G. W. (2012). Production of p-xylene from biomass by catalytic fast pyrolysis using ZSM-5 catalysts with reduced pore openings. *Angewandte Chemie International Edition, 51*(44), 11097-11100.

Choi, S. J., Park, S. H., Jeon, J.-K., Lee, I. G., Ryu, C., Suh, D. J., & Park, Y.-K. (2013). Catalytic conversion of particle board over microporous catalysts. *Renewable Energy, 54*, 105-110.

Corma, A., Huber, G., Sauvanaud, L., & Oconnor, P. (2007). Processing biomass-derived oxygenates in the oil refinery: Catalytic cracking (FCC) reaction pathways and role of catalyst. *Journal of Catalysis, 247*(2), 307-327.

Cruz-Cabeza, A. J., Esquivel, D., Jiménez-Sanchidrián, C., & Romero-Salguero, F. J. (2012). Metal-exchanged β zeolites as catalysts for the conversion of acetone to hydrocarbons. *Materials, 5*(12), 121-134.

Cypres, R. (1987). Aromatic hydrocarbons formation during coal pyrolysis. *Fuel Processing Technology, 15*, 1-15.

de Lucas, A., Canizares, P., Durán, A., & Carrero, A. (1997). Dealumination of HZSM-5 zeolites: effect of steaming on acidity and aromatization activity. *Applied Catalysis A: General, 154*(1–2), 221-240.

de Miguel Mercader, F., Groeneveld, M. J., Kersten, S. R. A., Way, N. W. J., Schaverien, C. J., & Hogendoorn, J. A. (2010). Production of advanced biofuels: Co-processing of upgraded pyrolysis oil in standard refinery units. *Applied Catalysis B: Environmental, 96*(1-2), 57-66.

Depeyre, D., Flicoteaux, C., & Chardaire, C. (1985). Pure n-hexadecane thermal steam cracking. *Industrial & Engineering Chemistry Process Design and Development, 24*(4), 1251-1258.

Evans Robert, J., & Milne, T. (1988). Molecular-beam, mass-spectrometric studies of wood vapor and model compounds over an HZSM-5 catalyst *Pyrolysis Oils from Biomass* (Vol. 376, pp. 311-327): American Chemical Society.

Fisk, C. A., Morgan, T., Ji, Y., Crocker, M., Crofcheck, C., & Lewis, S. A. (2009). Bio-oil upgrading over platinum catalysts using in situ generated hydrogen. *Applied Catalysis A: General, 358*(2), 150-156.

Fogassy, G., Thegarid, N., Toussaint, G., van Veen, A. C., Schuurman, Y., & Mirodatos, C. (2010). Biomass derived feedstock co-processing with vacuum gas oil for second-generation fuel production in FCC units. *Applied Catalysis B: Environmental, 96*(3-4), 476-485.

Foster, A. J., Jae, J., Cheng, Y.-T., Huber, G. W., & Lobo, R. F. (2012). Optimizing the aromatic yield and distribution from catalytic fast pyrolysis of biomass over ZSM-5. *Applied Catalysis A: General, 423-424*, 154-161.

French, R., & Czernik, S. (2010). Catalytic pyrolysis of biomass for biofuels production. *Fuel Processing Technology, 91*(1), 25-32.

Furimsky, E. (2000). Catalytic hydrodeoxygenation. *Applied Catalysis A: General, 199*(2), 147-190.

Gayubo, A. G., Aguayo, A. T., Atutxa, A., Aguado, R., & Bilbao, J. (2004). Transformation of oxygenate components of biomass pyrolysis oil on a HZSM-5 zeolite. I. alcohols and phenols. *Industrial & Engineering Chemistry Research, 43*(11), 2610-2618.

Gayubo, A. G., Aguayo, A. T., Atutxa, A., Aguado, R., Olazar, M., & Bilbao, J. (2004). Transformation of oxygenate components of biomass pyrolysis oil on a HZSM-5

zeolite. II. aldehydes, ketones, and acids. *Industrial & Engineering Chemistry Research, 43*(11), 2619-2626.

Gayubo, A. G., Aguayo, A. T., Atutxa, A., Prieto, R., & Bilbao, J. (2004). Deactivation of a HZSM-5 zeolite catalyst in the transformation of the aqueous fraction of biomass pyrolysis oil into hydrocarbons. *Energy & Fuels, 18*(6), 1640-1647.

Gayubo, A. G., Aguayo, A. T., Atutxa, A., Valle, B., & Bilbao, J. (2005). Undesired components in the transformation of biomass pyrolysis oil into hydrocarbons on an HZSM-5 zeolite catalyst. *Journal of Chemical Technology & Biotechnology, 80*(11), 1244-1251.

Gayubo, A. G., Valle, B., Aguayo, A. s. T., Olazar, M. n., & Bilbao, J. (2009). Attenuation of catalyst deactivation by cofeeding methanol for enhancing the valorisation of crude bio-oil. *Energy & Fuels, 23*(8), 4129-4136.

Gayubo, A. G., Valle, B., Aguayo, A. T., Olazar, M., & Bilbao, J. (2010). Olefin production by catalytic transformation of crude bio-oil in a two-step process. *Industrial & Engineering Chemistry Research, 49*(1), 123-131.

Gayubo, A. G., Valle, B., Aguayo, A. T., Olazar, M., & Bilbao, J. (2010). Pyrolytic lignin removal for the valorization of biomass pyrolysis crude bio-oil by catalytic transformation. *Journal of Chemical Technology & Biotechnology, 85*(1), 132-144.

Gong, F., Yang, Z., Hong, C., Huang, W., Ning, S., Zhang, Z., . . . Li, Q. (2011). Selective conversion of bio-oil to light olefins: Controlling catalytic cracking for maximum olefins. *Bioresource Technology, 102*(19), 9247-9254.

Graça, I., Comparot, J. D., Laforge, S., Magnoux, P., Lopes, J. M., Ribeiro, M. F., & Ribeiro, F. R. (2009). Effect of phenol addition on the performances of H–Y zeolite during methylcyclohexane transformation. *Applied Catalysis A: General, 353*(1), 123-129.

Graça, I., Fernandes, A., Lopes, J. M., Ribeiro, M. F., Laforge, S., Magnoux, P., & Ramôa Ribeiro, F. (2010). Effect of phenol adsorption on HY zeolite for n-heptane cracking: Comparison with methylcyclohexane. *Applied Catalysis A: General, 385*(1-2), 178-189.

Graça, I., Ribeiro, F. R., Cerqueira, H. S., Lam, Y. L., & de Almeida, M. B. B. (2009). Catalytic cracking of mixtures of model bio-oil compounds and gasoil. *Applied Catalysis B: Environmental, 90*(3-4), 556-563.

Graça, I. s., Comparot, J.-D., Laforge, S. b., Magnoux, P., Lopes, J. M., Ribeiro, M. F., & Ramôa Ribeiro, F. (2009). Influence of phenol addition on the H-ZSM-5 zeolite catalytic properties during methylcyclohexane transformation. *Energy & Fuels, 23*(9), 4224-4230.

Gujar, A. C., Guda, V. K., Nolan, M., Yan, Q., Toghiani, H., & White, M. G. (2009). Reactions of methanol and higher alcohols over H-ZSM-5. *Applied Catalysis A: General, 363*(1-2), 115-121.

Guo, X., Zheng, Y., Zhang, B., & Chen, J. (2009). Analysis of coke precursor on catalyst and study on regeneration of catalyst in upgrading of bio-oil. *Biomass and Bioenergy, 33*(10), 1469-1473.

Hellinger, M., Carvalho, H. W. P., Baier, S., Wang, D., Kleist, W., & Grunwaldt, J.-D. (2015). Catalytic hydrodeoxygenation of guaiacol over platinum supported on metal oxides and zeolites. *Applied Catalysis A: General, 490*, 181-192.

Hew, K. L., Tamidi, A. M., Yusup, S., Lee, K. T., & Ahmad, M. M. (2010). Catalytic cracking of bio-oil to organic liquid product (OLP). *Bioresource Technology, 101*(22), 8855-8858.

Hilten, R., Speir, R., Kastner, J., & Das, K. C. (2011). Production of aromatic green gasoline additives via catalytic pyrolysis of acidulated peanut oil soap stock. *Bioresource Technology, 102*(17), 8288-8294.

Hoang, T. Q., Zhu, X., Lobban, L. L., Resasco, D. E., & Mallinson, R. G. (2010). Effects of HZSM-5 crystallite size on stability and alkyl-aromatics product distribution from conversion of propanal. *Catalysis Communications, 11*(11), 977-981.

Hong, C., Gong, F., Fan, M., Zhai, Q., Huang, W., Wang, T., & Li, Q. (2013). Selective production of green light olefins by catalytic conversion of bio-oil with Mg/HZSM-5 catalyst. *Journal of Chemical Technology & Biotechnology, 88*(1), 109-118.

Horne, P. A., & Williams, P. T. (1996). Reaction of oxygenated biomass pyrolysis model compounds over a ZSM-5 catalyst. *Renewable Energy, 7*(2), 131-144.

Huang, W., Gong, F., Fan, M., Zhai, Q., Hong, C., & Li, Q. (2012). Production of light olefins by catalytic conversion of lignocellulosic biomass with HZSM-5 zeolite impregnated with 6wt.% lanthanum. *Bioresource Technology, 121*, 248-255.

Huber, G. W., & Corma, A. (2007). Synergies between bio- and oil refineries for the production of fuels from biomass. *Angewandte Chemie International Edition, 46*(38), 7184-7201.

Ibáñez, M., Valle, B., Bilbao, J., Gayubo, A. G., & Castaño, P. (2012). Effect of operating conditions on the coke nature and HZSM-5 catalysts deactivation in the transformation of crude bio-oil into hydrocarbons. *Catalysis Today, 195*(1), 106-113.

Iliopoulou, E. F., Antonakou, E. V., Karakoulia, S. A., Vasalos, I. A., Lappas, A. A., & Triantafyllidis, K. S. (2007). Catalytic conversion of biomass pyrolysis products by mesoporous materials: Effect of steam stability and acidity of Al-MCM-41 catalysts. *Chemical Engineering Journal, 134*(1-3), 51-57.

Iliopoulou, E. F., Stefanidis, S. D., Kalogiannis, K. G., Delimitis, A., Lappas, A. A., & Triantafyllidis, K. S. (2012). Catalytic upgrading of biomass pyrolysis vapors using transition metal-modified ZSM-5 zeolite. *Applied Catalysis B: Environmental, 127*, 281-290.

Jackson, M. A., Compton, D. L., & Boateng, A. A. (2009). Screening heterogeneous catalysts for the pyrolysis of lignin. *Journal of Analytical and Applied Pyrolysis, 85*(1-2), 226-230.

Jae, J., Tompsett, G. A., Foster, A. J., Hammond, K. D., Auerbach, S. M., Lobo, R. F., & Huber, G. W. (2011). Investigation into the shape selectivity of zeolite catalysts for biomass conversion. *Journal of Catalysis, 279*(2), 257-268.

Karanjkar, P. U., Coolman, R. J., Huber, G. W., Blatnik, M. T., Almalkie, S., de Bruyn Kops, S. M., . . . Conner, W. C. (2014). Production of aromatics by catalytic fast pyrolysis of cellulose in a bubbling fluidized bed reactor. *AIChE Journal, 60*(4), 1320-1335.

Katikaneni, S. P. R., Adjaye, J. D., & Bakhshi, N. N. (1995). Studies on the catalytic conversion of canola oil to hydrocarbons: influence of hybrid catalysts and steam. *Energy & Fuels, 9*(4), 599-609.

Kim, J.-Y., Lee, J. H., Park, J., Kim, J. K., An, D., Song, I. K., & Choi, J. W. (2015). Catalytic pyrolysis of lignin over HZSM-5 catalysts: effect of various parameters on the production of aromatic hydrocarbon. *Journal of Analytical and Applied Pyrolysis, 114*, 273-280.

Kim, J., Choi, M., & Ryoo, R. (2010). Effect of mesoporosity against the deactivation of MFI zeolite catalyst during the methanol-to-hydrocarbon conversion process. *Journal of Catalysis, 269*(1), 219-228.

Kwon, K. C., Mayfield, H., Marolla, T., Nichols, B., & Mashburn, M. (2011). Catalytic deoxygenation of liquid biomass for hydrocarbon fuels. *Renewable Energy, 36*(3), 907-915.

Lappas, A. A., Bezergianni, S., & Vasalos, I. A. (2009). Production of biofuels via co-processing in conventional refining processes. *Catalysis Today, 145*(1-2), 55-62.

Le Van Mao, R., & McLaughlin, G. P. (1989). Conversion of light alcohols to hydrocarbons over ZSM-5 zeolite and asbestos-derived zeolite catalysts. *Energy & Fuels, 3*(5), 620-624.

Lee, K.-H. (2012). Effects of the types of zeolites on catalytic upgrading of pyrolysis wax oil. *Journal of Analytical and Applied Pyrolysis, 94*, 209-214.

Lee, K.-H., & Oh, S. C. (2012). Thermal and catalytic degradation of pyrolytic waxy oil in a plug flow reactor. *Journal of Analytical and Applied Pyrolysis, 93*, 19-23.

Li, W., Pan, C., Zhang, Q., Liu, Z., Peng, J., Chen, P., . . . Zheng, X. (2011). Upgrading of low-boiling fraction of bio-oil in supercritical methanol and reaction network. *Bioresource Technology, 102*(7), 4884-4889.

Li, X., Su, L., Wang, Y., Yu, Y., Wang, C., Li, X., & Wang, Z. (2012). Catalytic fast pyrolysis of Kraft lignin with HZSM-5 zeolite for producing aromatic hydrocarbons. *Frontiers of Environmental Science & Engineering, 6*(3), 295-303.

Liu, J., Jiang, G., Liu, Y., Di, J., Wang, Y., Zhao, Z., . . . Jiang, L. (2014). Hierarchical macro-meso-microporous ZSM-5 zeolite hollow fibers with highly efficient catalytic cracking capability. *Scientific Reports, 4*, 7276.

Ma, Z., Troussard, E., & van Bokhoven, J. A. (2012). Controlling the selectivity to chemicals from lignin via catalytic fast pyrolysis. *Applied Catalysis A: General, 423-424*, 130-136.

Mante, O. D., Agblevor, F. A., & McClung, R. (2011). Fluid catalytic cracking of biomass pyrolysis vapors. *Biomass Conversion and Biorefinery, 1*(4), 189-201.

Mathews, J. F., Tepylo, M. G., Eager, R. L., & Pepper, J. M. (1985). Upgrading of aspen poplar wood oil over HZSM-5 zeolite catalyst. *The Canadian Journal of Chemical Engineering, 63*(4), 686-689.

Mihalcik, D. J., Mullen, C. A., & Boateng, A. A. (2011). Screening acidic zeolites for catalytic fast pyrolysis of biomass and its components. *Journal of Analytical and Applied Pyrolysis, 92*(1), 224-232.

Mohammed, M. A. A., Salmiaton, A., Wan Azlina, W. A. K. G., Mohammad Amran, M. S., Fakhru'l-Razi, A., & Taufiq-Yap, Y. H. (2011). Hydrogen rich gas from oil palm biomass as a potential source of renewable energy in Malaysia. *Renewable and Sustainable Energy Reviews, 15*(2), 1258-1270.

Mortensen, P. M., Grunwaldt, J. D., Jensen, P. A., Knudsen, K. G., & Jensen, A. D. (2011). A review of catalytic upgrading of bio-oil to engine fuels. *Applied Catalysis A: General, 407*(1-2), 1-19.

Mullen, C. A., & Boateng, A. A. (2010). Catalytic pyrolysis-GC/MS of lignin from several sources. *Fuel Processing Technology, 91*(11), 1446-1458.

Ni, Y., Sun, A., Wu, X., Hai, G., Hu, J., Li, T., & Li, G. (2011). The preparation of nano-sized H[Zn, Al]ZSM-5 zeolite and its application in the aromatization of methanol. *Microporous and Mesoporous Materials, 143*(2-3), 435-442.

Nie, L., de Souza, P. M., Noronha, F. B., An, W., Sooknoi, T., & Resasco, D. E. (2014). Selective conversion of m-cresol to toluene over bimetallic Ni–Fe catalysts. *Journal of Molecular Catalysis A: Chemical, 388-389*, 47-55.

Olcese, R. N., Bettahar, M., Petitjean, D., Malaman, B., Giovanella, F., & Dufour, A. (2012). Gas-phase hydrodeoxygenation of guaiacol over Fe/SiO_2 catalyst. *Applied Catalysis B: Environmental, 115-116*, 63-73.

Olcese, R. N., Francois, J., Bettahar, M. M., Petitjean, D., & Dufour, A. (2013). Hydrodeoxygenation of guaiacol, a surrogate of lignin pyrolysis vapors, over iron based catalysts: kinetics and modeling of the lignin to aromatics integrated process. *Energy & Fuels, 27*(2), 975-984.

Park, H. J., Dong, J. I., Jeon, J. K., Yoo, K. S., Yim, J. S., Sohn, J. M., & Park, Y. K. (2007). Conversion of the pyrolytic vapor of radiata pine over zeolites. *Journal of Industrial and Engineering Chemistry, 13*(2), 182-189.

Park, H. J., Heo, H. S., Jeon, J.-K., Kim, J., Ryoo, R., Jeong, K.-E., & Park, Y.-K. (2010). Highly valuable chemicals production from catalytic upgrading of radiata pine sawdust-derived pyrolytic vapors over mesoporous MFI zeolites. *Applied Catalysis B: Environmental*, *95*(3-4), 365-373.

Park, H. J., Park, K.-H., Jeon, J.-K., Kim, J., Ryoo, R., Jeong, K.-E., . . . Park, Y.-K. (2012). Production of phenolics and aromatics by pyrolysis of miscanthus. *Fuel, 97*, 379-384.

Peralta, M. A., Sooknoi, T., Danuthai, T., & Resasco, D. E. (2009). Deoxygenation of benzaldehyde over CsNaX zeolites. *Journal of Molecular Catalysis A: Chemical, 312*(1-2), 78-86.

Perego, C., & Bosetti, A. (2011). Biomass to fuels: The role of zeolite and mesoporous materials. *Microporous and Mesoporous Materials, 144*(1-3), 28-39.

Prasomsri, T., To, A. T., Crossley, S., Alvarez, W. E., & Resasco, D. E. (2011). Catalytic conversion of anisole over HY and HZSM-5 zeolites in the presence of different hydrocarbon mixtures. *Applied Catalysis B: Environmental*, *106*(1–2), 204-211.

Putun, E., Uzun, B. B., & Putun, A. E. (2006). Fixed-bed catalytic pyrolysis of cotton-seed cake: effects of pyrolysis temperature, natural zeolite content and sweeping gas flow rate. *Bioresource Technology*, *97*(5), 701-710.

R. Marinangeli, T. Marker, J. Petri, T. Kalnes, M. McCall, D. Mackowiak, . . . Shonnard, D. (2006). Opportunities for biorenewables in oil refineries. UOP.

Rezaei, P. S., Shafaghat, H., & Daud, W. M. A. W. (2014). Production of green aromatics and olefins by catalytic cracking of oxygenate compounds derived from biomass pyrolysis: A review. *Applied Catalysis A: General, 469*, 490-511.

Sad, M. E., Padró, C. L., & Apesteguía, C. R. (2008). Synthesis of cresols by alkylation of phenol with methanol on solid acids. *Catalysis Today, 133-135*, 720-728.

Samolada, M. C., Papafotica, A., & Vasalos, I. A. (2000). Catalyst evaluation for catalytic biomass pyrolysis. *Energy & Fuels, 14*(6), 1161-1167.

Serrano-Ruiz, J. C., & Dumesic, J. A. (2011). Catalytic routes for the conversion of biomass into liquid hydrocarbon transportation fuels. *Energy & Environmental Science, 4*(1), 83-99.

Sharma, R. K., & Bakhshi, N. N. (1991). Upgrading of wood-derived bio-oil over HZSM-5. *Bioresource Technology, 35*(1), 57-66.

Sharma, R. K., & Bakhshi, N. N. (1993). Catalytic upgrading of pyrolysis oil. *Energy & Fuels, 7*(2), 306-314.

Shen, D., Zhao, J., Xiao, R., & Gu, S. (2015). Production of aromatic monomers from catalytic pyrolysis of black-liquor lignin. *Journal of Analytical and Applied Pyrolysis, 111*, 47-54.

Shin, E.-J., & Keane, M. A. (2000). Gas-phase hydrogenation/hydrogenolysis of phenol over supported nickel catalysts. *Industrial & Engineering Chemistry Research, 39*(4), 883-892.

Song, M., Zhong, Z., & Dai, J. (2010). Different solid acid catalysts influence on properties and chemical composition change of upgrading bio-oil. *Journal of Analytical and Applied Pyrolysis, 89*(2), 166-170.

Srinivasan, V., Adhikari, S., Chattanathan, S. A., Tu, M., & Park, S. (2014). Catalytic pyrolysis of raw and thermally treated cellulose using different acidic zeolites. *BioEnergy Research, 7*(3), 867-875.

Stefanidis, S. D., Kalogiannis, K. G., Iliopoulou, E. F., Lappas, A. A., & Pilavachi, P. A. (2011). In-situ upgrading of biomass pyrolysis vapors: catalyst screening on a fixed bed reactor. *Bioresource Technology, 102*(17), 8261-8267.

Stephanidis, S., Nitsos, C., Kalogiannis, K., Iliopoulou, E. F., Lappas, A. A., & Triantafyllidis, K. S. (2011). Catalytic upgrading of lignocellulosic biomass pyrolysis vapours: Effect of hydrothermal pre-treatment of biomass. *Catalysis Today, 167*(1), 37-45.

Thangalazhy-Gopakumar, S., Adhikari, S., & Gupta, R. B. (2012). Catalytic pyrolysis of biomass over H^+ZSM-5 under hydrogen pressure. *Energy & Fuels, 26*(8), 5300-5306.

Thegarid, N., Fogassy, G., Schuurman, Y., Mirodatos, C., Stefanidis, S., Iliopoulou, E. F., . . . Lappas, A. A. (2014). Second-generation biofuels by co-processing catalytic pyrolysis oil in FCC units. *Applied Catalysis B: Environmental, 145*, 161-166.

Thilakaratne, R., Wright, M. M., & Brown, R. C. (2014). A techno-economic analysis of microalgae remnant catalytic pyrolysis and upgrading to fuels. *Fuel, 128*, 104-112.

Thring, R. W., Katikaneni, S. P. R., & Bakhshi, N. N. (2000). The production of gasoline range hydrocarbons from Alcell® lignin using HZSM-5 catalyst. *Fuel Processing Technology, 62*(1), 17-30.

Toor, S. S., Rosendahl, L., & Rudolf, A. (2011). Hydrothermal liquefaction of biomass: a review of subcritical water technologies. *Energy, 36*(5), 2328-2342.

Valle, B., Castaño, P., Olazar, M., Bilbao, J., & Gayubo, A. G. (2012). Deactivating species in the transformation of crude bio-oil with methanol into hydrocarbons on a HZSM-5 catalyst. *Journal of Catalysis, 285*(1), 304-314.

Valle, B., Gayubo, A. G., Aguayo, A. s. T., Olazar, M., & Bilbao, J. (2010). Selective production of aromatics by crude bio-oil valorization with a nickel-modified HZSM-5 zeolite catalyst. *Energy & Fuels, 24*(3), 2060-2070.

Valle, B., Gayubo, A. G., Alonso, A., Aguayo, A. T., & Bilbao, J. (2010). Hydrothermally stable HZSM-5 zeolite catalysts for the transformation of crude bio-oil into hydrocarbons. *Applied Catalysis B: Environmental, 100*(1-2), 318-327.

Vieira, R. C., Pinto, J. C., Biscaia, E. C., Baptista, C. M. L. A., & Cerqueira, H. S. (2004). Simulation of catalytic cracking in a fixed-fluidized-bed unit. *Industrial & Engineering Chemistry Research, 43*(19), 6027-6034.

Vispute, T. P., Zhang, H., Sanna, A., Xiao, R., & Huber, G. W. (2010). Renewable chemical commodity feedstocks from integrated catalytic processing of pyrolysis oils. *Science, 330*(6008), 1222-1227.

Vitolo, S., Bresci, B., Seggiani, M., & Gallo, M. G. (2001). Catalytic upgrading of pyrolytic oils over HZSM-5 zeolite: behaviour of the catalyst when used in repeated upgrading–regenerating cycles. *Fuel, 80*(1), 17-26.

Vitolo, S., Seggiani, M., Frediani, P., Ambrosini, G., & Politi, L. (1999). Catalytic upgrading of pyrolytic oils to fuel over different zeolites. *Fuel, 78*(10), 1147-1159.

Wang, J.-J., Chang, J., & Fan, J. (2010). Upgrading of bio-oil by catalytic esterification and determination of acid number for evaluating esterification degree. *Energy & Fuels, 24*(5), 3251-3255.

Wang, W., De Cola, P., Glaeser, R., Ivanova, I., Weitkamp, J., & Hunger, M. (2004). Methylation of phenol by methanol on acidic zeolite H–Y investigated by in situ CF MAS NMR spectroscopy. *Catalysis Letters, 94*(1-2), 119-123.

Wang, W., Yang, Y., Luo, H., Hu, T., & Liu, W. (2011). Amorphous Co–Mo–B catalyst with high activity for the hydrodeoxygenation of bio-oil. *Catalysis Communications, 12*(6), 436-440.

Weitkamp, J. (2000). Zeolites and catalysis. *Solid State Ionics, 131*(1–2), 175-188.

Williams, P. T., & Horne, P. A. (1995a). The influence of catalyst regeneration on the composition of zeolite-upgraded biomass pyrolysis oils. *Fuel, 74*(12), 1839-1851.

Williams, P. T., & Horne, P. A. (1995b). The influence of catalyst type on the composition of upgraded biomass pyrolysis oils. *Journal of Analytical and Applied Pyrolysis, 31*, 39-61.

Williams, P. T., & Nugranad, N. (2000). Comparison of products from the pyrolysis and catalytic pyrolysis of rice husks. *Energy, 25*(6), 493-513.

Williams, P. T., & Taylor, D. T. (1993). Aromatization of tyre pyrolysis oil to yield polycyclic aromatic hydrocarbons. *Fuel, 72*(11), 1469-1474.

Xue, H., Huang, X., Zhan, E., Ma, M., & Shen, W. (2013). Selective dealumination of mordenite for enhancing its stability in dimethyl ether carbonylation. *Catalysis Communications, 37*, 75-79.

Yu, W., Tang, Y., Mo, L., Chen, P., Lou, H., & Zheng, X. (2011). One-step hydrogenation-esterification of furfural and acetic acid over bifunctional Pd catalysts for bio-oil upgrading. *Bioresource Technology, 102*(17), 8241-8246.

Yu, Y., Li, X., Su, L., Zhang, Y., Wang, Y., & Zhang, H. (2012). The role of shape selectivity in catalytic fast pyrolysis of lignin with zeolite catalysts. *Applied Catalysis A: General, 447-448*, 115-123.

Zhang, H., Carlson, T. R., Xiao, R., & Huber, G. W. (2012). Catalytic fast pyrolysis of wood and alcohol mixtures in a fluidized bed reactor. *Green Chemistry, 14*(1), 98-110.

Zhang, H., Cheng, Y.-T., Vispute, T. P., Xiao, R., & Huber, G. W. (2011). Catalytic conversion of biomass-derived feedstocks into olefins and aromatics with ZSM-5: the hydrogen to carbon effective ratio. *Energy & Environmental Science, 4*(6), 2297.

Zhang, H., Xiao, R., Huang, H., & Xiao, G. (2009). Comparison of non-catalytic and catalytic fast pyrolysis of corncob in a fluidized bed reactor. *Bioresource Technology, 100*(3), 1428-1434.

Zhang, J., Luo, Z., Dang, Q., Wang, J., & Chen, W. (2012). Upgrading of bio-oil over bifunctional catalysts in supercritical monoalcohols. *Energy & Fuels, 26*(5), 2990-2995.

Zhang, M., & Moutsoglou, A. (2014). Catalytic fast pyrolysis of prairie cordgrass lignin and quantification of products by pyrolysis–gas chromatography–mass spectrometry. *Energy & Fuels, 28*(2), 1066-1073.

Zhang, M., Resende, F. L. P., & Moutsoglou, A. (2014). Catalytic fast pyrolysis of aspen lignin via Py-GC/MS. *Fuel, 116*, 358-369.

Zhang, Q., Chang, J., Wang, & Xu, Y. (2006). Upgrading bio-oil over different solid catalysts. *Energy & Fuels, 20*(6), 2717-2720.

Zhang, Y., Brown, T. R., Hu, G., & Brown, R. C. (2013). Techno-economic analysis of two bio-oil upgrading pathways. *Chemical Engineering Journal, 225*, 895-904.

Zhao, Y., Deng, L., Liao, B., Fu, Y., & Guo, Q.-X. (2010). Aromatics production via catalytic pyrolysis of pyrolytic lignins from bio-Oil. *Energy & Fuels, 24*(10), 5735-5740.

Zhao, Y., Fu, Y., & Guo, Q. X. (2012). Production of aromatic hydrocarbons through catalytic pyrolysis of gamma-valerolactone from biomass. *Bioresource Technology, 114*, 740-744.

Zhu, X., Lobban, L. L., Mallinson, R. G., & Resasco, D. E. (2011). Bifunctional transalkylation and hydrodeoxygenation of anisole over a Pt/HBeta catalyst. *Journal of Catalysis, 281*(1), 21-29.

Zhu, X., Mallinson, R. G., & Resasco, D. E. (2010). Role of transalkylation reactions in the conversion of anisole over HZSM-5. *Applied Catalysis A: General, 379*(1-2), 172-181.

Zhu, X., Nie, L., Lobban, L. L., Mallinson, R. G., & Resasco, D. E. (2014). Efficient conversion of m-cresol to aromatics on a bifunctional Pt/HBeta catalyst. *Energy & Fuels, 28*(6), 4104-4111.

LIST OF PUBLICATIONS

- **Sirous Rezaei, Pouya**, Shafaghat, Hoda, & Wan Daud, Wan Mohd Ashri (2016). Aromatic hydrocarbon production by catalytic pyrolysis of palm kernel shell waste using a bifunctional Fe/HBeta catalyst: effect of lignin-derived phenolics on zeolite deactivation. *Green Chemistry, 18*, 1684-1693.
- **Sirous Rezaei, Pouya**, Shafaghat, Hoda, & Wan Daud, Wan Mohd Ashri (2015). Suppression of coke formation and enhancement of aromatic hydrocarbon production in catalytic fast pyrolysis of cellulose over different zeolites: effects of pore structure and acidity. *RSC Advances, 5*, 65408-65414.
- **Sirous Rezaei, Pouya**, Shafaghat, Hoda, & Wan Daud, Wan Mohd Ashri (2015). Origin of catalyst deactivation in atmospheric hydrogenolysis of *m*-cresol over Fe/HBeta. *RSC Advances, 5*, 51278-51285.
- **Sirous Rezaei, Pouya**, Shafaghat, Hoda, & Wan Daud, Wan Mohd Ashri (2014). Production of green aromatics and olefins by catalytic cracking of oxygenate compounds derived from biomass pyrolysis: A review. *Applied Catalysis A: General, 469*, 490-511.

Green Chemistry

PAPER

Cite this: *Green Chem.*, 2016, **18**, 1684

Aromatic hydrocarbon production by catalytic pyrolysis of palm kernel shell waste using a bifunctional Fe/HBeta catalyst: effect of lignin-derived phenolics on zeolite deactivation

Pouya Sirous Rezaei, Hoda Shafaghat and Wan Mohd Ashri Wan Daud*

Conversion of lignin to aromatic hydrocarbons over zeolites is a challenging issue due to low reactivity of lignin-derived phenolic compounds over zeolites as well as their high potential for strong adsorption on zeolite acid sites. Hence, pure zeolites are not appropriate catalysts for upgrading of the lignocellulosic biomass with high content of lignin. In this research, a bifunctional Fe/HBeta catalyst showed to be efficient for production of aromatic hydrocarbons in catalytic pyrolysis of palm kernel shell waste with a high lignin content of about 50 wt%. Lignin-derived phenolics were deoxygenated through a hydrogenolysis reaction promoted by Fe active sites. A comparison between catalytic behaviour of HBeta and HZSM-5 in conversion of palm kernel shells showed that catalyst deactivation *via* occupation of zeolite acid sites by lignin-derived phenolics is affected by catalyst pore size and strength of zeolite acid sites. Meanwhile, cellulose and lignin were compared in terms of reactivity over zeolite acid sites and influence on zeolite deactivation. It was also shown that the yield of aromatic hydrocarbons obtained from conversion of lignin was remarkably enhanced by incorporation of iron into the HBeta structure. However, both HBeta and Fe/HBeta resulted in approximately similar aromatic yield from conversion of cellulose.

Received 18th August 2015,
Accepted 2nd November 2015

DOI: 10.1039/c5gc01935d

www.rsc.org/greenchem

1. Introduction

Lignocellulosic biomass is of high potential to be a green source of valuable chemicals and fuels.[1,2] Pyrolysis is an economically feasible process for large-scale utilization of biomass.[3] Pyrolysis is a thermal decomposition technique in which organic compounds are degraded in the absence of oxygen producing non-condensable gases, solid residues containing carbon deposits and a liquid called bio-oil.[4] However, bio-oil has a high oxygen content causing some disadvantages such as high viscosity, poor heating value, corrosiveness, and chemical and thermal instability.[5–9] Hence, bio-oil needs to be deoxygenated to hydrocarbons in order to be used as a fuel additive. Catalytic pyrolysis is an efficient process for conversion of biomass materials into valuable hydrocarbons since it includes both steps of pyrolysis and catalytic upgrading in one unit. So far, different types of zeolites have been used as catalysts for atmospheric pressure upgrading of biomass derived feedstocks. Zeolites contain both Brønsted and Lewis acid sites which promote upgrading reactions such as dehydration, decarboxylation, decarbonylation, aromatization, isomerization, cracking, dehydrogenation, dealkylation and oligomerization.[2,10] Furthermore, the microporous structure of zeolites makes them shape selective catalysts. This shape selectivity makes it possible to control product distribution, and to promote reaction selectivity towards desired hydrocarbons.

It is well described in the literature that among the three lignocellulosic components (cellulose, hemicellulose and lignin), lignin is the most difficult one to be deoxygenated.[11–13] So far, catalytic pyrolysis processes for conversion of lignin into aromatic hydrocarbons have been conducted at high temperatures above 600 °C, high ratios of zeolite to lignin and fast heating rates.[14–18] In catalytic pyrolysis of lignin over HZSM-5 using a pyroprobe pyrolyzer, it was observed that aromatic hydrocarbon yield was significantly enhanced by an increase of the reaction temperature from 550 to 650 °C.[19,20] Xiangyu Li *et al.*[11] showed that aromatic hydrocarbon yield was a strong function of the catalyst to lignin ratio; the aromatic hydrocarbon production was maximized at a high HZSM-5 to lignin ratio of 15. However, cellulose could be remarkably converted into aromatic hydrocarbons by catalytic pyrolysis at lower temperatures (below 600 °C) and catalyst to feed ratios.[21,22] The reasons for difficulty in lignin deoxygenation are low reactivity of lignin-derived phenolics over zeolite acid sites and rapid deactivation of zeolites exposed to phenolic

Department of Chemical Engineering, Faculty of Engineering, University of Malaya, 50603 Kuala Lumpur, Malaysia. E-mail: pouya.sr@gmail.com, h.shafaghat@gmail.com, ashri@um.edu.my; Fax: +60 3 79675319; Tel: +60 3 79675297

RSC Advances

PAPER

Cite this: *RSC Adv.*, 2015, **5**, 65408

Suppression of coke formation and enhancement of aromatic hydrocarbon production in catalytic fast pyrolysis of cellulose over different zeolites: effects of pore structure and acidity

Pouya Sirous Rezaei, Hoda Shafaghat and Wan Mohd Ashri Wan Daud*

Received 14th June 2015
Accepted 27th July 2015

DOI: 10.1039/c5ra11332f

www.rsc.org/advances

Rapid deactivation of zeolites caused by high formation and deposition of coke is a great challenge in catalytic conversion of biomass materials into value-added chemicals and fuels. The main purpose of this work was to reduce the formation of both types of thermal and catalytic coke over zeolites. It was revealed that there is a significant interaction between zeolite pore structure and the density of acid sites which could be optimized for reduced coke formation. In this study, catalytic pyrolysis of cellulose was conducted using HZSM-5 (Si/Al: 30), HY (Si/Al: 30) and physically mixed catalysts of HZSM-5 (Si/Al: 30) and dealuminated HY (Si/Al: 327). Coke formation over the physically mixed catalysts was remarkably lower than that over HZSM-5 and HY; the coke contents of HZSM-5, HY and physically mixed catalysts of HZSM-5 and dealuminated HY with a ratio of 70 : 30 wt% were 7.01, 11.47 and 4.82 wt%, respectively. The aromatic hydrocarbon yield was also considerably enhanced over the physically mixed catalysts compared to HZSM-5 and HY; the aromatic hydrocarbon yields achieved over HZSM-5, HY and the mixture of HZSM-5 and dealuminated HY (70 : 30 wt%) were 20.31, 8.91 and 27.01 wt%, respectively. This study shows that the interactive effects of zeolite characteristics such as pore structure and acidity could be taken into account for designing more efficient catalysts to achieve lower coke formation and higher production of desired products.

1. Introduction

The depletion of fossil fuels and the negative impacts of their utilization on the environment such as global warming and air pollution necessitate the discovery of renewable, sustainable and environmentally friendly alternative sources of energy.[1–3] Lignocellulosic biomass is of great potential to be considered as such an alternative since it is abundantly available, and the fuel obtained from biomass is carbon dioxide neutral.[4] Biomass pyrolysis which leads to a liquid product called bio-oil has gained extensive attention as an economically feasible technique for large-scale exploitation of biomass.[5] However, bio-oil is highly oxygenated and has poor fuel properties such as high viscosity, poor heating value, corrosiveness, and chemical and thermal instability.[6–9] It is also immiscible with conventional fossil fuels, and therefore needs to be upgraded. Catalytic pyrolysis is considered an efficient technology since it includes both steps of pyrolysis and catalytic upgrading in one unit. Zeolites have been the most common catalysts used for atmospheric pressure upgrading of pyrolysis vapors in catalytic pyrolysis of biomass feedstocks. The major challenge in this process is high formation and deposition of coke on zeolite which causes high deactivation of catalyst.[10] The reason for high yield of coke is low hydrogen to carbon effective ratio of biomass which leads to low hydrogen content in hydrocarbon pool inside catalyst. Coke deposited on catalyst is divided into two types of thermal and catalytic origin.[11] Thermal coke is produced by homogeneous thermal polymerization of compounds in gas phase, and is mainly deposited on outer surface of catalyst.[12] Catalytic coke is formed in the internal channels of catalyst as a result of heterogeneous transformation of oxygenate compounds over zeolite acid sites through reactions of oligomerization, cyclization, aromatization and condensation.[13–15] Coke deposition results in catalyst deactivation through poisoning zeolite acid sites and pore blockage. In addition to catalyst deactivation, coke formation is a competing reaction with production of desired products. Therefore, it is essential to optimize catalyst properties in order to lower coke formation.

Zeolite pore structure and acidity are the two significant catalyst properties which greatly affect the amount of coke formation. In catalytic upgrading of pine wood pyrolysis vapors, it was revealed that among beta, Y and ferrierite zeolites,

Department of Chemical Engineering, Faculty of Engineering, University of Malaya, 50603 Kuala Lumpur, Malaysia. E-mail: pouya.sr@gmail.com; h.shafaghat@gmail.com; ashri@um.edu.my; Fax: +60 3 79675319; Tel: +60 3 79675297

RSC Advances

PAPER

Cite this: *RSC Adv.*, 2015, **5**, 51278

Origin of catalyst deactivation in atmospheric hydrogenolysis of *m*-cresol over Fe/HBeta†

Pouya Sirous Rezaei, Hoda Shafaghat and Wan Mohd Ashri Wan Daud*

Received 23rd April 2015
Accepted 3rd June 2015

DOI: 10.1039/c5ra07420g

www.rsc.org/advances

Zeolites are the most common catalysts used for atmospheric deoxygenation of biomass pyrolysis derived feedstocks. The catalytic performance of the zeolite and the yield of deoxygenation greatly depend on the nature of the feedstock. Lignin is the most difficult part of biomass to be deoxygenated and lignin derived phenolic compounds cause rapid deactivation of zeolites. The main purpose of this research was to study the origin of zeolite deactivation in atmospheric deoxygenation of phenolic compounds. Phenol and *m*-cresol were selected as model compounds for lignin. In order to investigate their effect on zeolite deactivation, catalytic conversion of a mixture of methanol with *m*-cresol or phenol and a mixture of *m*-cresol with phenol were carried out over HBeta and Fe/HBeta, respectively. Co-feeding phenol or *m*-cresol with methanol caused high deactivation of HBeta and significant reduction in the aromatics yield. Meanwhile, these phenols had low reactivity over HBeta. Catalytic performance was enhanced by iron impregnation on zeolite, and Fe/HBeta could considerably convert *m*-cresol into aromatic hydrocarbons through hydrogenolysis. However, this catalyst was not efficient for deoxygenation of phenol. Strong adsorption of phenol molecules on zeolite acid sites resulting in high formation of coke was the main source of zeolite deactivation which was attenuated by an increase in reaction temperature.

1. Introduction

Considering the depletion of fossil fuels as well as the environmental threats caused by large-scale consumption of this source of energy, there is an increasing concern about the future of the hydrocarbon industry.[1–4] Lignocellulosic biomass seems to be a potential alternative to replace fossil fuels since it is renewable and abundantly available.[5,6] Pyrolysis is an effective technique for high exploitation of biomass and production of liquid fuel, called bio-oil.[7] However, pyrolysis bio-oil is highly oxygenated due to the high oxygen content of biomass.[8–10] In the last two decades, several different catalytic reactions operated at atmospheric pressure or high hydrogen pressure have been examined in order to achieve an efficient process for deoxygenation of biomass derived feedstocks. Atmospheric pressure processes seem more attractive due to lower operating costs. However, it is more difficult to achieve a high yield of deoxygenation at atmospheric pressure mainly due to a low hydrogen to carbon effective ratio of biomass derived feedstocks and catalyst deactivation caused by high coke deposition. Zeolites are the most widely used catalysts in the atmospheric transformation of biomass derived feedstocks for production of valuable hydrocarbons like aromatics and olefins.[5] The studies reported in the literature indicate that the nature of the feedstock greatly affects the catalytic performance of zeolites and yield of deoxygenation. Therefore, the composition of the biomass should be taken into account in order to design an efficient catalytic system. Ana G. Gayubo *et al.*[11,12] showed that alcohols, ketones and acids could be significantly converted to hydrocarbons through catalytic transformation over HZSM-5, while phenols and aldehydes had low reactivity to hydrocarbons and caused a large amount of coke deposited on this zeolite. As a result, it was suggested to separate phenols and aldehydes prior to catalytic upgrading of pyrolysis bio-oil. It has been indicated in several researches that lignin is the most difficult fraction of biomass to be converted to hydrocarbons.[13–15] This is due to the phenolic structure of lignin and low reactivity of lignin derived phenolic compounds over zeolites. In a study by Charles A. Mullen *et al.*,[16] it was revealed that the lignin with higher content of *p*-hydroxyphenyl units and lower contents of guaiacyl and syringyl units caused higher deactivation of HZSM-5. The reason for this was declared to be higher concentration of simple phenolics compared to that of guaiacols and syringols obtained by pyrolysis of the lignin with higher proportion of *p*-hydroxyphenyl units; simple phenols have more potential than guaiacols and syringols to be tightly bound to the active sites of zeolites causing higher catalyst deactivation. In transformation of methylcyclohexane over HZSM-5, it was revealed that addition of phenol to methylcyclohexane significantly increased catalyst deactivation due to strong adsorption of phenol on zeolite acid sites.[17] The loss of

Department of Chemical Engineering, Faculty of Engineering, University of Malaya, 50603 Kuala Lumpur, Malaysia. E-mail: pouya.sr@gmail.com; h.shafaghat@gmail.com; ashri@um.edu.my; Fax: +60 3 79675319; Tel: +60 3 79675297

† Electronic supplementary information (ESI) available. See DOI: 10.1039/c5ra07420g

Applied Catalysis A: General 469 (2014) 490–511

Contents lists available at ScienceDirect

Applied Catalysis A: General

journal homepage: www.elsevier.com/locate/apcata

Production of green aromatics and olefins by catalytic cracking of oxygenate compounds derived from biomass pyrolysis: A review

Pouya Sirous Rezaei, Hoda Shafaghat, Wan Mohd Ashri Wan Daud *

Department of Chemical Engineering, University of Malaya, 50603 Kuala Lumpur, Malaysia

ARTICLE INFO

Article history:
Received 12 June 2013
Received in revised form 27 August 2013
Accepted 22 September 2013
Available online xxx

Keywords:
Bio-oil
Catalytic cracking
Reaction selectivity
Aromatics
Olefins

ABSTRACT

The concern for depletion of fossil fuels and their growing environmental threats necessitates to develop efficient techniques for utilization of biomass as an alternative fuel source which is renewable and environmentally safe. Catalytic cracking of biomass pyrolysis derived feedstock could be an economical process for production of high value added chemicals which are currently obtained from fossil fuels. However, promotion of reaction selectivity toward valuable chemicals is a great challenge in this process. Coke formation in catalytic cracking of biomass pyrolysis vapors/bio-oil is a competing reaction with production of valuable hydrocarbons like aromatics and olefins. Coke is one major undesired product of this process which its high yield is due to low hydrogen to carbon effective ratio of biomass and in turn low hydrogen content in hydrocarbon pool inside catalyst. Catalytic cracking of biomass pyrolysis vapors/bio-oil is a highly shape selective reaction with strong dependency on catalyst acidity and reaction conditions. This paper, for the first time, reviews the effects of catalyst properties and reaction conditions on reaction selectivity toward aromatics and olefins in catalytic cracking of biomass pyrolysis vapors/bio-oil and bio-oil model compounds.

Contents

1. Introduction

Current utilization rate of fossil fuels is much higher than their natural regeneration rate leading to the shortage of fossil fuels. Considering the depletion of fossil fuel reserves as well as the increasing environmental threats like global warming and air pollution caused by large-scale consumption of fossil fuels, there is a growing demand for renewable, sustainable and environmentally friendly fuels [1–5]. Lignocellulosic biomass seems to be a highly potential renewable source of energy. Fuels obtained from biomass are considered carbon dioxide neutral since CO_2 produced from biofuel combustion has been previously absorbed from atmosphere through photosynthesis process of plants [6].

* Corresponding author. Tel.: +60 3 79675297; fax: +60 3 79675319.
E-mail addresses: pouya.sr@gmail.com (P.S. Rezaei), h.shafaghat@gmail.com (H. Shafaghat), ashri@um.edu.my (W.M.A.W. Daud).

0926-860X/$ – see front matter © 2013 Elsevier B.V. All rights reserved.
http://dx.doi.org/10.1016/j.apcata.2013.09.036